

IOWA STATE UNIVERSITY

Digital Repository

Graduate Theses and Dissertations

Iowa State University Capstones, Theses and
Dissertations

2018

Moment matching technique for fast and robust uncertainty quantifications of complex systems

Ya-Lu Teng
Iowa State University

Follow this and additional works at: <https://lib.dr.iastate.edu/etd>

 Part of the [Civil Engineering Commons](#)

Recommended Citation

Teng, Ya-Lu, "Moment matching technique for fast and robust uncertainty quantifications of complex systems" (2018). *Graduate Theses and Dissertations*. 16887.
<https://lib.dr.iastate.edu/etd/16887>

This Thesis is brought to you for free and open access by the Iowa State University Capstones, Theses and Dissertations at Iowa State University Digital Repository. It has been accepted for inclusion in Graduate Theses and Dissertations by an authorized administrator of Iowa State University Digital Repository. For more information, please contact digirep@iastate.edu.



**Moment matching technique for fast and robust uncertainty quantifications of
complex systems**

by

Ya-Lu Teng

A thesis submitted to the graduate faculty
in partial fulfillment of the requirements for the degree of
MASTER OF SCIENCE

Major: Civil Engineering (Structural Engineering)

Program of Study Committee:
Inho Cho, Major Professor
An Chen
Jin Tian

The student author, whose presentation of the scholarship herein was approved by the program of study committee, is solely responsible for the content of this thesis. The Graduate College will ensure this thesis is globally accessible and will not permit alterations after a degree is conferred.

Iowa State University

Ames, Iowa

2018

Copyright © Ya-Lu Teng, 2018. All rights reserved.

TABLE OF CONTENTS

	Page
LIST OF FIGURES	iii
LIST OF TABLES	vi
NOMENCLATURE	x
ACKNOWLEDGMENTS	xi
ABSTRACT.....	xii
CHAPTER 1. REVIEW OF LITERATURE	1
1.1 Introduction	1
CHAPTER 2. METHODS AND PROCEDURES	18
2.1 Methods	18
2.1.1 Reduce Sample Points of Moment Matching.....	18
2.1.2 Study Variables for Moment Matching.....	19
2.1.3 Microphysical Mechanisms and Validations of the Adopted PM-FEA Platform	20
2.2 Procedures	27
2.2.1 Simple Uncertainty Estimation Procedure of Moment Matching	27
2.2.2 Predicted Uncertainty Behind Shear Force-Resisting Capacity	29
2.2.3 Predicted Uncertainty Behind Progressive Bar Buckling	34
CHAPTER 3. EXPERIMENTAL DATA AND RESULTS	38
3.1 Results of progressive bar buckling.....	38
3.2 Results of shear force-resisting capacity	52
CHAPTER 4. MOMENT MATCHING ON VULNERABILITY	60
4.1 Conventional ranges of the collapse capacity and GANMM results.....	60
CHAPTER 5. CONCLUSION.....	97
5.1 Remark on Limitation of the Proposed Method	97
5.2 Conclusion	99
REFERENCES	102

LIST OF FIGURES

	Page
Figure 1.1. Ching <i>et al.</i> (2009) [16] applied MM technique to uncertainty propagation behind seismic loss estimation.	3
Figure 1.2. The prototype building used to apply SP-BELA.....	9
Figure 1.3. The dimension of (a) TUA; and (b) TUB (cited from Beyer 2008 [21]).	11
Figure 1.4. The locations of installation of the three actuators (cited from Beyer 2008 [21]).	12
Figure 1.5. The loading patterns (cited from Beyer 2008 [21]). μ represents the levels of ductility.	13
Figure 1.6. Permanent plastic deformation occurs at soft matrix part excited by cyclic loadings. (cited from Cho 2013 [22])	14
Figure 2.1. (a) Irregular asperity pattern (inset) along the aggregate boundaries within a damaged concrete (cited from Cho 2017 [26]). Bottom figure shows a random-sized particle distribution; (b) Shear mechanism; (c) Solid element containing rigid particles (cited from Cho and Porter 2014 [27]; Cho 2013 [22])......	21
Figure 2.2. Schematic illustration of evolving buckling lengths of smart longitudinal bars: (a) intact state with 5 bar elements with initial buckling lengths of the effective length factor k (i.e. 0.5 for fixed-ends condition) times unstretched length L_0 ; (cited from Cho and Hall 2014 [24])......	21
Figure 2.3. (a) Popular confinement model using a simplified distinction between core and cover parts; (b) real-scale RC column used for test; (c) proximity index plot on horizontal cross section and (d) on vertical cross section (cited from Cho and Hall 2014 [24]).	22
Figure 2.4. Finite element models of (a) TUA and (b) TUB shear walls.	23
Figure 2.5. Displacement and moment responses in square-root-of-sum-of-squares from experiments of (a) TUA and (b) TUB shear walls (cited from Beyer et al. 2008 [21]); from PM-FEA simulations of (c) TUA and (d) TUB. The SRSS moment is expressed as $M_{WE2} + M_{SN2} \cdot (\pm 1)$, and the SRSS displacement is represented by $D_{WE2} + D_{SN2} \cdot (\pm 1)$, where the (± 1) is the sign representing the directions such as north and south.	24

Figure 2.6. Predicted progressive bar buckling and concrete spalling zone of U-shaped wall system (TUA): (a) inset photo shows concrete damage state (Beyer et al., [21]); (b) progressive bar state at end of test where the blue color represents bar without buckling (outside the dashed box) show zones without buckling and the red colored bar (inside the dashed box) indicates zone with PBB; buckling of the longitudinal bar was observed for the first time during the cycle in the diagonal direction at $\mu = 6.0$ when at position V the D12 bar in the outer corner of the west flange buckled (Beyer et al., [21]); (c), (d), (e), and (f) show that steel strain-stress behaviors within PBB zone (i.e., zone within dashed box)..... 25

Figure 2.7. Predicted progressive bar buckling and concrete spalling zone of U-shaped wall system (TUB): (a) inset photo shows concrete damage state (Beyer et al., [21]); (b) progressive bar state at the end of experiment where the blue colored bar (outside the dashed box) show zones without buckling and the red colored bar (inside the dashed box) indicates zone with PBB; buckling was observed when at $\mu = 4.0$ during NS cycle (Beyer et al., [21]); (c), (d), (e), and (f) show that steel strain-stress behaviors within PBB zone (i.e., zone within dashed box)..... 26

Figure 2.8. Three index points and weights for 1D MM of normal distribution of (a) fc' ; (b) fy ; (c) A_b ; (d) F_{axial} 28

Figure 2.9. Nine index points and weights for 4D MM of normal distributions of fc' , fy , A_b , and F_{axial} 28

Figure 2.10. Wall dimensions and loading directions of (a) TUA and TUB; (b) Wall 1, 2, and 3; (c) “Butterfly” bi-directional loading patterns of TUA and TUB; (d) Complex bi-directional loading pattern of Wall 3 30

Figure 2.11. Expectations of the maximum shear force-resisting capacity (denoted as $E[F_{max}]$) predicted by PM-FEA coupled with multi-dimensional MM ranging from 1D through 4D: (a) Wall 1; (b) Wall 2; (c) Wall 3; (d) TUA; (e) TUB. Error bar indicates $\pm\sigma$. Irregular, large error bars of Wall 3 imply relatively larger uncertainty in F_{max} of Wall 3 than other four U-walls 31

Figure 2.12. $COV[F_{min}]$ and $COV[F_{max}]$ obtained from 1D through 4D MM for (a) Wall 1; (b) Wall 2; (c) Wall 3; (d) TUA; (e) TUB. The variability of F_{axial} appears to govern the uncertainty of force-resisting capacity of Wall 3 while f_y appears to dominate the uncertainty of other four U-walls 33

Figure 2.13.COV of the crushed area ratio (denoted as COV[CA]) obtained from PM-FEA coupled with multi-dimensional MM ranging from 1D through 4D: (a) TUA; (b) TUB; (c) Wall 1; (d) Wall 2; (e) Wall 3. Among four variables, F_{axial} appears to hold the least impact on the uncertainty of TUA whereas f_y has the smallest impact on that of TUB. Uncertainties of Wall 1 and Wall 2 are nearly evenly affected by the variabilities of all four variables. Contrarily, f_c' appears to dominate the uncertainty of Wall 3 (as marked by a circle).	36
Figure 2.14. Expectations of the crushed area ratio (denoted as E[CA]) derived from PM-FEA coupled with multi-dimensional MM ranging from 1D through 4D: (a) TUA; (b) TUB; (c) Wall 1; (d) Wall 2; (e) Wall 3. Error bar indicates $\pm\sigma$. Large error bars are produced by MM which implies there are substantial uncertainties in the crushed areas and progressive bar buckling of five U-walls.	37
Figure 3.1. (a)3D model of TUA; (b)2D model of TUA; (c)3D model of TUB; (d)2D model of TUB.	38
Figure 5.1. Expectations of the crushed area ratio (denoted as E[CA]) derived from PM-FEA coupled with multi-dimensional MM ranging from 1D through 4D: (a) TUA; (b) TUB; (c) Wall 1; (d) Wall 2; (e) Wall 3. Error bar indicates $\pm\sigma$. Large error bars are produced by MM which implies there are substantial uncertainties in the crushed areas and progressive bar buckling of five U-walls.	98
Figure 5.2. (a) PDF of variable X; (b) True and simulated responses at various X.	99

LIST OF TABLES

	Page
Table 1.1 Wall thickness of TUA and TUB	10
Table 2.1. Mean and standard distribution of four study variables [21][25]	20
Table 2.2. For 1D MM [subscript $j = 1, 2, 3, 4$ corresponds to fc' , fy , A_b , and $Faxial$, respectively	29
Table 2.3. Nine indexes and weights for 4D MM [subscripts 1 through 4 correspond to fc' , fy , A_b , and $Faxial$, respectively	29
Table 3.1. Height, width and area of TUA	39
Table 3.2. Crushed Area, ratio and its average ratio of initial condition of TUA	39
Table 3.3. Crushed Area, ratio and its average ratio of $A_{b-5\%}$	39
Table 3.4. Crushed Area, ratio and its average ratio of $A_{b+5\%}$	39
Table 3.5. Crushed Area, ratio and its average ratio of $Faxial - 4\%$	39
Table 3.6. Crushed Area, ratio and its average ratio of $Faxial + 4\%$	40
Table 3.7.Crushed Area, ratio and its average ratio of $fc' - 4\%$	40
Table 3.8. Crushed Area, ratio and its average ratio of $fc' + 4\%$	40
Table 3.9. Crushed Area, ratio and its average ratio of $fy - 8.3\%$	40
Table 3.10. Crushed Area, ratio and its average ratio of $fy + 8.3\%$	40
Table 3.11. Moment matching result for TUA	41
Table 3.12. Height, width and area of TUB.....	41
Table 3.13. Crushed Area, ratio and its average ratio of initial condition of TUB.....	41
Table 3.14. Crushed Area, ratio and its average ratio of $A_{b-5\%}$	41
Table 3.15. Crushed Area, ratio and its average ratio of $A_{b+5\%}$	42
Table 3.16. Crushed Area, ratio and its average ratio of $Faxial - 4\%$	42

Table 3.17. Crushed Area, ratio and its average ratio of $Faxial + 4\%$	42
Table 3.18. Crushed Area, ratio and its average ratio of $fc' - 4\%$	42
Table 3.19. Crushed Area, ratio and its average ratio of $fc' + 4\%$	42
Table 3.20. Crushed Area, ratio and its average ratio of $fy - 8.3\%$	43
Table 3.21. Crushed Area, ratio and its average ratio of $fy + 8.3\%$	43
Table 3.22. Moment matching result for TUB	43
Table 3.23. Height, width and area of Wall1	44
Table 3.24. Crushed Area, ratio and its average ratio of initial condition of Wall1	44
Table 3.25. Crushed Area, ratio and its average ratio of $A_{b-5\%}$	44
Table 3.26. Crushed Area, ratio and its average ratio of $A_{b+5\%}$	44
Table 3.27. Crushed Area, ratio and its average ratio of $Faxial - 4\%$	44
Table 3.28. Crushed Area, ratio and its average ratio of $Faxial + 4\%$	45
Table 3.29. Crushed Area, ratio and its average ratio of $fc' - 4\%$	45
Table 3.30. Crushed Area, ratio and its average ratio of $fc' + 4\%$	45
Table 3.31. Crushed Area, ratio and its average ratio of $fy - 8.3\%$	45
Table 3.32. Crushed Area, ratio and its average ratio of $fy + 8.3\%$	45
Table 3.33. Moment matching result for Wall1	46
Table 3.34. Height, width and area of Wall2	46
Table 3.35. Crushed Area, ratio and its average ratio of initial condition of Wall2	46
Table 3.36. Crushed Area, ratio and its average ratio of $A_{b-5\%}$	46
Table 3.37. Crushed Area, ratio and its average ratio of $A_{b+5\%}$	47
Table 3.38. Crushed Area, ratio and its average ratio of $Faxial - 4\%$	47
Table 3.39. Crushed Area, ratio and its average ratio of $Faxial + 4\%$	47

Table 3.40. Crushed Area, ratio and its average ratio of $fc' - 4\%$	47
Table 3.41. Crushed Area, ratio and its average ratio of $fc' + 4\%$	47
Table 3.42. Crushed Area, ratio and its average ratio of $fy - 8.3\%$	48
Table 3.43. Crushed Area, ratio and its average ratio of $fy + 8.3\%$	48
Table 3.44. Moment matching result for Wall2.....	48
Table 3.45. Height, width and area of Wall3	49
Table 3.46. Crushed Area, ratio and its average ratio of initial condition of Wall3.....	49
Table 3.47. Crushed Area, ratio and its average ratio of $A_{b-5\%}$	49
Table 3.48. Crushed Area, ratio and its average ratio of $A_{b+5\%}$	49
Table 3.49. Crushed Area, ratio and its average ratio of $Faxial - 4\%$	49
Table 3.50. Crushed Area, ratio and its average ratio of $Faxial + 4\%$	50
Table 3.51. Crushed Area, ratio and its average ratio of $fc' - 4\%$	50
Table 3.52. Crushed Area, ratio and its average ratio of $fc' + 4\%$	50
Table 3.53. Crushed Area, ratio and its average ratio of $fy - 8.3\%$	50
Table 3.54. Crushed Area, ratio and its average ratio of $fy + 8.3\%$	50
Table 3.55. Moment matching result for Wall3.....	51
Table 3.56. The max and min forces of TUA in various conditions	52
Table 3.57. The max and min forces of TUB in various conditions.....	53
Table 3.58. The max and min forces of Wall 1 in various conditions	53
Table 3.59. The max and min forces of Wall 2 in various conditions	54
Table 3.60. The max and min forces of Wall 3 in various conditions.....	54
Table 3.61. MM result of TUA	55
Table 3.62. MM result of TUB	56

Table 3.63. MM result of Wall 1	57
Table 3.64. MM result of Wall 2	58
Table 3.65. MM result of Wall3	59
Table 4.1. The ranges of μ and σ of investigated references	60
Table 4.2. Exact results of GANMM.....	62
Table 4.3. Percentile locations for x_1 , x_2 and x_3	73
Table 4.4. The result of common remedy	74
Table 4.5. Relocation of x_1 , x_2 and x_3 ; P_k represents k -th percentile location	85
Table 4.6. Results of GANMM with x_1^- , x_2^- and x_3^-	86

NOMENCLATURE

AFR	Axial Force Ratio
COV	Coefficient of Variance
FOSM	First-Order Second-Moment
MM	Moment Matching
PBB	Progressive Bar Buckling
PDF	Probability Density Function
PMF	Probability Mass Function
PM-FEA	parallel multiscale finite element analysis

ACKNOWLEDGMENTS

I would like to dedicate this thesis to my major professor Inho Cho without whose support I would not have been able to complete this work. Professor Cho acknowledges me the importance of combining knowledge from different fields, civil engineering, computer science, and statistics in this thesis. In addition, professor Cho encourages me to attempt many developing languages, such as C++ and R, which helps me complete this thesis. Professor Cho's encouragement allows me to broaden my vision and extend my knowledge to obtain a wider view of aspect that not only on this thesis, but also on opening more opportunities for my future.

I would like to thank my committee member professor An Chen. Professor Chen has taught me the knowledge of reinforced concrete and that helps me to understand the behavior of reinforced concrete and prestressed concrete, which further helps me to develop this thesis completely.

Besides, I am very thankful to my committee member from computer science department, professor Jin Tian. Professor Tian taught me the mathematical and statistical theory, and application of machine learning, which consists of computer science, mathematics, and statistics inseparably. The tight combination of the three disciplines impacts me to accomplish this thesis successfully.

Last but not the least, I would like to thank my mom for supporting me mentally as well as financially. When I encountered troubles during studying and writing this work, she encouraged me to keep my faith and finish this thesis.

ABSTRACT

Despite the growing popularity of reinforced concrete (RC) core walls, robust uncertainty quantification of their global and local performances remains an intractable challenge. A combination of a random sampling technique in conjunction with a simplified structural analysis has been widely used, but substantial ambiguity remains in the simulation accuracy and the resultant uncertainties. As a fast and robust alternative, this study suggests a moment matching (MM) technique. MM can dramatically reduce required sample points to only a few, which enables a direct use of a high-precision parallel multiscale finite element analysis (PM-FEA) for uncertainty quantification. This study demonstrates how to apply the combination of MM and PM-FEA to quantify uncertainties behind complex RC core walls, notably in terms of global force-resisting capacity and microscopic progressive bar buckling of five U-shaped walls. Results suggest that the combination of MM and PM-FEA will serve as a promising method to improve our understanding of uncertainties behind complex RC structure.

CHAPTER 1. REVIEW OF LITERATURE

1.1 Introduction

In the past decades, to enhance the safety of living and use of structures, increasing the strength of structures economically has been a significant issue for both structural engineers and researchers. On the other hand, finding the uncertain vulnerable parameters that decrease strength of a structure is significantly essential as well. In [1], Heredia-Zavoni provides a model to obtain an analytical solution for the probability distribution of cumulative damage after an earthquake ground motion. To further analyze the relation between fragility curves and various uncertainties statistically, [2] exploited a regression-based method for structural design. A probabilistic methodology is presented by Aslani [3] to estimate the economic losses both at the component-level (local level) and at the system-level (global level). Nevertheless, except the known factors that would affect the strength of a structure, such as concrete strength and the number of rebars, there exists many uncertainties that would increase the vulnerability of a structure, i.e. the ground motion intensity, fundamental period of vibration, yield strength, and global drift [4]. In the aspect of statistics, a large number of structures should be considered, instead of considering merely a single structure, i.e. [5] evaluates vulnerability without assuming a single structure is representative at the class level. In Bal's research [6], in order to seek the possible parameters that increase the seismic vulnerability, geometrical, functional, and material properties of the building stock built by reinforced concrete around Istanbul have been investigated by employing statistical parameters (i.e. mean values and standard deviations), and the probability density function. A comparison of two surveys regarding seismic vulnerability in Haiti and Turkey has been done in [7]. Haiti appears to be more seismically vulnerable than Turkey. However,

the exposure data of earthquakes loss model available is very aggregated spatially. [8] presents a mean damage ratio to express the total damage over an urban area. If a large number of ground-motion simulations are employed, the mean damage ratio is insensitive compared to the spatial resolution of the exposure data. In Akkar's study, the uncertainties are expressed by using statistical distributions. In Avsar's study [9], he concludes that the uncertainties, the skew angles and number of bent columns, affect the vulnerabilities. Many empirical studies consider intensity as the parameter to describe the expected ground motion during an earthquake representing building vulnerability.

More recent studies tend to employ analytical methodologies to overcome the lack of post-earthquake data. To compare with the empirical methodology, [10] selects Dehradun, India and presents a comparison between two widely used methodologies, the empirical and analytical methodologies, for damage assessment. The author concludes that the analytical approach appears to be preferred in cases when reliably calibrated vulnerability models are available. Another analytical methodology based on multiple linear regression is employed for rapid vulnerability assessment of buildings in Turkey after a catastrophic earthquake [11]. [11] newly introduced the span index, priority index, existence of captive columns, and soft story index that play a dominant role in vulnerability. To test the accuracy of the derived regression function, a leave-one-out cross validation method is applied. The result shows that the correct classification rate is nearly 90 percent. Except the indexes, [12] adopts an extensive study on static and dynamic procedures to estimate the nonlinear response of buildings and concludes that N2[13]+DAP[14] is the best methodology considering both accuracy and efficiency in analytical computation.

With the contribution from all aforementioned authors, the research and articles inspire me to apply a statistical method, moment matching, to reduce the computational complexity of uncertainties estimation. The initial mathematical form of moment matching (MM) technique appears to be the work of Rosenblueth (1975) [15] who proposes n -point estimates for several variables. Let X and Y be real random variables and $Y = Y(X)$. He suggests that the accuracy of an expected value of X can be improved by taking the probability density to be concentrated at more than two points when its skewness coefficient, v_X , is negligible and the probability distribution is approximately Guassian. For an estimate of three points, the concentrations are P_+ at x_+ , P at \bar{X} , and P_- at $x_- = 2\bar{X} - x_+$, which is subjected to Eq. (1.1) to Eq. (1.3).

$$2P_+ + P = 1 \quad (1.1)$$

$$2P_+(x_+ - \bar{X})^2 = \sigma_X^2 \quad (1.2)$$

$$2P_+(x_+ - \bar{X})^4 = 3\sigma_X^2 \quad (1.3)$$

Solution of Eqs. 1-3 gives $P_+ = 1/6$, $P = 2/3$, $x_+ = \bar{X} + \sqrt{3}\sigma_X$ and $x_- = \bar{X} - \sqrt{3}\sigma_X$.

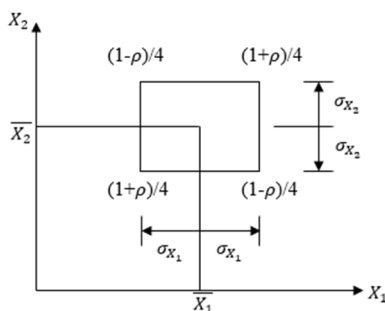


Figure 1.1. Ching *et al.* (2009) [16] applied MM technique to uncertainty propagation behind seismic loss estimation.

With two real-world buildings as examples, Ching [16] compares the moment matching technique with other methodologies, such as First-Order Second-Moment (FOSM) technique, and Monte Carlo simulation which requires more computational demand. The moment matching technique shows better accuracy than FOSM, and performs satisfactorily compared to Monte Carlo simulation.

The moment matching technique is to replace a continuous probability density function (PDF), i.e. PDF of \mathbf{X} , by a discrete probability mass function. The moment matching technique can be considered as a relation: $\mathbf{Y} = g(\mathbf{X})$, where the expected value $E(\mathbf{Y})$ is derived from some lower-order moments of \mathbf{X} . Thus, unlike the FOSM technique, the moment matching technique approximates PDF of \mathbf{X} by a sum of delta functions with corresponding moments, instead of simplifying $g(\mathbf{X})$.

The author then concludes two important equations (Eq. 1.4 and Eq. 1.5) as shown below:

$$E(\mathbf{X}^k) = \sum_{i=1}^q w_i \chi_i^k \quad (1.4)$$

$$\sum_{i=1}^q w_i = 1 \quad (1.5)$$

When the PDF of \mathbf{X} is a certain type, such as Gaussian, the solutions of locations and weights are associated with Gauss-quadrature integration points and weights. Thereby, this inspires me to apply the moment matching technique under Gaussian distribution to test the performance of combinations from one-dimension to four dimensions.

In essence, the MM technique transfers a continuous probability density function (PDF) of a random variable to an equivalent discrete probability mass function (PMF) consisting of weights and positions. The resulting position of PMF is called “index” hereafter. The indexes

and associated weights can be generated by matching the first few moments of \mathbf{x} PDFs, and if a PDF is a standard form, one can leverage off well-documented tables (e.g. Abramowitz and Stegun, 1972 [17]; Rosenblueth, 1975 [15]). By virtue of the PMF, complex integration can be replaced with simpler weighted summation. For instance, suppose $\mathbf{x} \in \mathbb{R}^n$ is n -dimensional random variable ($\mathbf{x} = \{x_1, \dots, x_n\}$) and $y \in \mathbb{R}$ is a final response through a relation function $g: \mathbb{R}^n \rightarrow \mathbb{R}$, $y = g(\mathbf{x})$. Then, MM can be used to efficiently estimate the expectation of y , $E[y]$ as

$$E[y] = \int \text{PDF}(\mathbf{x})g(\mathbf{x})d\mathbf{x} \approx \sum_{i=1}^q w_i g(\mathbf{x}_i) \quad (1.6)$$

where $i = 1, \dots, q$ denotes index (e.g., sample, specimen, etc.) and q denotes the number of total indexes. High-precision accuracy is noteworthy. With the first p^{th} moments of \mathbf{x} PDF, p^{th} -order accuracy of $E[y]$ can be achieved and $[p/2]_{th}$ -order accuracy of variance $\text{Var}[y]$ can be obtained. To briefly explain the accuracy preservation, consider a multivariate Taylor series expansion of $g(\mathbf{x})$ around $E[\mathbf{x}]$:

$$E[y] = g(E[\mathbf{x}]) + E \left[\sum_{j=1}^n \frac{\partial}{\partial x_j} (x_j - E[x_j])g(\mathbf{x}) \right] + \frac{1}{2!} E \left[\left(\sum_{j=1}^n \frac{\partial}{\partial x_j} (x_j - E[x_j]) \right)^2 g(\mathbf{x}) \right] + \dots \quad (1.7)$$

As shown above, if $E[x_i^2]$ is known, $E[y]$ can be exactly estimated up to the second-order term of the expansion (for further details see Cho and Porter (2016) [18] or Ching et al. (2009) [16]). Cho and Porter [4] address the methodology to depict a class with only a few buildings that contain the attributes which impact the seismic behavior of the class. Then a general numerical moment matching technique is proposed to those seismic attributes. On the other hand, the general numerical moment matching enables second-generation based earthquake engineering methods to capture seismic risk assessment of a building class. There are four suggested steps. First, select key seismic features, such as plan irregularity,

vertical irregularity or height. Second, in the class, quantify the joint distributions of those features. Third, apply moment matching technique, which is mainly adopted to replace a probability density function by a discrete equivalent probability mass function, to select sample points to match the first several moments (I.e., first five moments). Finally, select or design index buildings with the desired attributes, such as height or plan irregularity.

The authors let \mathbf{X} be the features of the asset in the class, such as heights, plan and vertical irregularity, and let \mathbf{Y} represent a vector of uncertain measures of performance of the asset class. Thereby, $\mathbf{Y} = g(\mathbf{X})$ describes the relationship. Then the expectation value of \mathbf{Y} , $E[\mathbf{Y}]$, becomes the target. To solve this, the authors expand the expectation value by Taylor series expansion and conclude that $E[\mathbf{Y}]$ of p th-order accuracy can be obtained with the first p th moment of probability density function of \mathbf{X} while the variance of \mathbf{Y} of $[p/2]$ th-order accuracy can be obtained as well. Eq. (1.8) gives the abovementioned theory. $E[\mathbf{Y}]$ represents the expectation of \mathbf{Y} .

$$E[\mathbf{Y}] = \int PDF(\mathbf{X})g(\mathbf{X})d\mathbf{X} \approx \sum_{n=1}^f w_n g(\chi_n) \quad (1.8)$$

where n represents i th delta function; f indicates the total number of delta functions.

In the paper, authors give an instance of assuming \mathbf{X} is a three-dimensional random variable, which means nine delta functions are required (i.e., three delta functions for the probability density functions in each dimension). The question then becomes solving 18 unknowns ($\chi = \{\chi_n, w_n\}$, where $n = 1 \sim 18$) with 18 conditions and can be solved by adopting multivariate Newton-Raphson iteration.

Cho and Porter [18] mention the merit of using the general moment matching technique is

that the technique requires considerably fewer points than similar works, such as μ & σ method. For instance, for 5 seismic features, the moment matching technique requires $2 \times 5 + 1 = 11$ points, while the μ & σ method needs $3^5 = 243$ points. It demonstrates that moment matching technique saves $243 - 11 = 232$ points.

The authors propose that the mean seismic vulnerability function can be denoted as $y(x)$ as Eq. (1.9). Higher moment can be described as Eq. (1.10).

$$y(x) = \sum_{i=0}^{2n+1} w_i \cdot y_i(x) \quad (1.9)$$

$$E[y^k(x)] = \sum_{i=0}^{2n+1} w_i \cdot y_i^k(x) \quad (1.10)$$

The general moment matching technique applied in the paper shows a strong advantage that it requires merely $2n + 1$ samples to match the first five moments of the target population, where n represents the number of interested attributes, while other methods require a number of samples exponentially with n .

It is instructive to touch upon differences of MM from other popular random sampling methods including First-Order Second-Moment (Baker and Cornell 2003 [19]). It is essential to calculate the total uncertainty in the result of estimation of the repair cost in future earthquakes. Monte Carlo simulation is a promising approach for estimation; however, it is computationally expensive. Therefore, the authors propose approximate first-order second-moment (FOSM) method to separate high-dimensional vectors of random of conditional variables into a single random conditional variable. A numerical integration is then applied, and thus the ground motion hazard, which is the dominant contributor to the total uncertainty, can be incorporated. To do the calculation and estimation, three assumptions are considered:

(1) Markovian dependence is assumed for all distributions in the framework; (2) All damage is considered to appear on an element level; (3) All relations in the framework are scalar functions. As a result, with the three assumptions, the expected annual loss, variance in annual loss, and the mean annual rate of exceeding a given loss can be computed. To calculate the total uncertainty, combining both aleatory and epistemic uncertainty is necessary. Notably, since the two uncertainties have no correlation, it is recommended to compute them separately, and then incorporate their effects to obtain the total uncertainty for simplicity.

Also, for the aleatory and epistemic variables, such as element repair cost, where the amount of data is literally rare, the authors suggest adopting the representation taking the form of generalization of the concept of “equi-correlation.”

Moreover, Latin Hypercubes (Borzi *et al.* 2008 [20]) is also a popular random sampling method. Recently, analytical methods are applied to large-scale assessment of the seismic vulnerability of RC buildings. However, the long computational time of running nonlinear dynamic analyses is a critical problem of the original procedures. To resolve the problem, Borzi [20] suggests applying a simplified pushover-based earthquake loss assessment (SP-BELA) and displacement-based earthquake loss assessment (DBELA) procedure to define the nonlinear behavior of a random population of buildings. Figure 1.2 is the prototype building used to apply SP-BELA, noting that only the flexural collapse mechanism is taken into consideration for beams.

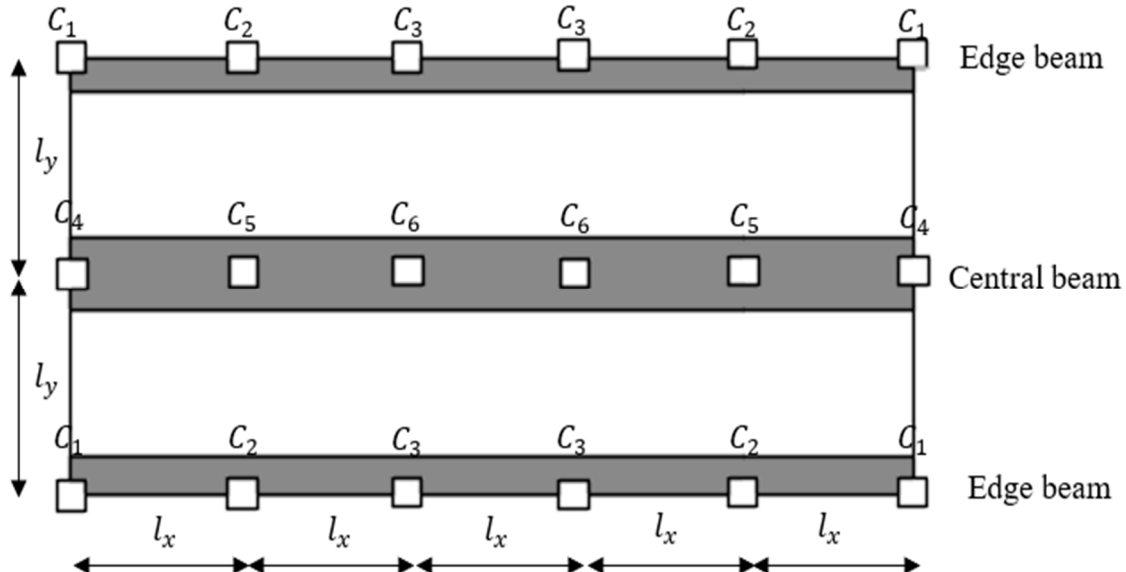


Figure 1.2. The prototype building used to apply SP-BELA.

Compare to the conventional methods, with adopting the simplified methodology, the analysis of hundreds of randomly generated frames can be estimated within a reasonable time span. Moreover, the comparison between the vulnerability curves predicted with SP-BELA and DBELA procedures has highlighted the merit of the SP-BELA procedure that accounts for the proportion of buildings which will have beam-sway, column-sway, or a combination of the abovementioned two sways.

Existing sample methods require sufficiently many sample points for a higher accuracy. But, in relation to the present goal, a final response of each sample requires separate structural analysis, and therefore a simplified structural analysis is often preferred in existing sampling methods. Contrarily, the present MM technique dramatically reduces the sample points, enabling a direct use of a high-precision structural analysis. Even a parallel multiscale finite element analysis (PM-FEA) platform can be used for uncertainty

quantification as being done herein, which may mark a notable advance compared to the existing methods that are often relying upon simplified or idealized structural analyses.

Objective of this study is to demonstrate 1) how MM can dramatically reduce the sample sizes; 2) how MM can be coupled with a high-precision PM-FEA platform, 3) how the combination of MM and PM-FEA can quantify uncertainty behind global and microscopic phenomena of complex RC structures. Importantly, the demonstrations using realistic five U-shaped walls under multi-directional loading paths shows that the proposed method can help elucidate the uncertainty behind microscopic progressive bar buckling (PBB). Herein, the term “intrinsic uncertainty” means the unavoidable uncertainty that may exist despite performing laboratory tests in an exceptionally excellent condition to realize the intended values of materials and design parameter.

The sample walls used in this thesis are based on Beyer’s paper [21]. Despite U-shaped or channel-shaped walls are commonly used as lateral strength providing members, such as accommodate elevators, the experimental results which chiefly focus on the influence of seismic loadings are scarce. Thus, the authors decide to do the experiments to investigate mainly the bending behaviors (damages or failures) after the U-shaped or channel-shaped walls encounter cyclic loading regime. In Beyer’s research, two U-shaped walls, Test Unit A (TUA) and Test Unit B (TUB), are designed with different thickness. The difference on wall thickness of TUA and TUB are shown in Table 1.1. Figure 1.3 shows the dimensions of TUA and TUB. The sizes of bars used are 6 mm and 12 mm diameter.

Table 1.1 Wall thickness of TUA and TUB

	TUA	TUB
Wall Thickness	0.15 (m)	0.10 (m)

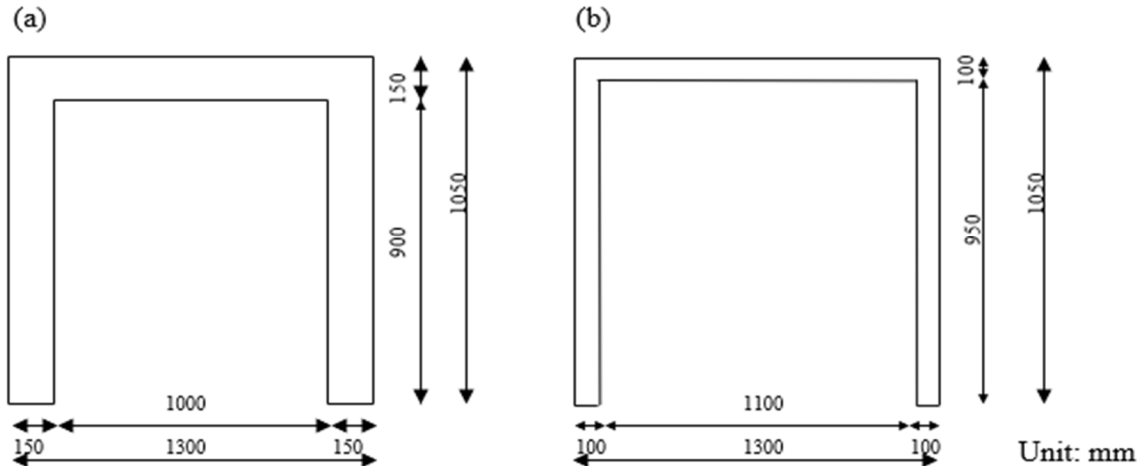


Figure 1.3. The dimension of (a) TUA; and (b) TUB (cited from Beyer 2008 [21]).

To control the twist of the wall head and the two translational degrees of freedom, three actuators are installed. One east-west (EW) actuator loads the web at where height equals to 3 meters while two north-south (NS) actuator loads the flanges at where height equals to 2.95 meters. To correctly document the behavior of the wall, in total, 120 hard-wired instruments are installed to measure required data, i.e. local and global displacements, strains of selected transverse reinforcing bars. Additionally, Demec measurements are taken at the lower part of the walls to record its deformation pattern. Figure 1.4 shows the entire view of the installations.

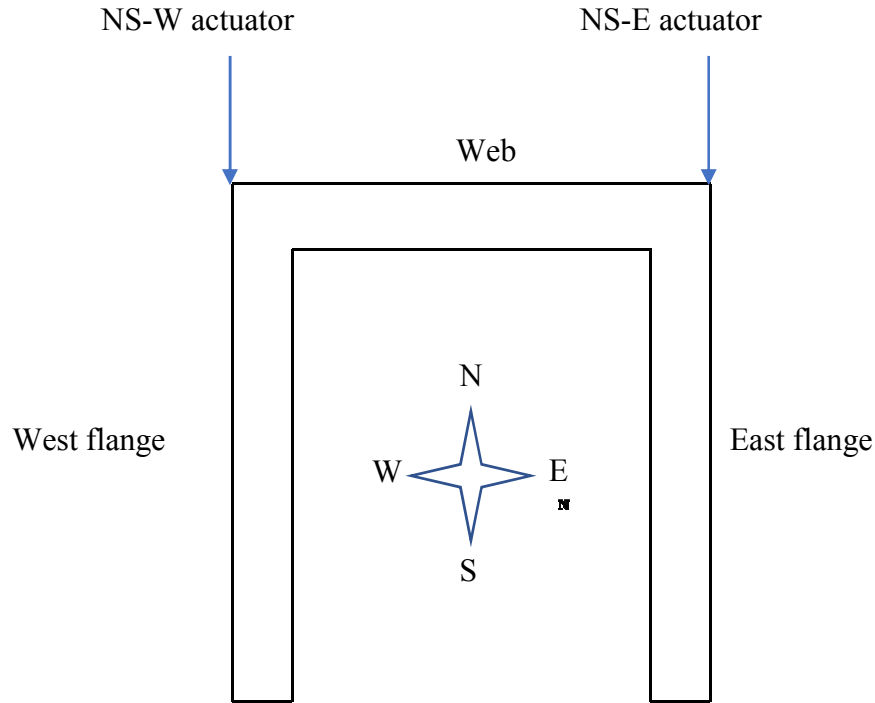


Figure 1.4. The locations of installation of the three actuators (cited from Beyer 2008 [21]).

After setting all the required installations for the walls, the loading patterns are designed according to Figure 1.5. The full cycle of EW direction is parallel to the web from O to A, A to B, and B to O. The NS cycle is from O to C, C to D, and D to O. The diagonal cycle is from O to E, E to F, and F to O. The final cycle “sweep” starts from O to A, A to G, G to D, D to C, C to H, H to B, and finally B to O.

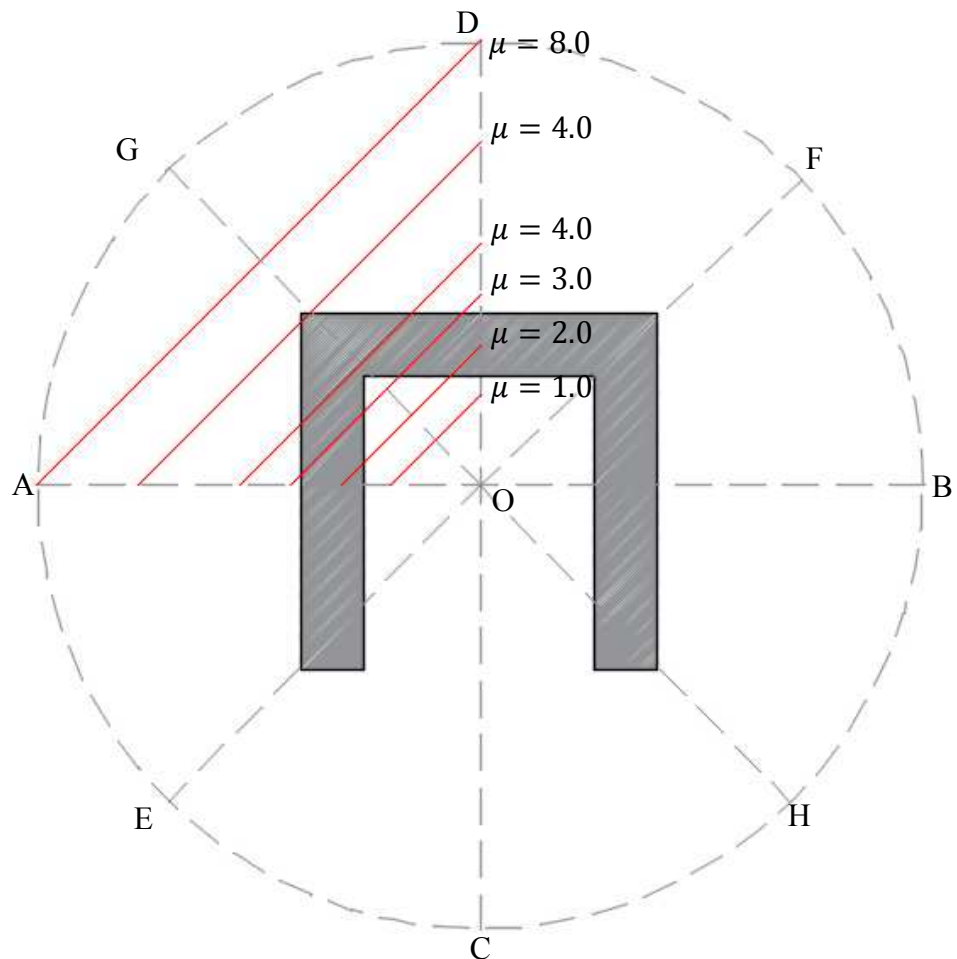


Figure 1.5. The loading patterns (cited from Beyer 2008 [21]). μ represents the levels of ductility.

The test results are presented in three ways: (1) failure mechanism; (2) force-displacement hystereses; (3) displacement components. TUA fails since the longitudinal reinforcing bars fracture. The first buckling of the longitudinal bars appears during the cycle in the diagonal direction. However, the failure of concrete does not appear for TUA. TUB failed due to the crushing of compression during sweep process at $\mu = 6.0$. Notably, the concrete spalling is observed at $\mu = 2.0$; however, the longitudinal reinforcing bars are invisible at the stage.

By comparison with typical failures of common walls, the failures of TUA and TUB are not

catastrophic since TUA and TUB are capable to transfer the lateral load to the well-confined boundary elements.

In the light of “Quasi-Static Cyclic Tests of Two U-Shaped Reinforced Concrete Walls” from Beyer [21], our research use the Test Unit A and Test Unit B to investigate the performance of moment matching technique with normal distribution assumed.

Also, in this thesis, the part which investigates progressive bar buckling is based on Cho’s paper (2013) [22]. The author proposed a tribology-inspired three-dimensional interlocking mechanism to show the strong correlation between random material property and localized damage at global system level. Also, Cho proposes an automated platform to capture progressive bar buckling. In his work, he assumes that the permanent plastic deformation happens at the soft matrix part merely (Figure 1.6) while the ideal sphere remains intact during resisting cyclic loadings.

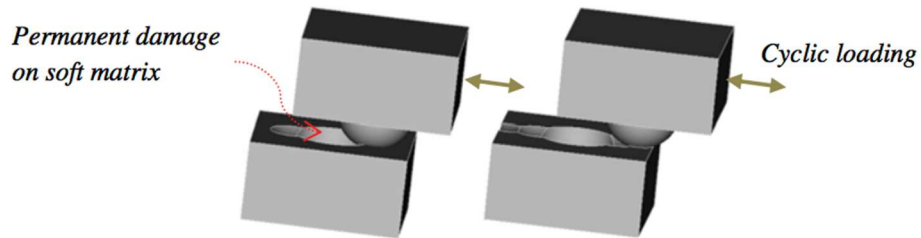


Figure 1.6. Permanent plastic deformation occurs at soft matrix part excited by cyclic loadings. (cited from Cho 2013 [22])

In this paper, a “smart” reinforcing steel model is also proposed. Since the topological transition can be triggered, meaning the bar buckling can be detected, only when all surrounding elements enter at least partially crushed state, the energy threshold is also proposed to evaluate the energy of surrounding elements to further detect bar buckling. Eq. (1.11) shows the abovementioned description.

$$\int_{S_m} \sigma dV \geq E_{th} \quad (1.11)$$

where S_m represents the dissipated energy of surrounding elements, and E_{th} is the energy threshold. Thereby, the bar buckling can then be detected in a sense of energy from surrounding elements.

The topic of uncertainty is also significantly important when applying moment matching. The work from Rossetto and Elnashai (2005) [23] investigates uncertainty. Rossetto and Elnashai [23] proposed a clear methodology for the derivation of vulnerability curves using analytical damage statistics. Through appropriate calibration in modeling, the methodology is applicable to various types of structures and seismo-tectonic environment. Furthermore, the post-earthquake damage can also be predicted.

The analytical curve generation methodology contains four steps. First, define the system by the selection and design of a single structure with material, configuration, and seismic resistance. Second, define ground motion input by selecting appropriate records of earthquakes for the analysis. Third, evaluate the model using adaptive pushover analysis (APO) technique within a capacity spectrum framework of assessment. APO follows the conventional pushover analysis mostly, but it updates the lateral applied load distribution to take varying stiffness, modal properties and consequent ground motion demand into account. Thereby, APO reduces the computational time by decreasing the required number of analysis from several thousands to a few hundred. Finally, process the analysis result statistically by defining response surface equations, which are defined for each hazard scenario, and relating inter-story drift response to the ground motion and the structural property. The vulnerability curves are plotted based on the building damage statistics generated from the response

surfaces by adopting re-sampling technique. For the validation, the authors applied the methodology to the case of low-rise, infilled RC frames with inadequate seismic provisions. The derived curves are proved with observational post-earthquake damage statistics. Notably, the U-shaped walls used in this thesis is very complicated, and thus we must consider the general confinement effect. In the light of work from Cho and Hall (2014) [24], the authors investigate non-local information-based confinement model. Confinement effect is significantly trivial for improving resilience against extreme compression loading, i.e., seismic excitations. The previous approaches are often based on structure-dependent parameters, and their formulations are defined on idealized points, small portion, or certain sections of the structures. Therefore, the previous approaches limit the cases of applications. In “General Confinement Model Based on Nonlocal Information,” a general confinement model, which can harness physical information inside real-scale systems, is proposed. With information index (Eq. 1.12), nonlocal information that provides the proximity to adjacent stiff materials and boundaries is adopted.

$$d_{ic} = \begin{cases} 1 - d, & \text{Linear Form} \\ 1/\exp(d), & \text{Exponential Form} \end{cases} \quad (1.12)$$

where d_{ic} is the information index having a continuous value from 0 to 1, representing the free boundary and fully fixed conditions, respectively.

In this paper, the authors applied this novel methodology on RC columns of solid and hollow sections, 4-story T-shaped shear wall, and tall rectangular walls with and without opening. According to the experimental results of these three cases, the higher accuracy is obtained with the help of nonlocal information. For instant, in the application of 4-story T-shaped wall, due to the large compression loading, the large error has been investigated in the negative displacement loading without the help of nonlocal information. Contrarily, with the

inclusion of nonlocal information-based confinement model, the large error has been eliminated.

The merits of this general confinement model are as below: it can apply on broad situations; the entire system can be used instead of a certain portion or part of the structure; reduction of calibration on a large number of parameters is made possible.

This thesis is structured as follows: chapter 2 introduces methods and procedures applied in this thesis. chapter 3 describes how to create a few sample points using MM that rigorously cover salient design variables' space. Next sections summarize microscopic mechanisms and preliminary validations of the adopted PM-FEA. Then, following sections present how the combination of MM and PM-FEA can describe uncertainties behind the global performance and progressive bar buckling phenomenon. Chapter 4 describes the experimental data and resultant 1D to 4D MM. The last section before conclusion touches upon some limits of the proposed methodology.

CHAPTER 2. METHODS AND PROCEDURES

2.1 Methods

2.1.1 Reduce Sample Points of Moment Matching

In view of the objective of this paper, we apply a three-point MM technique on each variable of interest which is assumed mutually independent following a normal distribution. For higher precision, one can increase the number of points of MM by expanding the following algebraic derivations. It should be noted that if variable's probabilistic distribution is sufficiently different from any standard distribution (which appears more realistic), then one is referred to the corresponding author's "numerical" moment matching technique (Cho and Porter 2016 [18]) since it has no reliance upon distribution assumption. Also, if the variables are mutually dependent, one may refer to the so-called "rotation of axes" (Ching *et al.* 2009 [16]) which are not required in the present study. According to the work of Rosenblueth (1975) [15], three index points' locations (denoted as x_i ; $i = 1, 2, 3$) and weights (w_i) of normally distributed variable are calculated by using symmetry conditions (i.e., $w_1 = w_3$; $|x_1 - E[x]| = |x_3 - E[x]|$; $x_2 = E[x]$) and the relationship of the plain central moment, i.e., $E[x^p] = \sigma^p(p - 1)!!$ if p is even and $E[x^p] = 0$ otherwise. Here, $E[x]$ is the expectation of x ; σ is the standard deviation; p is a positive integer; $k!!$ denotes the double factorial. As a resultant, we have the system of equations (i.e., $2w_1 + w_2 = 1$; $2w_1(x_1 - E[x])^2 = \sigma^2$; $2w_1(x_1 - E[x])^4 = 3\sigma^4$), from which we can obtain weights of three samples as

$$\begin{aligned} \text{3 Locations: } & \{x_1, x_2, x_3\} = \{E[x] - \sqrt{3}\sigma, E[x], E[x] + \sqrt{3}\sigma\} \\ \text{3 Weights: } & \{w_1, w_2, w_3\} = \{1/6, 4/6, 1/6\} \end{aligned} \quad (2.1)$$

Throughout the paper, these three sample points for the MM are used in various performances, such as seismic shear-force resisting capacity, and progressive bar buckling.

2.1.2 Study Variables for Moment Matching

Four variables are identified and investigated in this study: i.e., the compressive strength of concrete (f'_c), the yielding strength (f_y) and area (A_b) of longitudinal reinforcement, and the axial force ratio (AFR) defined by $F_{axial}/f'_c A_g$ with A_g being the gross cross section area of the wall. Since the “excellent control” of experiment is defined as the coefficient of variation ($\text{COV} \equiv \sigma/\mu$) of less than 10%, this study considers less than 5% perturbation of the intended values of the four variables (i.e., f'_c , f_y , A_b , $F_{axial}/f'_c A_g$). In particular, we increase and decrease f'_c and $F_{axial}/f'_c A_g$ (AFR) by 4% from their mean. For A_b , we increase and decrease primary bar’s area by 5% from its mean to slightly add more intrinsic uncertainty resulting from spatial misallocation of rebars. For f_y , we increase and decrease the value by 8.4%, roughly two times more uncertainty from other variables. This larger uncertainty for yield strength is in line with a comparable work of (Rossetto and Elnashai 2005 [15]), in which they documented $\text{COV}[f'_c] = 0.12$ and $\text{COV}[f_y] = 0.25$ for RC building’s population. It should be noted that one may have objections to these statistical assumptions of f'_c , f_y , and so on, since different statistics may exist in other structures population. Still, this study’s objective is to demonstrate the efficacy and reliability of the combination of MM and PM-FEA for applications to complex walls. Hence, the present study will be meaningful for future extensions to other populations with different statistical features.

In view of 3-point MM, each variable’s three index points are easily calculated by Eq. (1.3). Now, we can construct a normal distribution $N(\mu, \sigma^2)$ that satisfies the aforementioned variabilities of salient variables (i.e., $\pm 4\%$ for AFR and f'_c ; $\pm 5\%$ for A_b ; $\pm 8.4\%$ for f_y). For instance, the third index point x_3 of AFR is away from the mean by +4%, leading to $x_3 =$



$1.04E[AFR] = E[AFR] + \sqrt{3}\sigma_{AFR}$, and therefore $\sigma_{AFR} = 0.04E[AFR]/\sqrt{3}$. Table 2.1 [21][25] summarizes the means and standard deviations of four study variables, which will be used for the following MM technique.

Table 2.1. Mean and standard distribution of four study variables [21][25]

Name	$E[f_y]$ [MPa]	σ_{f_y} [MPa]	$E[A_b]$ [mm ²]	σ_{A_b} [mm ²]	$E[f'_c]$ [MPa]	$\sigma_{f'_c}$ [MPa]	$E[AFR]$	σ_{AFR} [%]
TUA*	488	23.667	113.1	3.264	77.90	1.799	2.00%	0.046%
TUB*	471	22.842	113.1	3.264	54.70	1.263	4.00%	0.092%
Wall 1\$	516	25.025	113.1	3.264	23.73	0.548	9.63%	0.222%
Wall 2\$	516	25.025	113.1	3.264	23.73	0.548	9.63%	0.222%
Wall 3\$	516	25.025	113.1	3.264	20.83	0.481	9.63%	0.222%

2.1.3 Microphysical Mechanisms and Validations of the Adopted PM-FEA Platform

To investigate the delicate impact of the intrinsic uncertainty of structural and material properties on U-shaped wall system behaviors, this study adopted a parallel multiscale finite element analysis platform, called VEEL (Virtual Earthquake Engineering Laboratory developed by Cho 2013 [22]). Running on parallel computers, VEEL can capture millimeter length scale's physical damage mechanisms through multiscale analysis paradigm. VEEL models entire reinforcement system as it is (including all horizontal stirrups and longitudinal bars) and three-dimensional concrete body. VEEL incorporates nonlinear shear of cracked concrete by using cement-aggregate interlocking mechanism defined on multi-directional micro crack surfaces (see Figure 2.1).

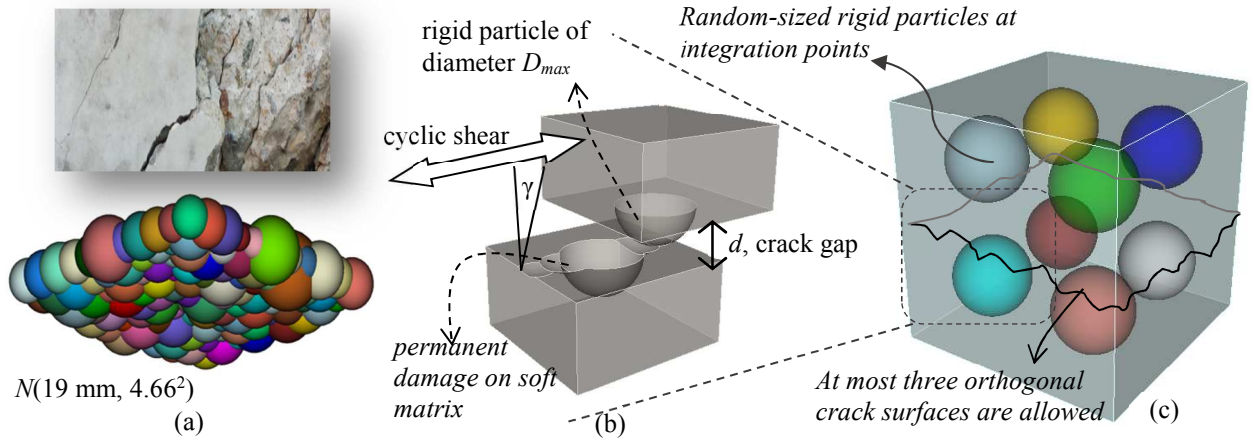


Figure 2.1. (a) Irregular asperity pattern (inset) along the aggregate boundaries within a damaged concrete (cited from Cho 2017 [26]). Bottom figure shows a random-sized particle distribution; (b) Shear mechanism; (c) Solid element containing rigid particles (cited from Cho and Porter 2014 [27]; Cho 2013 [22]).

Random-sized rigid particles are used for the nonlinear interlocking mechanism on a separate domain. Importantly, VEEL can capture progressive bar buckling phenomena. Admittedly, bar buckling is a complex process depending upon the surrounding concrete damages. Bars may buckle over one stirrup spacing or sometimes multiple stirrup spacing as illustrated in Figure 2.2.

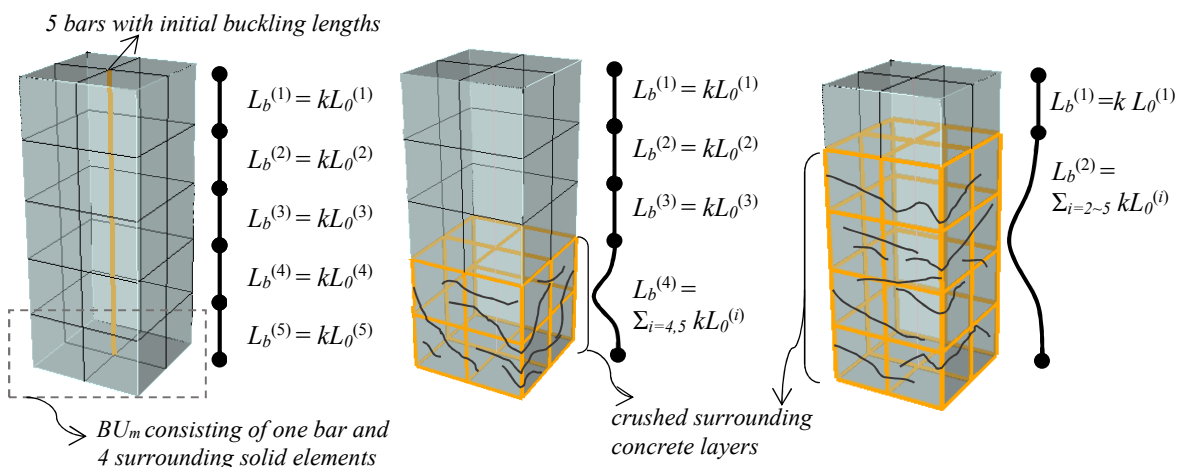


Figure 2.2. Schematic illustration of evolving buckling lengths of smart longitudinal bars: (a) intact state with 5 bar elements with initial buckling lengths of the effective length factor k (i.e. 0.5 for fixed-ends condition) times unstretched length L_0 ; (cited from Cho and Hall 2014 [24]).

VEEL automatically considers current damage of surrounding concrete and new boundary conditions of longitudinal bars, thereby capturing progressive buckling in any 3D RC structures (see details in Cho 2013). To consider general confinement effect of complex three-dimensional wall systems, nonlocal information-based confinement model (Cho and Hall 2014 [24]), which utilizes physical information of the proximity between concrete integration points and adjacent reinforcing bars (see Figure 2.3).

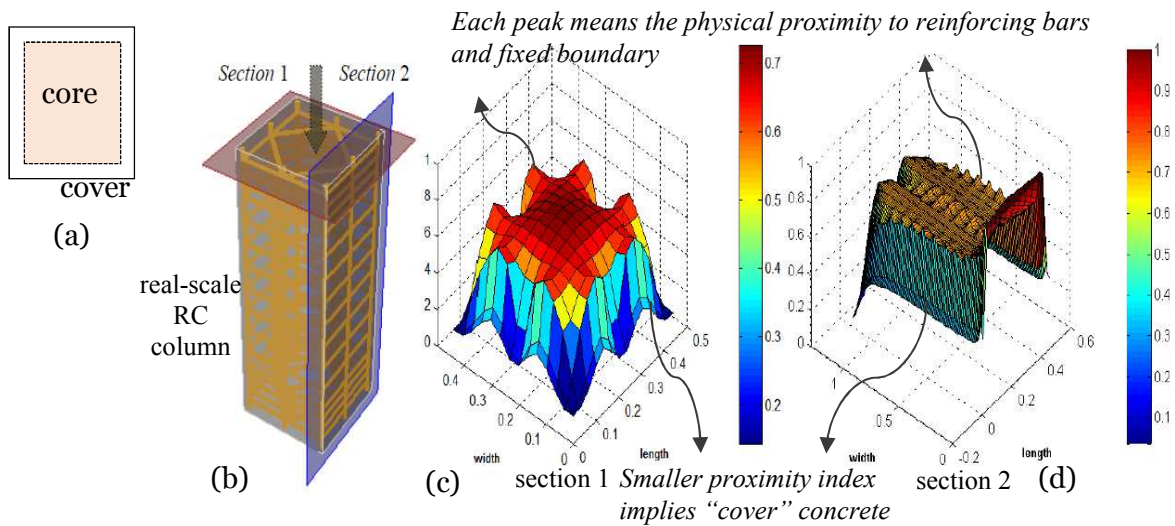


Figure 2.3. (a) Popular confinement model using a simplified distinction between core and cover parts; (b) real-scale RC column used for test; (c) proximity index plot on horizontal cross section and (d) on vertical cross section (cited from Cho and Hall 2014 [24]).

To demonstrate the high-precision fidelity of the adopted analysis tool VEEL, some simulation results of two U-shaped shear walls, TUA and TUB tested by Beyer *et al.* (2008) [21], are presented. Notably, the simulation results demonstrate accuracy not only in the global response prediction, but also in the localized damage phenomena reproduction such as progressive bar buckling in conjunction with localized compressive damages.

The finite element models of TUA and TUB used in this study are shown in Figure 2.4, and the only difference between TUA and TUB is thickness. TUA and TUB were loaded in the bi-directional horizontal loads, and the reproduced global responses are shown in Figure 2.5. The global responses of the square-root-of-sum-of-squares (SRSS) displacements show good agreement with the experimental results.

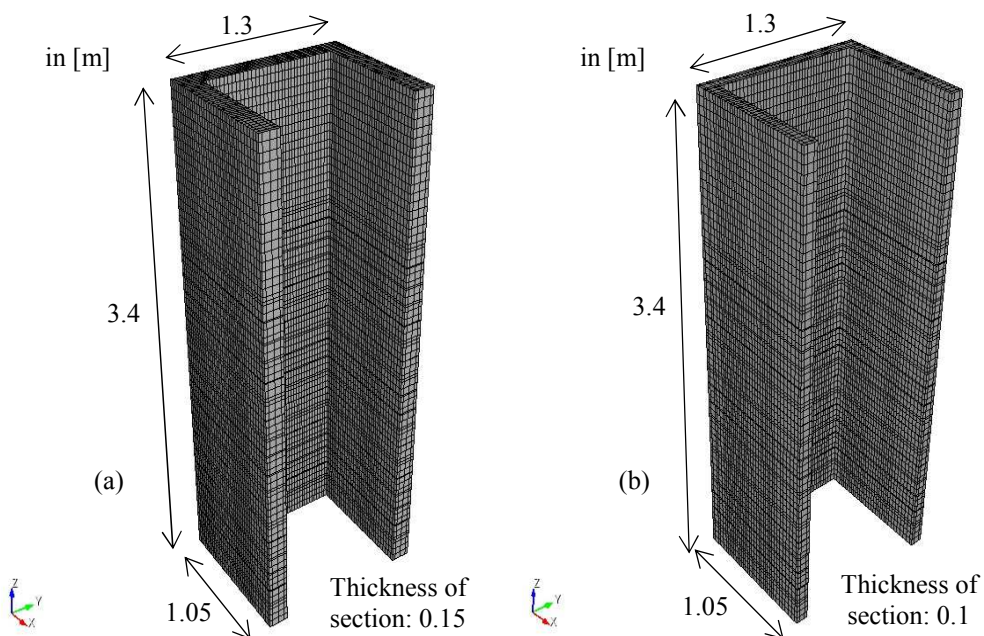


Figure 2.4. Finite element models of (a) TUA and (b) TUB shear walls.

In the later section, more comparisons will be conducted. In this study, we discuss about the shear-force resisting capacity and the progressive bar buckling. Moreover, the collapse capacity and vulnerability curve are discussed as well.

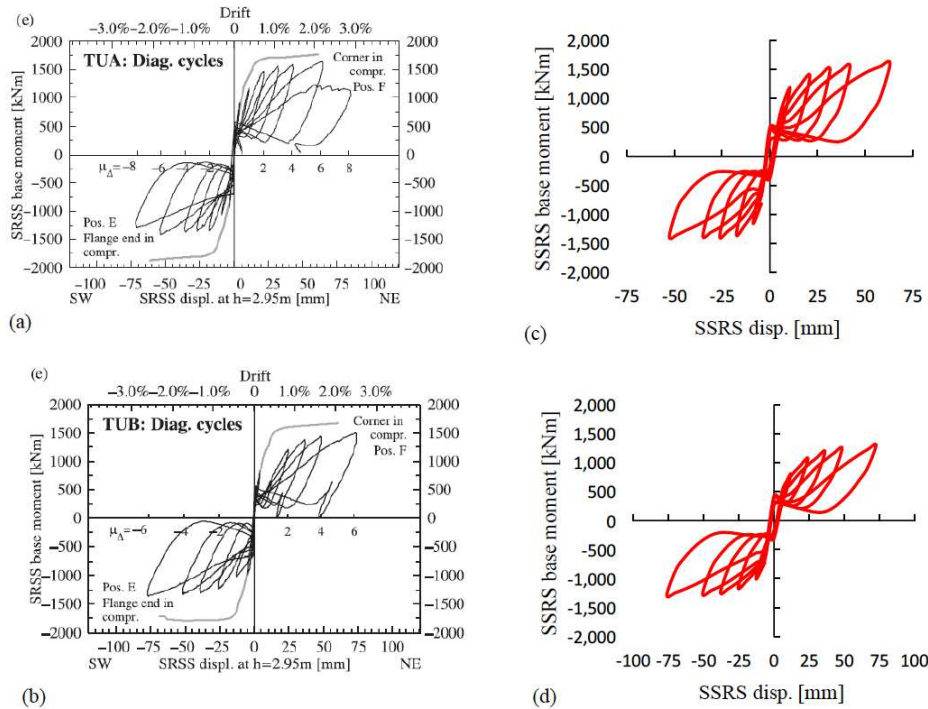


Figure 2.5. Displacement and moment responses in square-root-of-sum-of-squares from experiments of (a) TUA and (b) TUB shear walls (cited from Beyer et al. 2008 [21]); from PM-FEA simulations of (c) TUA and (d) TUB. The SRSS moment is expressed as $\sqrt{M_{WE}^2 + M_{SN}^2} \cdot (\pm 1)$, and the SRSS displacement is represented by $\sqrt{D_{WE}^2 + D_{SN}^2} \cdot (\pm 1)$, where the (± 1) is the sign representing the directions such as north and south.

In Figure 2.6 and 2.7, the green box represents the predicted zone of PBB. Compared to the photo of actual damage state (insets of Figure 6 and 7), VEEL appears to be able to capture the zone of PBB and spalling. It should be noted that another advanced computational tool may be chosen for the comparable study as long as it can capture both macro and micro damage behavior of U-shaped walls and also address bi-directional loading conditions.

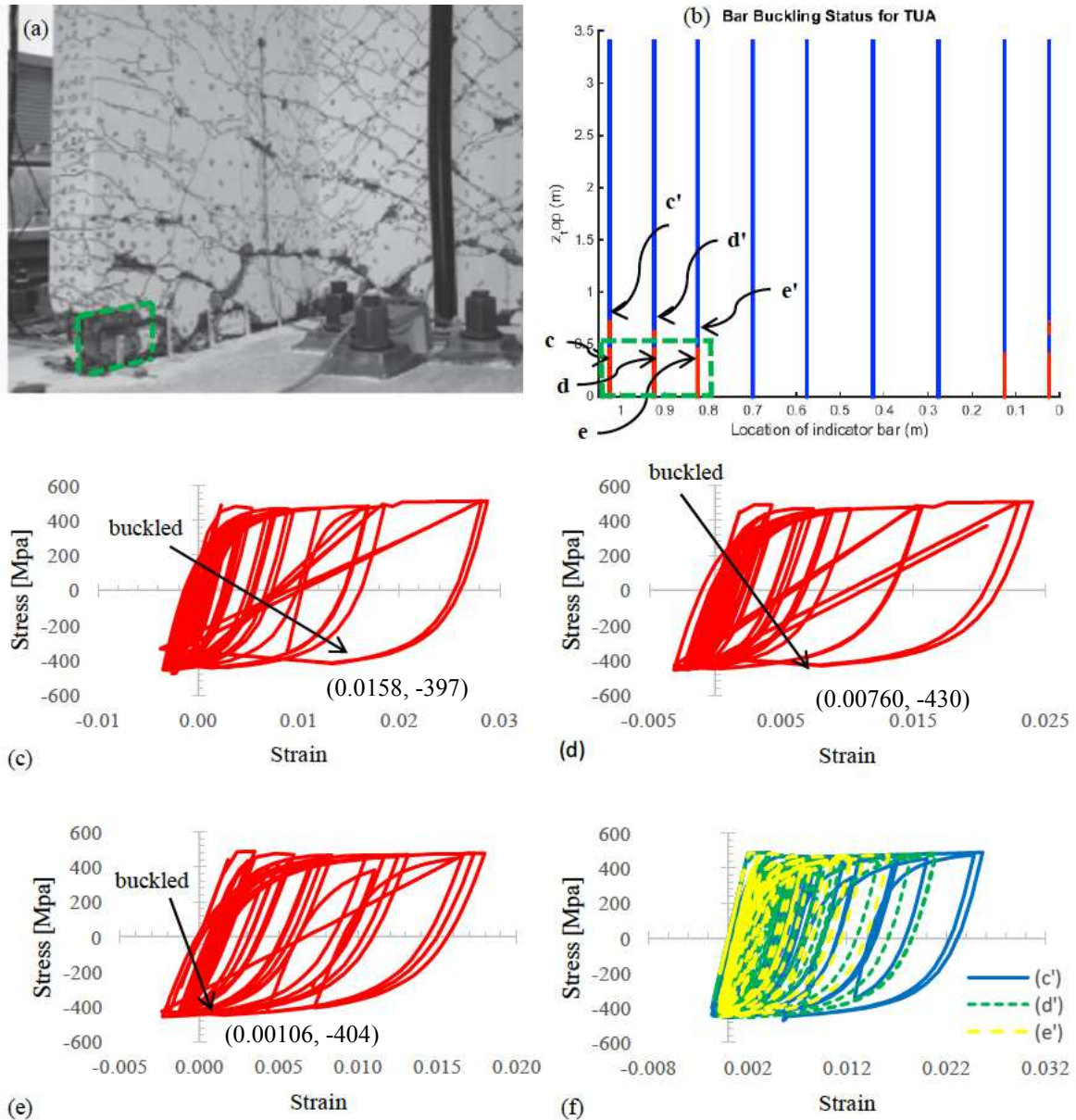


Figure 2.6. Predicted progressive bar buckling and concrete spalling zone of U-shaped wall system (TUA): (a) inset photo shows concrete damage state (Beyer et al., [21]); (b) progressive bar state at end of test where the blue color represents bar without buckling (outside the dashed box) show zones without buckling and the red colored bar (inside the dashed box) indicates zone with PBB; buckling of the longitudinal bar was observed for the first time during the cycle in the diagonal direction at $\mu = 6.0$ when at position V the D12 bar in the outer corner of the west flange buckled (Beyer et al., [21]); (c), (d), (e), and (f) show that steel strain-stress behaviors within PBB zone (i.e., zone within dashed box).

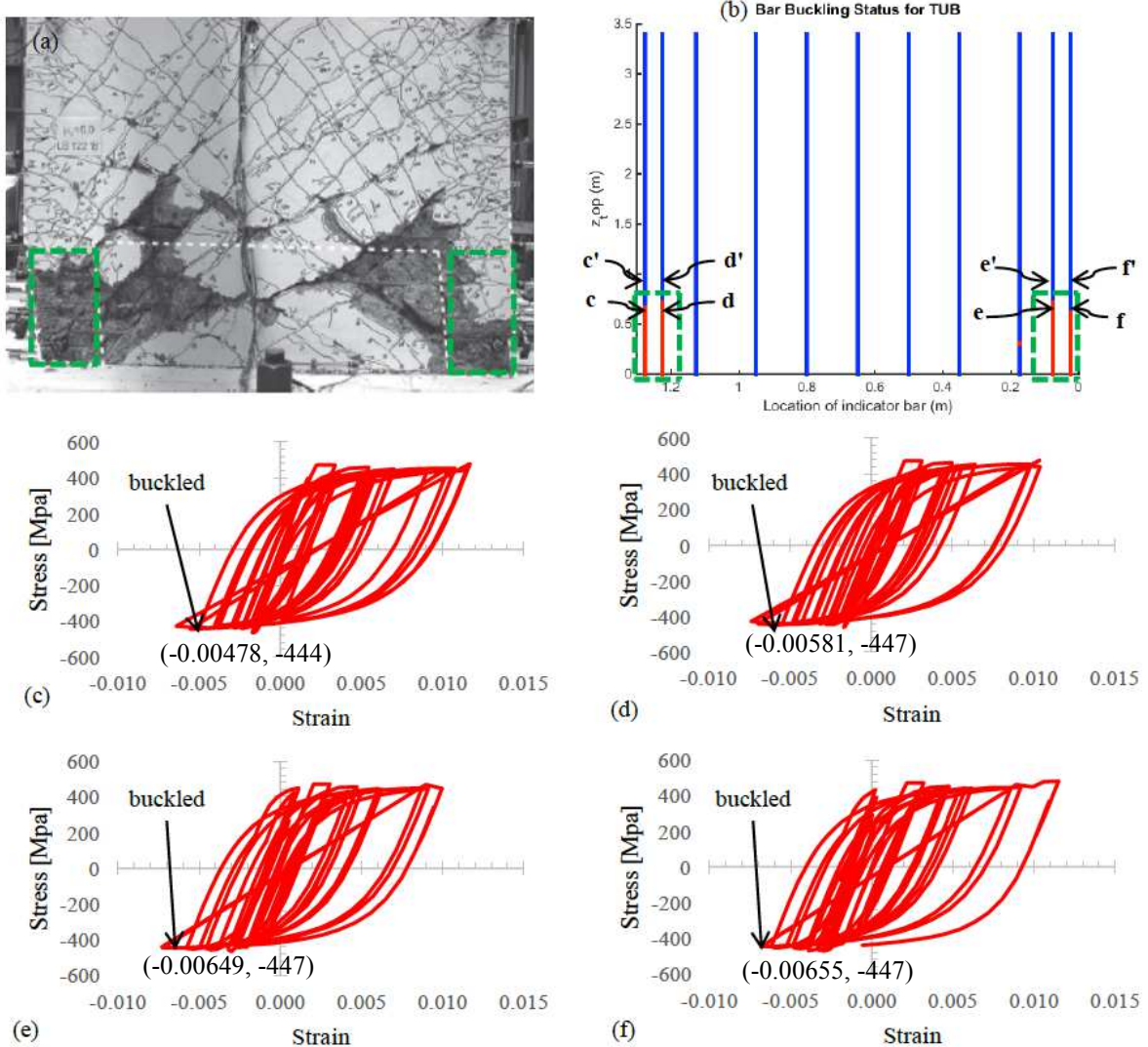


Figure 2.7. Predicted progressive bar buckling and concrete spalling zone of U-shaped wall system (TUB): (a) inset photo shows concrete damage state (Beyer et al., [21]); (b) progressive bar state at the end of experiment where the blue colored bar (outside the dashed box) show zones without buckling and the red colored bar (inside the dashed box) indicates zone with PBB; buckling was observed when at $\mu = 4.0$ during NS cycle (Beyer et al., [21]); (c), (d), (e), and (f) show that steel strain-stress behaviors within PBB zone (i.e., zone within dashed box).

2.2 Procedures

2.2.1 Simple Uncertainty Estimation Procedure of Moment Matching

The focus of this study is to demonstrate how to leverage MM coupled with PM-FEA to efficiently and rigorously investigate the uncertainties of complex RC structures in the presence of intrinsic variability of salient design variables. Particularly, intrinsic variability is assumed to arise from salient test variables, even under an excellent control. To quantitatively measure the impact, the present study summarizes coefficient of variation (COV) of maximum shear force-resisting capacity (denoted as $\text{COV}[F_{max}]$) where $\text{COV}[F_{max}] = |\sigma(F_{max})/\text{E}[F_{max}]|$. By virtue of the MM technique, to obtain final expectation of the force-resisting capacity with n variables, we simply need to calculate the weighted summation as

$$\text{E}[F_{max}] = \sum_{i=1}^{2n+1} w_i \text{E}[F_{max,i}] \quad (2.2)$$

$$\text{E}[F_{max}^2] = \sum_{i=1}^{2n+1} w_i \text{E}[F_{max,i}^2] \quad (2.3)$$

where $w_i = 1/6$ owing to the normal distribution assumption, $w_{2n+1} = 1 - \sum_{i=1}^{2n} w_i$, $F_{max,i}$ is the simulated maximum force at the i^{th} index point. Here, the $(2n + 1)^{\text{th}}$ index point represents the intersection points of the n variables. In a similar manner, the final standard deviation can be obtained by

$$\sigma(F_{max}) = \sqrt{\text{E}[F_{max}^2]^2 - (\text{E}[F_{max}])^2} \quad (2.4)$$

For brevity, we use μ_j as the mean of property j , where $j = 1, \dots, 4$. Subscript $j=1$ corresponds to f_c' , 2 to f_y , 3 to A_b , and 4 to F_{axial} . For the j^{th} variable, the three index points are denoted as μ_j^- , μ_j , μ_j^+ where μ_j^- means the index with the smallest value. Figure 2.8

shows the examples of three index points of each salient variable obtained from 1D MM, and Figure 2.9 shows nine index points of 4D MM that cover all four variables space.

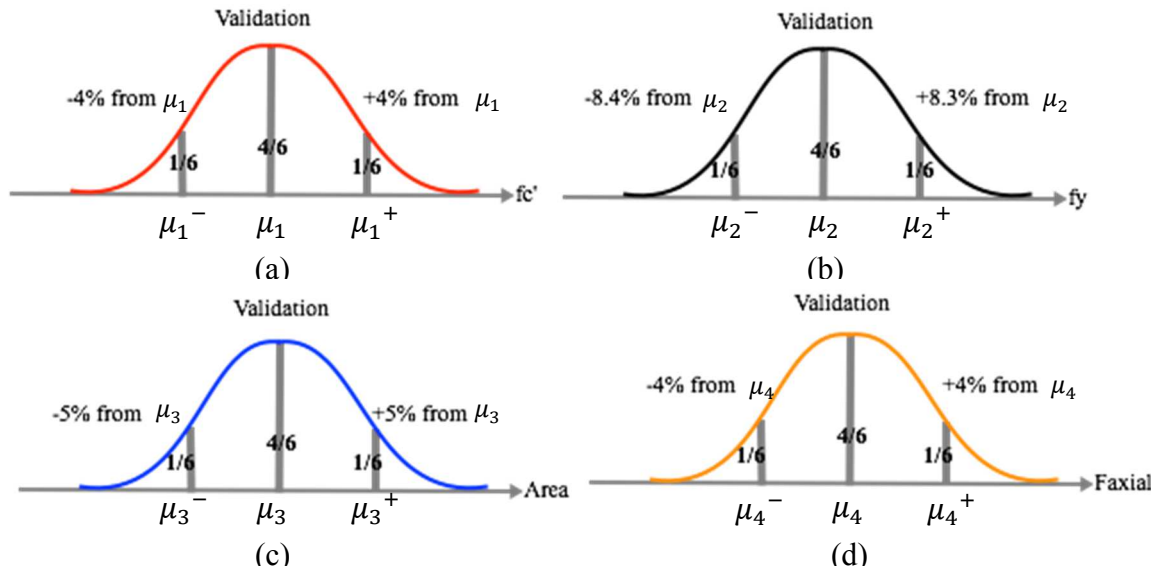


Figure 2.8. Three index points and weights for 1D MM of normal distribution of (a) f'_c ; (b) f_y ; (c) A_b ; (d) F_{axial} .

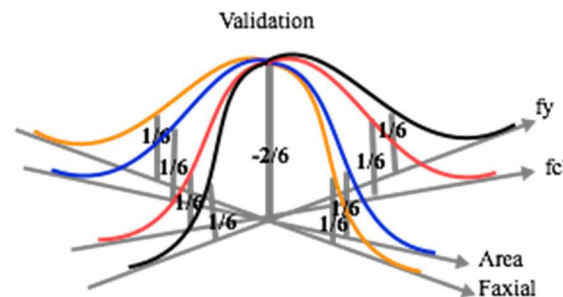


Figure 2.9. Nine index points and weights for 4D MM of normal distributions of f'_c , f_y , A_b , and F_{axial} .

Table 2.2 summarizes the three indexes and weights used for 1D MM, and Table 2.3 presents nine indices and weights for 4D MM. It is noteworthy that for the multi-dimensional moment matching, weights can be negative from the simple mathematical calculation, and also can be zero for a special case of the three-dimensional MM with the normal distribution assumption.

Table 2.2. For 1D MM [subscript $j = 1, 2, 3, 4$ corresponds to f_c' , f_y , A_b , and F_{axial} , respectively]

Index (i)	x_i	w_i
1	μ_j^+	1/6
2	μ_j^-	1/6
3	μ_j	4/6

Table 2.3. Nine indexes and weights for 4D MM [subscripts 1 through 4 correspond to f_c' , f_y , A_b , and F_{axial} , respectively]

Index (i)	x_{i1}	x_{i2}	x_{i3}	x_{i4}	w_i
1	μ_1^-	μ_2	μ_3	μ_4	1/6
2	μ_1^+	μ_2	μ_3	μ_4	1/6
3	μ_1	μ_2^-	μ_3	μ_4	1/6
4	μ_1	μ_2^+	μ_3	μ_4	1/6
5	μ_1	μ_2	μ_3^-	μ_4	1/6
6	μ_1	μ_2	μ_3^+	μ_4	1/6
7	μ_1	μ_2	μ_3	μ_4^-	1/6
8	μ_1	μ_2	μ_3	μ_4^+	1/6
9	μ_1	μ_2	μ_3	μ_4	-2/6

2.2.2 Predicted Uncertainty Behind Shear Force-Resisting Capacity

Figure 2.10 summarizes complex loading patterns of the five U-walls. Figure 2.11 summarizes expectations of maximum shear force-resisting capacities (denoted as $E[F_{max}]$) of the five U-walls obtained from the combination of PM-FEA and MM. Error bar is added to indicate $\pm\sigma$ in Figure 2.11. In each panel of Figure 2.11, four bars from the left correspond to

1D MM, the next 6 bars correspond to 2D MM, and the right-most bar corresponds to the prediction from 4D MM. 3D MM results are also shown between the 2D and 4D. Details are marked in the legend of Figure 2.11.

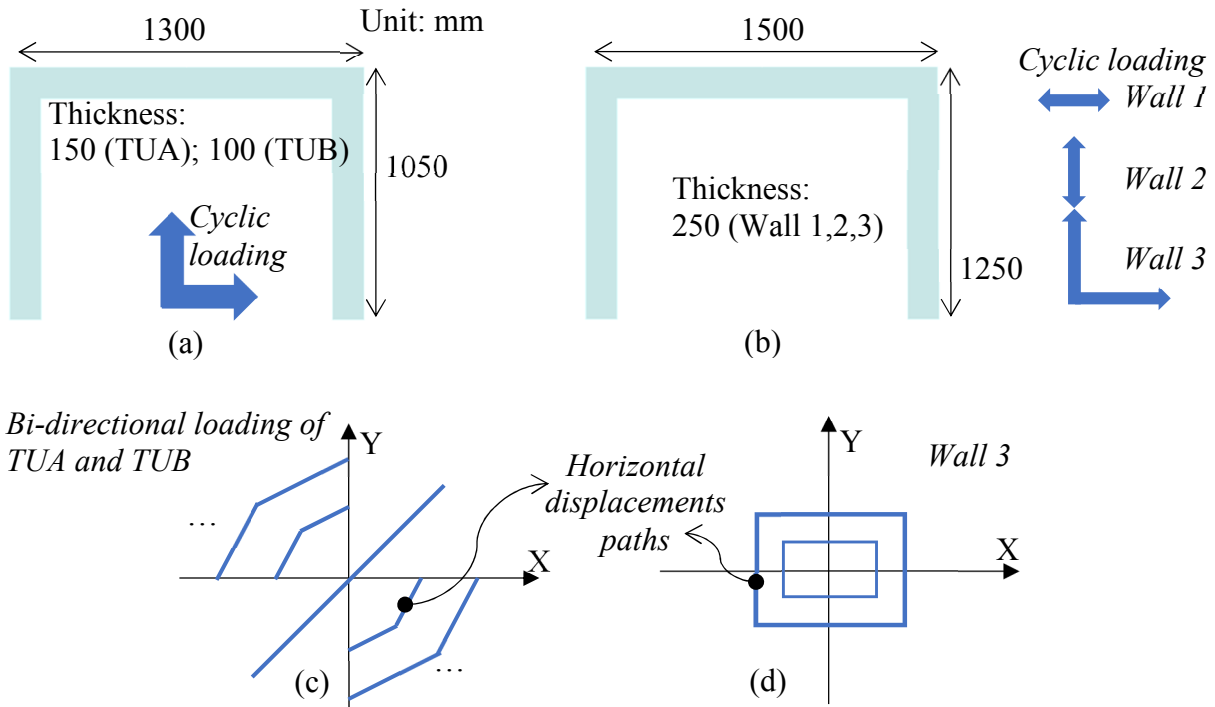


Figure 2.10. Wall dimensions and loading directions of (a) TUA and TUB; (b) Wall 1, 2, and 3; (c) “Butterfly” bi-directional loading patterns of TUA and TUB; (d) Complex bi-directional loading pattern of Wall 3.

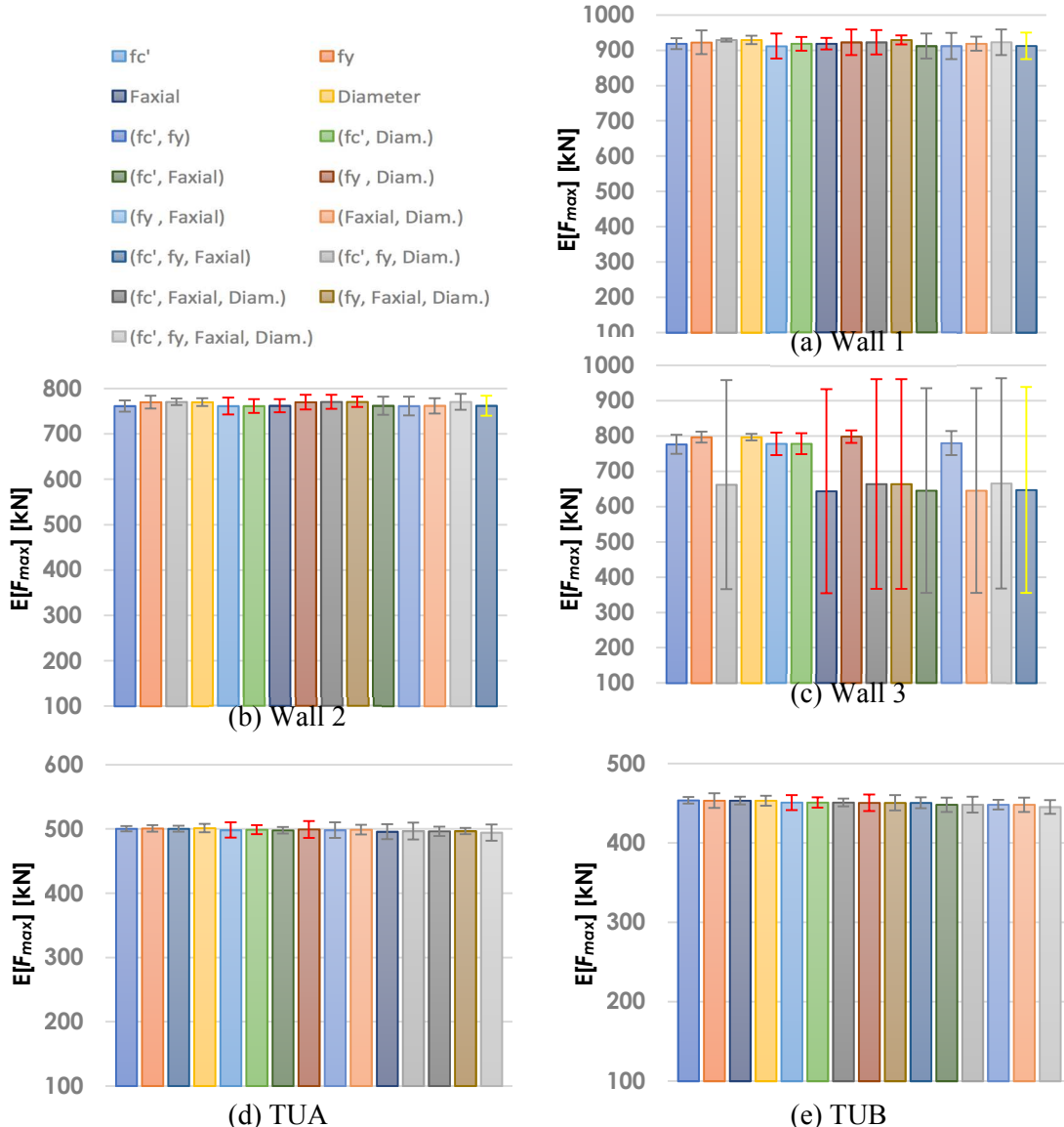


Figure 2.11. Expectations of the maximum shear force-resisting capacity (denoted as $E[F_{max}]$) predicted by PM-FEA coupled with multi-dimensional MM ranging from 1D through 4D: (a) Wall 1; (b) Wall 2; (c) Wall 3; (d) TUA; (e) TUB. Error bar indicates $\pm\sigma$. Irregular, large error bars of Wall 3 imply relatively larger uncertainty in F_{max} of Wall 3 than other four U-walls.

Figure. 2.12 presents COV of the maximum shear force-resisting capacity in negative and positive directions, denoted as $\text{COV}[F_{min}]$ and $\text{COV}[F_{max}]$, respectively. Since the five U-walls are all subject to reversely cyclic loads, F_{min} corresponds to the maximum capacity in the “negative” direction, opposite to that of F_{max} . All the values associated with bar plots are presented in Appendix.

The results of PM-FEA coupled with 1D~4D MM suggest that the variability of f_y appears to dominate the uncertainties of the four U-walls (i.e. Wall 1, Wall 2, TUA, and TUB), whereas the axial force ratio appears to dominate Wall 3. In particular, the four panels of Figure 2.12, except that of Wall 3, clearly shows the dominance of f_y on the uncertainty of F_{max} and F_{min} . As marked by arrow in Figure 2.12a, in each category of 1D through 4D MM the largest uncertainty arises from the case involving f_y . Contrarily, Wall 3 the maximum uncertainty appears to arise from the case involving f_c' (see Figure 2.12c).

It should be noted that deriving a general rule that can precisely prescribe dominant factors that govern uncertainty behind the shear-force resisting capability of RC core walls shall necessitate in-depth investigations with sufficiently many experimental data, which is beyond the scope of this study and will be addressed by a future research. Still, this study’s methodology is meaningful since the proposed combination of MM and a high-precision FEA will enable researchers to further assess various uncertainties behind global and microscopic performance of complex RC structures.



Figure 2.12. COV[F_{min}] and COV[F_{max}] obtained from 1D through 4D MM for (a) Wall 1; (b) Wall 2; (c) Wall 3; (d) TUA; (e) TUB. The variability of F_{axial} appears to govern the uncertainty of force-resisting capacity of Wall 3 while f_y appears to dominate the uncertainty of other four U-walls.

Of particular importance is the difference between TUA and Wall 3 since both TUA and Wall 3 are excited by complex bi-directional cyclic loading patterns. But, TUA and Wall 3 have a different thickness (i.e., 150 mm for TUA; 250 mm for Wall 3), and also have different axial force ratio: Wall 3 under 9.63% of axial force ratio while TUA under only 2%. Hence, when a high level of F_{axial} (here, greater than 9%) may be linked with the changing dominance of F_{axial} on the uncertainty behind force-resisting capacity.

2.2.3 Predicted Uncertainty Behind Progressive Bar Buckling

One of the central novelty of the present methodology lies in the new access to the uncertainty behind microscopic damage phenomena of complex RC structures. As an apt example, this section demonstrates how the combination of MM and PM-FEA can quantify uncertainty of PBB behavior. We performed the same procedure of the aforementioned 3-point MM to investigate the impacts of intrinsic variabilities of f_c' , f_y , A_b , and F_{axial} on the PBB phenomena. To easily quantify PBB, we introduced a new term, crushed area (CA) over which vertical reinforcing bars experience PBB behavior. In this study, each U-shaped wall consists of three panels, and we calculated each panel's CA. Each panel of a U-wall has a fraction of the crushed zone (denoted as R_{CAi} , where $i = 1, 2, 3$), i.e., $R_{CAi} = A_{crushed,i}/A_{total,i}$ where $A_{total,i}$ and $A_{crushed,i}$ denote the total area and crushed area of the i th panel, respectively. Then, we averaged CAs of three panels, suggesting the average crushed area per wall (denoted as R_{avg} ; $R_{avg} = \sum_{i=1}^3 R_{CAi}/3$). Figure 2.7b illustrates how to extract CA from PM-FEA results.

Figure 2.13 presents COV of CA obtained from the combination of PM-FEA and MM (ranging from 1D through 4D). Figure 2.14 summarizes the expectations of CA (denoted as $E[CA]$). Error bar is added to indicate $\pm\sigma$. Overall, large error bars are produced

by MM, which implies that there are substantial uncertainties in the prediction of PBB of the five U-walls. By comparing to Figure 2.11 and Figure 2.14, uncertainty behind PBB appears substantially larger than uncertainty behind global force-resisting capacity. This possibly implies that subtle variabilities of design variables may largely influence the microscopic damages such as PBB, which underpins the significance of uncertainty quantification. Due care should be paid to interpreting prediction results of PBB and other microscopic damage phenomena.

In the presence of such a large uncertainty of PBB, we can glean practically meaningful trends. The results in Figure 2.13 suggest that all salient variables appear to hold relatively similar influence on uncertainty of PBB of four walls, i.e. TUA, TUB, Wall 1 and Wall 2 (Figure 2.13a-d). On the contrary, f_c' appears to dominate CA (thus, PBB) of Wall 3 (as marked by a circle in Figure 2.13e). Of particular interest is the difference between TUA and TUB since both walls have the same multi-axial loading paths, i.e. bi-directional “butterfly” loading sequences (Figure 2.10c) in the presence of the identical axial force (780 kN). But, wall thickness is different (150 mm for TUA and 100 mm for TUB; see Figure 2.10). The difference in thickness between TUA and TUB appears to be linked to the dominance of f_c' on uncertainty of PBB. As in the prior section, the difference of Wall 3 from Wall 1 and Wall 2 appears to be tied to the different loading directions. As shown in Figure 2.10, Wall 2 is loaded parallel to the two flanges (normal to the web). Wall 1 is loaded parallel to the web (normal to two flanges), and Wall 3 is subject to bi-direction loading. Unlike Wall 1 and Wall 2, Wall 3’s complex bi-directional loading paths allow extensive damage distribution throughout the three panel of U-shaped Wall 3, and thus severe compressive damage along with PBB may develop.

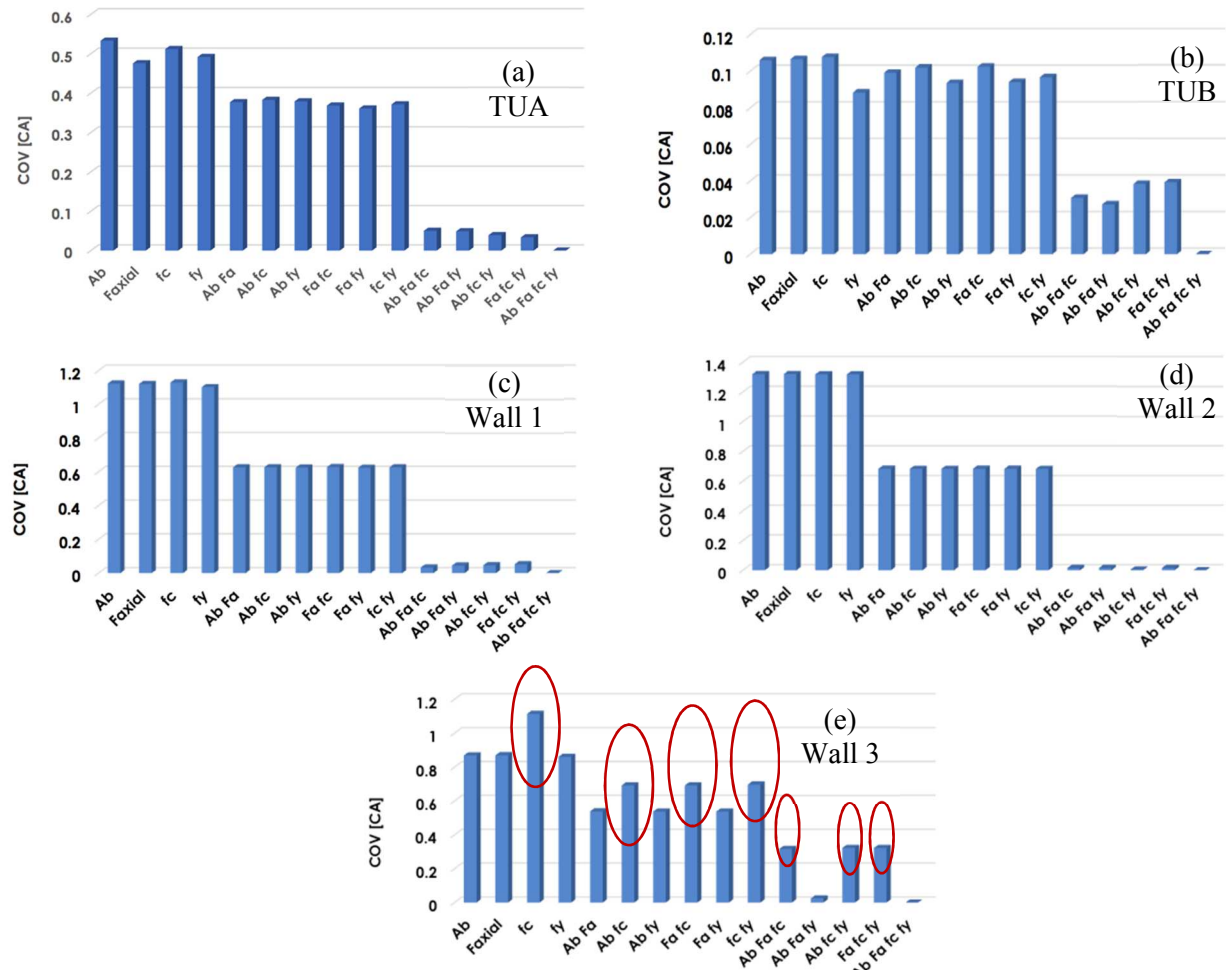


Figure 2.13. COV of the crushed area ratio (denoted as COV[CA]) obtained from PM-FEA coupled with multi-dimensional MM ranging from 1D through 4D: (a) TUA; (b) TUB; (c) Wall 1; (d) Wall 2; (e) Wall 3. Among four variables, F_{axial} appears to hold the least impact on the uncertainty of TUA whereas f_y has the smallest impact on that of TUB. Uncertainties of Wall 1 and Wall 2 are nearly evenly affected by the variabilities of all four variables. Contrarily, f_c' appears to dominate the uncertainty of Wall 3 (as marked by a circle).

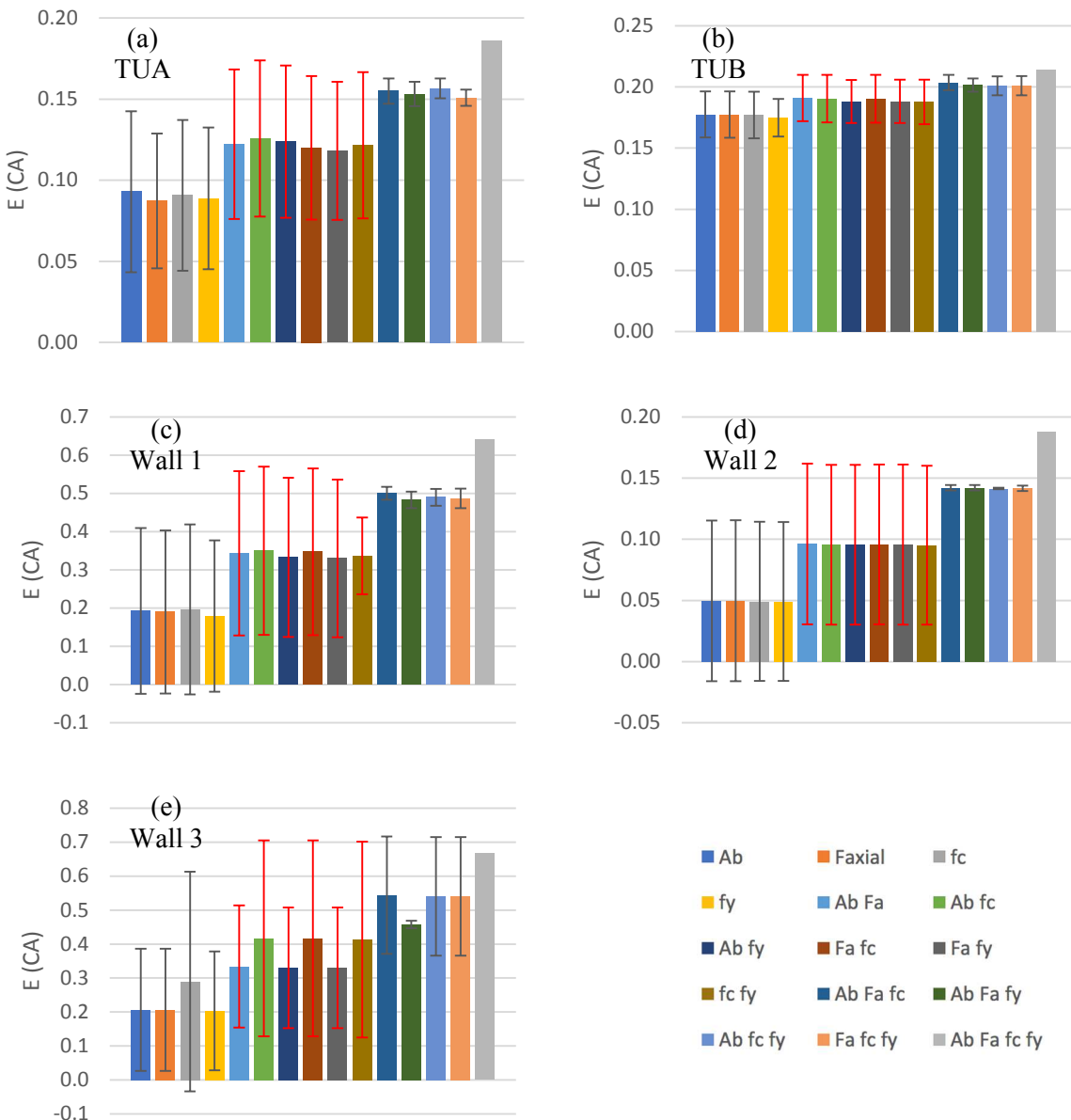


Figure 2.14. Expectations of the crushed area ratio (denoted as $E[CA]$) derived from PM-FEA coupled with multi-dimensional MM ranging from 1D through 4D: (a) TUA; (b) TUB; (c) Wall 1; (d) Wall 2; (e) Wall 3. Error bar indicates $\pm\sigma$. Large error bars are produced by MM which implies there are substantial uncertainties in the crushed areas and progressive bar buckling of five U-walls.

CHAPTER 3. EXPERIMENTAL DATA AND RESULTS

In this chapter, all the experimental data will be represented. The process of calculation will be demonstrated as well.

3.1 Results of progressive bar buckling

In chapter 2.2.3, we introduced the method we applied to predict uncertainty behind progressive bar buckling. First, we estimate crushed area (CA) for a panel. Second, we calculate the crushed ratio by using the CA divided by the total area (TA), which is $CA/TA = \text{crushed ratio}$. For example, TA of panel yz of TUA is $3.4 \times 1.3 = 4.42$, and its $CA = 0.225$. Therefore, we can obtain the crushed ratio by $0.225/4.42 = 0.051$ (Figure 3.1, Table 3.1 and Table 3.2). The results of TUA, TUB, Wall 1, Wall 2 and Wall 3 are shown as below (Table 3.2 to Table 3.55).

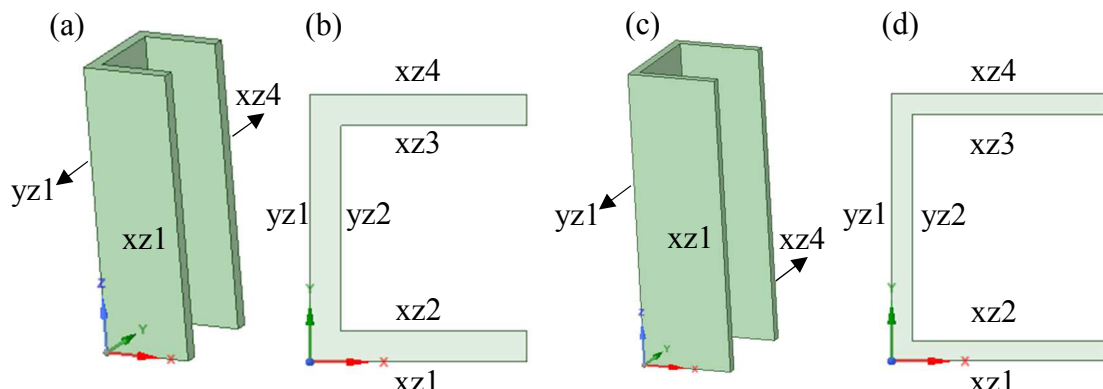


Figure 3.1. (a)3D model of TUA; (b)2D model of TUA; (c)3D model of TUB; (d)2D model of TUB.

Table 3.1. Height, width and area of TUA

Direction	Height (m)	Width (m)	Area (Total)
yz	3.4	1.3	4.42
xz	3.4	1.05	3.57

Table 3.2. Crushed Area, ratio and its average ratio of initial condition of TUA

Direction	CA	ratio	Average ratio
yz1	0.225	0.051	0.058
xz1	0.25875	0.072	
xz4	0.18	0.050	

Table 3.3. Crushed Area, ratio and its average ratio of $A_{b-5\%}$

Direction	CA	ratio	Average ratio
yz1	0.7725	0.175	0.166
xz1	0.535	0.150	
xz4	0.62375	0.175	

Table 3.4. Crushed Area, ratio and its average ratio of $A_{b+5\%}$

Direction	CA	ratio	Average ratio
yz1	0.7675	0.174	0.159
xz1	0.505	0.141	
xz4	0.5825	0.163	

Table 3.5. Crushed Area, ratio and its average ratio of $F_{axial-4\%}$

Direction	CA	ratio	Average ratio
yz1	0.7225	0.163	0.145
xz1	0.4725	0.132	
xz4	0.495	0.139	

Table 3.6. Crushed Area, ratio and its average ratio of $F_{axial+4\%}$

Direction	CA	ratio	Average ratio
yz1	0.6325	0.143	0.147
xz1	0.53125	0.149	
xz4	0.53375	0.150	

Table 3.7. Crushed Area, ratio and its average ratio of $f_c'_{-4\%}$

Direction	CA	ratio	Average ratio
yz1	0.82	0.186	0.161
xz1	0.5275	0.148	
xz4	0.53375	0.150	

Table 3.8. Crushed Area, ratio and its average ratio of $f_c'_{+4\%}$

Direction	CA	ratio	Average ratio
yz1	0.7525	0.170	0.152
xz1	0.5075	0.142	
xz4	0.5075	0.142	

Table 3.9. Crushed Area, ratio and its average ratio of $f_y_{-8.3\%}$

Direction	CA	ratio	Average ratio
yz1	0.715	0.162	0.150
xz1	0.475	0.133	
xz4	0.5525	0.155	

Table 3.10. Crushed Area, ratio and its average ratio of $f_y_{+8.3\%}$

Direction	CA	ratio	Average ratio
yz1	0.7375	0.167	0.151
xz1	0.5075	0.142	
xz4	0.51625	0.145	

Table 3.11. Moment matching result for TUA

MM	E(CA)	E(CA^2)	$\sigma(CA)$	COV CA
Ab	0.093	0.011	0.050	0.533
Faxial	0.087	0.009	0.042	0.476
fc	0.091	0.010	0.046	0.512
fy	0.089	0.010	0.044	0.492
Ab Fa	0.122	0.017	0.046	0.377
Ab fc	0.126	0.018	0.048	0.383
Ab fy	0.124	0.018	0.047	0.379
Fa fc	0.120	0.016	0.044	0.368
Fa fy	0.118	0.016	0.043	0.361
fc fy	0.122	0.017	0.045	0.371
Ab Fa fc	0.155	0.024	0.008	0.050
Ab Fa fy	0.153	0.024	0.007	0.049
Ab fc fy	0.157	0.025	0.006	0.039
Fa fc fy	0.151	0.023	0.005	0.033
Ab Fa fc fy	0.186	0.031	#NUM!	#NUM!

Table 3.12. Height, width and area of TUB

Direction	Height (m)	Width (m)	Area (Total)
yz	3.4	1.3	4.42
xz	3.4	1.05	3.57

Table 3.13. Crushed Area, ratio and its average ratio of initial condition of TUB

Direction	CA	ratio	Average ratio
yz1	1.1585	0.262	0.164
xz1	0.8225	0.230	
xz4	0	0.000	

Table 3.14. Crushed Area, ratio and its average ratio of $A_{b-5\%}$

Direction	CA	ratio	Average ratio
yz1	0.79675	0.180	0.205
xz1	0.7825	0.219	
xz4	0.77249	0.216	

Table 3.15. Crushed Area, ratio and its average ratio of $A_{b+5\%}$

Direction	CA	ratio	Average ratio
yz1	0.82075	0.186	0.203
xz1	0.79	0.221	
xz4	0.72	0.202	

Table 3.16. Crushed Area, ratio and its average ratio of $F_{axial-4\%}$

Direction	CA	ratio	Average ratio
yz1	0.766	0.173	0.201
xz1	0.7825	0.219	
xz4	0.751249	0.210	

Table 3.17. Crushed Area, ratio and its average ratio of $F_{axial+4\%}$

Direction	CA	ratio	Average ratio
yz1	0.7635	0.173	0.207
xz1	0.845	0.237	
xz4	0.75875	0.213	

Table 3.18. Crushed Area, ratio and its average ratio of $f_c'_{-4\%}$

Direction	CA	ratio	Average ratio
yz1	0.8465	0.192	0.213
xz1	0.83	0.232	
xz4	0.766249	0.215	

Table 3.19. Crushed Area, ratio and its average ratio of $f_c'_{+4\%}$

Direction	CA	ratio	Average ratio
yz1	0.742	0.168	0.192
xz1	0.76	0.213	
xz4	0.701249	0.196	

Table 3.20. Crushed Area, ratio and its average ratio of $f_{y-8.3\%}$

Direction	CA	ratio	Average ratio
yz1	0.78675	0.178	0.202
xz1	0.78875	0.221	
xz4	0.740625	0.207	

Table 3.21. Crushed Area, ratio and its average ratio of $f_{y+8.3\%}$

Direction	CA	ratio	Average ratio
yz1	0.78425	0.177	0.190
xz1	0.73625	0.206	
xz4	0.66625	0.187	

Table 3.22. Moment matching result for TUB

MM	E(CA)	E(CA^2)	$\sigma(CA)$	COV CA
Ab	0.177	0.032	0.019	0.106
Faxial	0.177	0.032	0.019	0.107
fc	0.177	0.032	0.019	0.108
fy	0.175	0.031	0.015	0.088
Ab Fa	0.191	0.037	0.019	0.099
Ab fc	0.190	0.037	0.019	0.102
Ab fy	0.188	0.036	0.018	0.094
Fa fc	0.190	0.037	0.020	0.103
Fa fy	0.188	0.036	0.018	0.094
fc fy	0.188	0.036	0.018	0.097
Ab Fa fc	0.204	0.042	0.006	0.031
Ab Fa fy	0.201	0.041	0.005	0.027
Ab fc fy	0.201	0.040	0.008	0.038
Fa fc fy	0.201	0.040	0.008	0.039
Ab Fa fc fy	0.214	0.045	#NUM!	#NUM!

Table 3.23. Height, width and area of Wall1

Direction	Height (m)	Width (m)	Area (Total)
yz	3.2	1.5	6.3
xz	3.2	1.25	5.25

Table 3.24. Crushed Area, ratio and its average ratio of initial condition of Wall1

Direction	CA	ratio	Average ratio
yz1	0.25	0.040	0.040
xz1	0.19175	0.037	
xz4	0.22375	0.043	

Table 3.25. Crushed Area, ratio and its average ratio of $A_{b-5\%}$

Direction	CA	ratio	Average ratio
yz1	3.31	0.525	0.503
xz1	2.28875	0.436	
xz4	2.8725	0.547	

Table 3.26. Crushed Area, ratio and its average ratio of $A_{b+5\%}$

Direction	CA	ratio	Average ratio
yz1	3.395	0.539	0.496
xz1	2.2975	0.438	
xz4	2.6849	0.511	

Table 3.27. Crushed Area, ratio and its average ratio of $F_{axial-4\%}$

Direction	CA	ratio	Average ratio
yz1	3.1	0.492	0.468
xz1	2.019375	0.385	
xz4	2.76375	0.526	

Table 3.28. Crushed Area, ratio and its average ratio of $F_{axial+4\%}$

Direction	CA	ratio	Average ratio
yz1	3.34375	0.531	0.513
xz1	2.283125	0.435	
xz4	3.01125	0.574	

Table 3.29. Crushed Area, ratio and its average ratio of $f_c'_{-4\%}$

Direction	CA	ratio	Average ratio
yz1	3.1875	0.506	0.522
xz1	2.49125	0.475	
xz4	3.06625	0.584	

Table 3.30. Crushed Area, ratio and its average ratio of $f_c'_{+4\%}$

Direction	CA	ratio	Average ratio
yz1	3.18	0.505	0.500
xz1	2.3825	0.454	
xz4	2.84375	0.542	

Table 3.31. Crushed Area, ratio and its average ratio of $f_y_{-8.3\%}$

Direction	CA	ratio	Average ratio
yz1	3.13	0.497	0.464
xz1	2.11375	0.403	
xz4	2.59	0.493	

Table 3.32. Crushed Area, ratio and its average ratio of $f_y_{+8.3\%}$

Direction	CA	ratio	Average ratio
yz1	3.0725	0.488	0.454
xz1	2.1825	0.416	
xz4	2.4125	0.460	

Table 3.33. Moment matching result for Wall1

MM	E(CA)	E(CA^2)	$\sigma(CA)$	COV CA
Ab	0.193	0.084	0.217	1.124
Faxial	0.190	0.081	0.213	1.121
fc	0.197	0.088	0.222	1.130
fy	0.180	0.071	0.198	1.102
Ab Fa	0.343	0.164	0.215	0.627
Ab fc	0.350	0.171	0.220	0.627
Ab fy	0.333	0.154	0.208	0.625
Fa fc	0.347	0.168	0.218	0.628
Fa fy	0.330	0.151	0.206	0.625
fc fy	0.337	0.158	0.211	0.627
Ab Fa fc	0.500	0.250	0.017	0.034
Ab Fa fy	0.483	0.234	0.022	0.045
Ab fc fy	0.490	0.240	0.023	0.047
Fa fc fy	0.487	0.238	0.026	0.053
Ab Fa fc fy	0.640	0.320	#NUM!	#NUM!

Table 3.34. Height, width and area of Wall2

Direction	Height (m)	Width (m)	Area (Total)
yz	3.2	1.5	6.3
xz	3.2	1.25	5.25

Table 3.35. Crushed Area, ratio and its average ratio of initial condition of Wall2

Direction	CA	ratio	Average ratio
yz1	0.0075	0.001	0.003
xz1	0.023125	0.004	
xz4	0.023125	0.004	

Table 3.36. Crushed Area, ratio and its average ratio of $A_{b-5\%}$

Direction	CA	ratio	Average ratio
yz1	1.215	0.193	0.142
xz1	0.62125	0.118	
xz4	0.61	0.116	

Table 3.37. Crushed Area, ratio and its average ratio of $A_{b+5\%}$

Direction	CA	ratio	Average ratio
yz1	1.1375	0.181	0.142
xz1	0.63625	0.121	
xz4	0.65625	0.125	

Table 3.38. Crushed Area, ratio and its average ratio of $F_{axial-4\%}$

Direction	CA	ratio	Average ratio
yz1	1.2	0.190	0.139
xz1	0.59625	0.114	
xz4	0.5975	0.114	

Table 3.39. Crushed Area, ratio and its average ratio of $F_{axial+4\%}$

Direction	CA	ratio	Average ratio
yz1	1.1775	0.187	0.146
xz1	0.6675	0.127	
xz4	0.6575	0.125	

Table 3.40. Crushed Area, ratio and its average ratio of $f_c'_{-4\%}$

Direction	CA	ratio	Average ratio
yz1	0.99	0.157	0.141
xz1	0.6775	0.129	
xz4	0.71875	0.137	

Table 3.41. Crushed Area, ratio and its average ratio of $f_c'_{+4\%}$

Direction	CA	ratio	Average ratio
yz1	1.02	0.162	0.141
xz1	0.6931249	0.132	
xz4	0.681249	0.130	

Table 3.42. Crushed Area, ratio and its average ratio of $f_{y-8.3\%}$

Direction	CA	ratio	Average ratio
yz1	1.2025	0.191	0.141
xz1	0.6025	0.115	
xz4	0.6125	0.117	

Table 3.43. Crushed Area, ratio and its average ratio of $f_{y+8.3\%}$

Direction	CA	ratio	Average ratio
yz1	1.195	0.190	0.141
xz1	0.615	0.117	
xz4	0.615	0.117	

Table 3.44. Moment matching result for Wall2

MM	E(CA)	E(CA^2)	$\sigma(CA)$	COV CA
Ab	0.050	0.007	0.066	1.319
Faxial	0.050	0.007	0.066	1.320
fc	0.049	0.007	0.065	1.319
fy	0.049	0.007	0.065	1.318
Ab Fa	0.096	0.014	0.066	0.683
Ab fc	0.096	0.013	0.065	0.682
Ab fy	0.096	0.013	0.065	0.682
Fa fc	0.096	0.013	0.065	0.683
Fa fy	0.096	0.013	0.065	0.683
fc fy	0.095	0.013	0.065	0.682
Ab Fa fc	0.142	0.020	0.002	0.015
Ab Fa fy	0.142	0.020	0.002	0.016
Ab fc fy	0.142	0.020	0.001	0.004
Fa fc fy	0.142	0.020	0.002	0.016
Ab Fa fc fy	0.188	0.027	#NUM!	#NUM!

Table 3.45. Height, width and area of Wall3

Direction	Height (m)	Width (m)	Area (Total)
yz	3.2	1.5	6.3
xz	3.2	1.25	5.25

Table 3.46. Crushed Area, ratio and its average ratio of initial condition of Wall3

Direction	CA	ratio	Average ratio
yz1	0.3575	0.057	0.080
xz1	0.4918749	0.094	
xz4	0.464375	0.088	

Table 3.47. Crushed Area, ratio and its average ratio of $A_{b-5\%}$

Direction	CA	ratio	Average ratio
yz1	3.165	0.502	0.466
xz1	2.34125	0.446	
xz4	2.365	0.450	

Table 3.48. Crushed Area, ratio and its average ratio of $A_{b+5\%}$

Direction	CA	ratio	Average ratio
yz1	3.165	0.502	0.455
xz1	2.193125	0.418	
xz4	2.33	0.444	

Table 3.49. Crushed Area, ratio and its average ratio of $F_{axial-4\%}$

Direction	CA	ratio	Average ratio
yz1	3.095	0.491	0.454
xz1	2.29	0.436	
xz4	2.28249	0.435	

Table 3.50. Crushed Area, ratio and its average ratio of $F_{axial+4\%}$

Direction	CA	ratio	Average ratio
yz1	3.21	0.510	0.468
xz1	2.338749	0.445	
xz4	2.36	0.450	

Table 3.51. Crushed Area, ratio and its average ratio of $f_c'_{-4\%}$

Direction	CA	ratio	Average ratio
yz1	3.18	0.505	0.491
xz1	2.483749	0.473	
xz4	2.6025	0.496	

Table 3.52. Crushed Area, ratio and its average ratio of $f_c'_{+4\%}$

Direction	CA	ratio	Average ratio
yz1	5.85	0.929	0.929
xz1	4.8749	0.929	
xz4	4.8749	0.929	

Table 3.53. Crushed Area, ratio and its average ratio of $f_y_{-8.3\%}$

Direction	CA	ratio	Average ratio
yz1	3.1725	0.504	0.465
xz1	2.275	0.433	
xz4	2.4018749	0.457	

Table 3.54. Crushed Area, ratio and its average ratio of $f_y_{+8.3\%}$

Direction	CA	ratio	Average ratio
yz1	3.05125	0.484	0.436
xz1	2.1525	0.410	
xz4	2.165	0.412	

Table 3.55. Moment matching result for Wall3

MM	E(CA)	E(CA^2)	$\sigma(CA)$	COV CA
Ab	0.207	0.075	0.180	0.869
Faxial	0.207	0.075	0.180	0.870
fc	0.290	0.188	0.323	1.114
fy	0.203	0.072	0.175	0.861
Ab Fa	0.334	0.144	0.180	0.539
Ab fc	0.417	0.257	0.288	0.692
Ab fy	0.330	0.140	0.177	0.537
Fa fc	0.417	0.257	0.288	0.692
Fa fy	0.330	0.141	0.178	0.538
fc fy	0.413	0.254	0.288	0.697
Ab Fa fc	0.544	0.325	0.172	0.317
Ab Fa fy	0.457	0.209	0.011	0.024
Ab fc fy	0.540	0.322	0.174	0.323
Fa fc fy	0.540	0.322	0.174	0.323
Ab Fa fc fy	0.667	0.391	#NUM!	#NUM!

It should be noted that deriving a general rule that can precisely prescribe dominant factors that govern uncertainty behind PBB of RC core walls shall necessitate in-depth investigations with sufficiently many experimental data, which is beyond the scope of this study and will be addressed by a future research. Still, this study's methodology is meaningful since the proposed combination of MM and a high-precision FEA will enable researchers to further assess various uncertainties behind global and microscopic performance of complex RC structures.

3.2 Results of shear force-resisting capacity

In Chapter 2.2.2, we introduced the method applied to predict uncertainty behind the shear force-resisting capacity. Table 3.56 to Table 3.2.60 represent the simulated results of the maximum and minimum shear force-resisting capability. Maximum and minimum shear force-resisting capability represent the concept of different directions. Based on the maximum and minimum forces, with adopting Eq 2.4 to 2.6 in Chapter 2.2.2, we subsequently calculate the results of 1D to 4D MM (see Table 3.61 to 3.65). For four variables (features), various percentage of behaviors are simulated and recorded.

Table 3.56. The max and min forces of TUA in various conditions

Condition	Max Force	Min Force
Validation	5.03E+05	-5.59E+05
$F_{axial-4\%}$	4.90E+05	-5.03E+05
$F_{axial+4\%}$	5.01E+05	-5.12E+05
$A_{b-5\%}$	4.88E+05	-4.96E+05
$A_{b+5\%}$	5.09E+05	-5.20E+05
$f_c'_{-4\%}$	4.99E+05	-5.12E+05
$f_c'_{+4\%}$	4.92E+05	-5.04E+05
$f_y_{-8.3\%}$	5.16E+05	-5.28E+05
$f_y_{+8.3\%}$	4.77E+05	-4.89E+05

Table 3.57. The max and min forces of TUB in various conditions

Condition	Max Force	Min Force
Validation	4.56E+05	-4.97E+05
$F_{axial-4\%}$	4.43E+05	-4.63E+05
$F_{axial+4\%}$	4.52E+05	-4.72E+05
$A_{b-5\%}$	4.39E+05	-4.58E+05
$A_{b+5\%}$	4.56E+05	-4.80E+05
$f_c'_{-4\%}$	4.53E+05	-4.73E+05
$f_c'_{+4\%}$	4.45E+05	-4.66E+05
$f_y_{-8.3\%}$	4.62E+05	-4.83E+05
$f_y_{+8.3\%}$	4.33E+05	-4.51E+05

Table 3.58. The max and min forces of Wall 1 in various conditions

Condition	Max Force	Min Force
Validation	9.29E+05	-9.43E+05
$F_{axial-4\%}$	9.22E+05	-9.34E+05
$F_{axial+4\%}$	9.37E+05	-9.44E+05
$A_{b-5\%}$	9.09E+05	-9.18E+05
$A_{b+5\%}$	9.50E+05	-9.60E+05
$f_c'_{-4\%}$	9.03E+05	-8.94E+05
$f_c'_{+4\%}$	8.91E+05	-8.81E+05
$f_y_{-8.3\%}$	9.66E+05	-9.72E+05
$f_y_{+8.3\%}$	8.53E+05	-9.02E+05

Table 3.59. The max and min forces of Wall 2 in various conditions

Condition	Max Force	Min Force
Validation	7.70E+05	-6.71E+05
$F_{axial-4\%}$	7.60E+05	-6.65E+05
$F_{axial+4\%}$	7.84E+05	-6.78E+05
$A_{b-5\%}$	7.55E+05	-6.54E+05
$A_{b+5\%}$	7.85E+05	-6.90E+05
$f_c'_{-4\%}$	7.44E+05	-6.53E+05
$f_c'_{+4\%}$	7.44E+05	-6.47E+05
$f_y_{-8.3\%}$	7.94E+05	-6.99E+05
$f_y_{+8.3\%}$	7.46E+05	-6.42E+05

Table 3.60. The max and min forces of Wall 3 in various conditions

Condition	Max Force	Min Force
Validation	7.95E+05	-8.25E+05
$F_{axial-4\%}$	7.94E+05	-8.20E+05
$F_{axial+4\%}$	8.05E+05	-8.27E+05
$A_{b-5\%}$	7.85E+05	-8.22E+05
$A_{b+5\%}$	8.16E+05	-8.36E+05
$f_c'_{-4\%}$	7.27E+05	-7.89E+05
$f_c'_{+4\%}$	7.52E+05	-7.66E+05
$f_y_{-8.3\%}$	8.26E+05	-8.45E+05
$f_y_{+8.3\%}$	7.73E+05	-8.08E+05

Table 3.61. MM result of TUA

	E(F _{max})	$\sigma(F_{max})$	E(F _{min})	$\sigma(F_{min})$	COV/F _{max}]	COV/F _{min}]
f_c'	500.50	4.07	-542.00	23.15	0.01	0.04
f_y	500.83	11.67	-542.17	26.33	0.02	0.05
F_{axial}	500.50	4.75	-541.83	24.42	0.01	0.05
A_b	501.50	6.42	-542.00	25.02	0.01	0.05
(f_c' , f_y)	498.33	11.91	-525.17	26.54	0.02	0.05
(f_c' , A_b)	499.00	7.09	-525.00	25.13	0.01	0.05
(f_c' , F_{axial})	498.00	5.16	-524.83	24.41	0.01	0.05
(f_y , A_b)	499.33	13.07	-525.17	27.33	0.03	0.05
(f_y , F_{axial})	498.33	12.16	-525.00	26.68	0.02	0.05
(F_{axial} , A_b)	499.00	7.51	-524.83	25.27	0.02	0.05
(f_c' , f_y , F_{axial})	495.83	11.88	-508.00	11.79	0.02	0.02
(f_c' , f_y , A_b)	496.83	13.01	-508.17	13.42	0.03	0.03
(f_c' , F_{axial} , A_b)	496.50	7.27	-507.83	7.75	0.01	0.02
(f_y , F_{axial} , A_b)	496.83	13.23	-508.00	13.48	0.03	0.03
(f_c' , f_y , F_{axial} , A_b)	494.33	12.68	-491.00	#NUM!	0.03	#NUM!

Table 3.62. MM result of TUB

	E(F _{max})	$\sigma(F_{max})$	E(F _{min})	$\sigma(F_{min})$	COV[F _{max}]	COV[F _{min}]
f'_c	453.67	4.03	-487.83	13.12	0.01	0.03
f_y	453.17	9.28	-487.00	16.89	0.02	0.03
F_{axial}	453.17	4.78	-487.17	13.15	0.01	0.03
A_b	453.17	6.34	-487.67	14.65	0.01	0.03
(f'_c, f_y)	450.83	9.44	-477.83	16.56	0.02	0.03
(f'_c, A_b)	450.83	6.57	-478.50	14.68	0.01	0.03
(f'_c, F_{axial})	450.83	5.08	-478.00	13.86	0.01	0.03
(f_y, A_b)	450.33	10.50	-477.67	17.70	0.02	0.04
(f_y, F_{axial})	450.33	9.64	-477.17	16.99	0.02	0.04
(F_{axial}, A_b)	450.33	6.85	-477.83	15.20	0.02	0.03
(f'_c, f_y, F_{axial})	448.00	9.09	-468.00	9.87	0.02	0.02
(f'_c, f_y, A_b)	448.00	10.00	-468.50	11.44	0.02	0.02
(f'_c, F_{axial}, A_b)	448.00	6.06	-468.67	7.20	0.01	0.02
(f_y, F_{axial}, A_b)	448.00	9.09	-468.00	9.87	0.02	0.02
($f'_c, f_y, F_{axial}, A_b$)	445.17	8.80	-458.67	#NUM!	0.02	#NUM!

Table 3.63. MM result of Wall 1

	E(F _{max})	$\sigma(F_{max})$	E(F _{min})	$\sigma(F_{min})$	COV/F _{max}]	COV/F _{min}]
f'_c	918.33	15.48	-924.50	26.43	0.02	0.03
f_y	922.50	33.89	-941.00	20.40	0.04	0.02
F_{axial}	929.17	4.34	-941.67	3.45	0.00	0.00
A_b	929.17	11.84	-941.67	12.27	0.01	0.01
(f'_c, f_y)	911.83	35.35	-922.50	32.26	0.04	0.03
(f'_c, A_b)	918.50	19.58	-923.17	28.28	0.02	0.03
(f'_c, F_{axial})	918.50	16.18	-923.17	25.71	0.02	0.03
(f_y, A_b)	922.67	35.93	-939.67	23.70	0.04	0.03
(f_y, F_{axial})	922.67	33.20	-939.67	20.56	0.04	0.02
(F_{axial}, A_b)	929.33	12.61	-940.33	12.61	0.01	0.01
(f'_c, f_y, F_{axial})	912.00	35.69	-921.17	31.59	0.04	0.03
(f'_c, f_y, A_b)	912.00	37.35	-921.17	33.72	0.04	0.04
(f'_c, F_{axial}, A_b)	918.67	20.14	-921.83	27.55	0.02	0.03
(f_y, F_{axial}, A_b)	922.83	36.22	-938.33	23.76	0.04	0.03
($f'_c, f_y, F_{axial}, A_b$)	912.17	37.68	-919.83	33.02	0.04	0.04

Table 3.64. MM result of Wall 2

	E(F _{max})	$\sigma(F_{max})$	E(F _{min})	$\sigma(F_{min})$	COV/F _{max}]	COV/F _{min}]
f'_c	761.33	12.26	-664.00	10.05	0.02	0.02
f_y	770.00	13.86	-670.83	16.46	0.02	0.02
F_{axial}	770.67	6.99	-671.17	3.76	0.01	0.01
A_b	770.00	8.66	-671.33	10.40	0.01	0.02
(f'_c, f_y)	761.33	18.50	-663.83	19.22	0.02	0.03
(f'_c, A_b)	761.33	15.01	-664.33	14.62	0.02	0.02
(f'_c, F_{axial})	762.00	14.51	-663.17	10.84	0.02	0.02
(f_y, A_b)	770.00	16.34	-671.17	19.47	0.02	0.03
(f_y, F_{axial})	770.67	15.52	-671.00	16.88	0.02	0.03
(Faxial, A_b)	770.67	11.13	-671.50	11.06	0.01	0.02
(f'_c, f_y, F_{axial})	762.00	20.07	-664.00	19.65	0.03	0.03
(f'_c, f_y, A_b)	761.33	20.43	-663.17	21.97	0.03	0.03
(f'_c, F_{axial}, A_b)	762.00	16.90	-664.50	15.17	0.02	0.02
(f_y, F_{axial}, A_b)	770.67	17.77	-671.33	19.83	0.02	0.03
($f'_c, f_y, F_{axial}, A_b$)	762.00	21.86	-664.33	22.34	0.03	0.03

Table 3.65. MM result of Wall3

	E(F _{max})	$\sigma(F_{max})$	E(F _{min})	$\sigma(F_{min})$	COV/F _{max}]	COV/F _{min}]
f'_c	776.50	27.14	-809.17	23.36	0.03	0.03
f_y	796.50	15.45	-825.50	10.70	0.02	0.01
F_{axial}	662.33	296.20	-686.67	307.09	0.45	0.45
A_b	796.83	9.32	-826.33	4.46	0.01	0.01
(f'_c, f_y)	778.00	32.10	-809.67	26.00	0.04	0.03
(f'_c, A_b)	778.33	29.85	-810.50	24.65	0.04	0.03
(f'_c, F_{axial})	643.83	289.08	-670.83	300.78	0.45	0.45
(f_y, A_b)	798.33	17.89	-810.50	24.65	0.02	0.03
(f_y, F_{axial})	663.83	297.28	-687.17	307.50	0.45	0.45
(Faxial, A_b)	663.17	297.17	-688.00	307.72	0.45	0.45
(f'_c, f_y, F_{axial})	645.33	290.27	-671.33	301.23	0.45	0.45
(f'_c, f_y, A_b)	779.83	34.35	-811.00	27.14	0.04	0.03
(f'_c, F_{axial}, A_b)	645.67	290.18	-672.17	301.50	0.45	0.45
(f_y, F_{axial}, A_b)	665.67	298.23	-688.50	308.13	0.45	0.45
($f'_c, f_y, F_{axial}, A_b$)	647.17	291.36	-672.67	301.94	0.45	0.45

CHAPTER 4. MOMENT MATCHING ON VULNERABILITY

4.1 Conventional ranges of the collapse capacity and GANMM results

In seismic engineering, the collapse capacity of a building or a component, in terms of ground acceleration (g), is significantly important to estimate vulnerability. Most of the capacity appears to follow a lognormal distribution.

In [28], the range of the mean value μ of collapse capacity is between 0.3g to 1.3g, and the lognormal standard deviation (σ) is between 0.7g to 0.9g. In [16], μ is 1 and σ is 0.8g. In [29], the range of μ is between 0.9g to 2.4g, and the σ is between 0.3g to 4.6g. In [30], the range of μ is between 0.9g to 2.7g, and the σ is between 0.4g to 0.8g. In [23], the μ is 2.99g and the σ is 0.62g. In [31], the μ is between 0.7g to 5.2g, and σ is between 0.2g to 0.8g. Table 4.1 shows the investigated references and corresponding ranges of μ and σ .

Table 4.1. The ranges of μ and σ of investigated references

References	Range of μ (g)	Range of σ (g)
16	1	0.8
23	2.99	0.62
28	0.3-1.3	0.7-0.9
29	0.9-2.4	0.3-4.6
30	0.9-2.7	0.4-0.8
31	0.7-5.2	0.2-0.8

According to the previous researches during the past decade, the common range of the collapse capacity of a building or a component appears to be from 0.3g to 5.5g having a

range of lognormal standard deviation (σ) between 0.2g to 0.9g. Instead of estimating by the continuous PDF, herein, we simplify it by adopting GANMM [32][33] to enable the use of moment matching technique. To apply GANMM, raw moments of the intended lognormal distribution should be provided. Equation (4.1) [34] shows the mathematical formula to generate intended raw moments.

$$E[X^n] = e^{n\mu + \frac{1}{2}n^2\sigma^2} \quad (4.1)$$

where n means the order of moments; μ and σ represent the mean value and the lognormal standard deviation.

By adopting GANMM, we can extend the original MM, which applied on a normal distribution in chapter 3, to a lognormal distribution that most seismic vulnerability tend to follow. Herein, the thesis offers a table consisting of the mean value μ , lognormal standard deviation σ , three locations (x_1 , x_2 and x_3), their corresponding weights (ω_1 , ω_2 , and ω_3) and final errors (F.E.) up to 5th moment (F. E.¹ to F. E.⁵). Equation 4.2 to 4.4 show how to calculate F.E. for $j - th$ moment,

$$eer_{\omega} = \frac{(1 - \sum_{k=1}^{k=3} \omega_k)}{1} \quad (4.2)$$

$$eer_j = \frac{E[X^j] - E[X^j]_{GA-NMM}}{E[X^j]} \quad (4.3)$$

$$F. E. ^j = \frac{(\sum_{i=1}^j eer_i) + eer_{\omega}}{j + 1} \quad (4.4)$$

where $F. E. ^j$ is the F.E. of $j - th$ moment, $E[X^j]$ is the real $j - th$ moment, $E[X^j]_{GA-NMM}$ is the $j - th$ moment calculated by GA-NMM,

Table 4.2 shows the final result obtained by proceeding GANMM in the order of μ ranging from 0.3 to 5.5 along with σ ranging from 0.2 to 0.9.

Table 4.2 obtained by GANMM technique enables future researchers and engineers who have the need to investigate uncertainties on vulnerability of collapse capacity to simply look up the table and acquire their intended uncertainty investigation with the proper μ and σ . Notably, the type of F.E. is set as double-precision which can store fifteen full decimals (10^{-15}) and F.A.E. is presented by percentage. Therefore, the actual error is that F.E. multiplied by 10^{-2} , which accounts for the acceptable F.E. should be at least smaller than 10^{-14} making the actual error smaller than 10^{-16} . In the cases that F.E. is smaller than 10^{-14} , they are equivalent to that F.E. is zero since double-precision stores till 10^{-15} at most. The decimals starting from 10^{-16} are arbitrary and meaningless.

Table 4.2. Exact results of GANMM

μ	σ	x_1'	x_2'	x_3'	ω_1'	ω_2'	ω_3'	F.E. ¹	F.E. ²	F.E. ³	F.E. ⁴	F.E. ⁵
0.3	0.2	1.050	1.491	2.116	0.344	0.596	0.060	0.00E+00	3.75E-15	1.04E-14	1.61E-14	2.34E-14
0.3	0.3	0.992	1.691	2.883	0.452	0.516	0.031	1.34E-14	8.94E-15	6.71E-15	7.97E-15	6.64E-15
0.3	0.4	0.974	2.013	4.161	0.561	0.424	0.015	7.59E-15	5.06E-15	8.19E-15	9.53E-15	1.15E-14
0.3	0.5	0.993	2.522	6.403	0.665	0.329	0.006	0.00E+00	4.93E-15	9.56E-15	1.92E-14	2.30E-14
0.3	0.6	1.046	3.320	10.533	0.757	0.241	0.002	0.00E+00	3.95E-15	2.97E-15	4.78E-15	6.33E-15
0.3	0.7	1.135	4.595	18.610	0.833	0.167	0.001	1.75E-14	1.17E-14	1.28E-14	3.40E-14	7.27E-14
0.3	0.8	1.260	6.686	35.466	0.891	0.109	0.000	0.00E+00	4.52E-15	3.39E-15	6.80E-15	1.47E-14
0.3	0.9	1.428	10.227	73.237	0.933	0.067	0.000	0.00E+00	6.43E-15	4.82E-15	3.86E-15	7.55E-15
0.4	0.2	1.160	1.647	2.338	0.342	0.597	0.061	1.84E-14	1.84E-14	1.66E-14	1.33E-14	1.11E-14
0.4	0.3	1.095	1.867	3.183	0.451	0.517	0.032	0.00E+00	5.56E-15	4.17E-15	3.33E-15	7.98E-15
0.4	0.4	1.077	2.225	4.600	0.561	0.424	0.015	0.00E+00	4.83E-15	3.62E-15	2.90E-15	6.75E-15
0.4	0.5	1.098	2.787	7.076	0.665	0.328	0.006	1.21E-14	1.21E-14	1.34E-14	1.46E-14	1.78E-14
0.4	0.6	1.157	3.669	11.641	0.757	0.241	0.002	6.22E-15	4.14E-15	3.11E-15	2.49E-15	7.77E-15
0.4	0.7	1.254	5.078	20.567	0.833	0.167	0.001	5.55E-15	8.69E-15	6.52E-15	9.77E-15	1.71E-14
0.4	0.8	1.393	7.389	39.196	0.891	0.109	0.000	1.08E-14	7.21E-15	5.40E-15	9.81E-15	1.37E-14
0.4	0.9	1.578	11.302	80.939	0.933	0.067	0.000	0.00E+00	5.27E-15	9.54E-15	7.63E-15	6.36E-15
0.5	0.2	1.283	1.822	2.586	0.345	0.595	0.060	1.22E-14	8.10E-15	1.02E-14	1.17E-14	1.08E-14
0.5	0.3	1.212	2.066	3.522	0.453	0.516	0.031	6.44E-15	8.84E-15	9.93E-15	1.03E-14	8.57E-15
0.5	0.4	1.190	2.460	5.083	0.561	0.424	0.015	0.00E+00	3.95E-15	2.97E-15	7.72E-15	9.06E-15
0.5	0.5	1.213	3.080	7.821	0.665	0.328	0.006	1.15E-14	1.43E-14	1.39E-14	1.37E-14	1.49E-14

Table 4.2. (continued)

μ	σ	x_1'	x_2'	x_3'	ω_1'	ω_2'	ω_3'	F.E. ¹	F.E. ²	F.E. ³	F.E. ⁴	F.E. ⁵
0.5	0.6	1.278	4.055	12.865	0.757	0.241	0.002	5.62E-15	9.05E-15	1.46E-14	1.60E-14	1.68E-14
0.5	0.7	1.386	5.612	22.730	0.833	0.167	0.001	1.11E-14	7.40E-15	5.55E-15	1.36E-14	3.58E-14
0.5	0.8	1.539	8.166	43.318	0.891	0.109	0.000	0.00E+00	6.06E-15	8.99E-15	1.09E-14	1.24E-14
0.5	0.9	1.744	12.491	89.451	0.933	0.067	0.000	8.98E-15	1.03E-14	1.19E-14	1.33E-14	1.74E-14
0.6	0.2	1.420	2.016	2.862	0.347	0.594	0.059	0.00E+00	0.00E+00	3.07E-15	4.79E-15	2.15E-14
0.6	0.3	1.339	2.282	3.890	0.452	0.516	0.031	5.82E-15	3.88E-15	7.81E-15	6.25E-15	5.21E-15
0.6	0.4	1.315	2.718	5.618	0.561	0.424	0.015	1.67E-14	1.76E-14	1.32E-14	1.77E-14	2.12E-14
0.6	0.5	1.341	3.404	8.642	0.665	0.329	0.006	0.00E+00	0.00E+00	0.00E+00	3.49E-15	9.13E-15
0.6	0.6	1.413	4.482	14.218	0.757	0.241	0.002	5.55E-15	8.04E-15	1.18E-14	9.47E-15	7.89E-15
0.6	0.7	1.532	6.203	25.120	0.833	0.167	0.001	0.00E+00	0.00E+00	0.00E+00	4.09E-15	3.41E-15
0.6	0.8	1.701	9.025	47.873	0.891	0.109	0.000	0.00E+00	9.92E-15	1.40E-14	1.37E-14	1.55E-14
0.6	0.9	1.928	13.804	98.859	0.933	0.067	0.000	0.00E+00	7.06E-15	8.36E-15	1.43E-14	1.96E-14
0.7	0.2	1.564	2.221	3.153	0.340	0.599	0.061	0.00E+00	6.74E-15	9.60E-15	1.08E-14	2.41E-14
0.7	0.3	1.480	2.523	4.302	0.453	0.516	0.031	5.55E-15	9.80E-15	1.10E-14	8.78E-15	9.64E-15
0.7	0.4	1.454	3.005	6.210	0.561	0.424	0.015	0.00E+00	0.00E+00	0.00E+00	0.00E+00	0.00E+00
0.7	0.5	1.482	3.763	9.553	0.665	0.328	0.006	1.11E-14	7.40E-15	9.08E-15	7.27E-15	8.57E-15
0.7	0.6	1.561	4.953	15.714	0.757	0.241	0.002	0.00E+00	0.00E+00	0.00E+00	3.88E-15	5.78E-15
0.7	0.7	1.693	6.855	27.762	0.833	0.167	0.001	8.63E-15	5.75E-15	9.11E-15	7.29E-15	1.21E-14
0.7	0.8	1.880	9.974	52.909	0.891	0.109	0.000	8.01E-15	1.35E-14	1.01E-14	1.14E-14	1.44E-14
0.7	0.9	2.130	15.257	109.258	0.933	0.067	0.000	0.00E+00	0.00E+00	0.00E+00	3.39E-15	7.52E-15
0.8	0.2	1.727	2.451	3.481	0.338	0.600	0.062	2.93E-14	2.51E-14	2.22E-14	2.19E-14	3.41E-14
0.8	0.3	1.635	2.788	4.753	0.452	0.516	0.031	9.54E-15	6.36E-15	1.01E-14	1.09E-14	9.11E-15
0.8	0.4	1.606	3.320	6.862	0.561	0.424	0.015	9.21E-15	1.92E-14	4.18E-14	5.60E-14	7.25E-14
0.8	0.5	1.638	4.158	10.557	0.665	0.328	0.006	0.00E+00	0.00E+00	5.23E-15	4.19E-15	6.54E-15
0.8	0.6	1.725	5.474	17.366	0.757	0.241	0.002	0.00E+00	0.00E+00	3.19E-15	2.55E-15	8.29E-15
0.8	0.7	1.871	7.576	30.683	0.833	0.167	0.001	0.00E+00	4.49E-15	1.76E-14	4.72E-14	8.55E-14
0.8	0.8	2.078	11.023	58.474	0.891	0.109	0.000	0.00E+00	6.65E-15	8.60E-15	1.13E-14	1.54E-14
0.8	0.9	2.354	16.861	120.748	0.933	0.067	0.000	1.33E-14	1.36E-14	1.36E-14	1.54E-14	1.28E-14
0.9	0.2	1.919	2.725	3.870	0.350	0.591	0.058	0.00E+00	0.00E+00	4.99E-15	1.24E-14	6.27E-15
0.9	0.3	1.806	3.080	5.250	0.452	0.517	0.031	0.00E+00	4.09E-15	7.05E-15	5.64E-15	4.70E-15
0.9	0.4	1.775	3.669	7.583	0.561	0.424	0.015	0.00E+00	7.11E-15	8.24E-15	1.09E-14	7.30E-15
0.9	0.5	1.810	4.595	11.667	0.665	0.328	0.006	0.00E+00	0.00E+00	3.88E-15	7.30E-15	1.35E-14
0.9	0.6	1.907	6.050	19.193	0.757	0.241	0.002	0.00E+00	0.00E+00	9.45E-15	1.45E-14	1.59E-14
0.9	0.7	2.067	8.373	33.909	0.833	0.167	0.001	7.07E-15	1.94E-14	3.56E-14	5.07E-14	6.58E-14
0.9	0.8	2.297	12.183	64.624	0.891	0.109	0.000	0.00E+00	5.44E-15	1.48E-14	1.18E-14	9.87E-15
0.9	0.9	2.602	18.634	133.446	0.933	0.067	0.000	6.02E-15	7.89E-15	1.09E-14	8.72E-15	7.27E-15
1.0	0.2	2.118	3.008	4.271	0.347	0.594	0.059	8.01E-15	1.27E-14	1.32E-14	1.44E-14	1.78E-14
1.0	0.3	1.997	3.405	5.805	0.452	0.516	0.031	0.00E+00	6.69E-15	1.09E-14	1.63E-14	1.98E-14
1.0	0.4	1.962	4.054	8.380	0.561	0.424	0.015	5.55E-15	9.52E-15	1.14E-14	9.16E-15	7.63E-15

Table 4.2. (continued)

μ	σ	x_1'	x_2'	x_3'	ω_1'	ω_2'	ω_3'	F.E. ¹	F.E. ²	F.E. ³	F.E. ⁴	F.E. ⁵
1.0	0.5	2.000	5.078	12.893	0.665	0.329	0.006	0.00E+00	4.86E-15	1.23E-14	1.26E-14	1.50E-14
1.0	0.6	2.107	6.686	21.211	0.757	0.241	0.002	1.79E-14	2.76E-14	3.12E-14	4.83E-14	6.75E-14
1.0	0.7	2.285	9.254	37.476	0.833	0.167	0.001	0.00E+00	6.02E-15	8.41E-15	6.73E-15	1.28E-14
1.0	0.8	2.538	13.464	71.419	0.891	0.109	0.000	5.93E-15	3.95E-15	6.94E-15	5.55E-15	9.01E-15
1.0	0.9	2.876	20.594	147.481	0.933	0.067	0.000	1.09E-14	1.36E-14	1.39E-14	1.52E-14	1.27E-14
1.1	0.2	2.338	3.320	4.714	0.344	0.596	0.060	5.55E-15	9.76E-15	1.28E-14	1.53E-14	1.51E-14
1.1	0.3	2.207	3.762	6.414	0.452	0.517	0.031	0.00E+00	5.48E-15	4.11E-15	3.29E-15	7.77E-15
1.1	0.4	2.168	4.482	9.263	0.561	0.424	0.015	6.82E-15	9.31E-15	1.02E-14	1.20E-14	1.52E-14
1.1	0.5	2.211	5.613	14.250	0.665	0.328	0.006	0.00E+00	0.00E+00	4.25E-15	7.18E-15	8.71E-15
1.1	0.6	2.329	7.389	23.443	0.757	0.241	0.002	0.00E+00	6.39E-15	9.98E-15	1.42E-14	1.46E-14
1.1	0.7	2.525	10.227	41.416	0.833	0.167	0.001	0.00E+00	0.00E+00	2.89E-15	1.12E-14	1.58E-14
1.1	0.8	2.805	14.880	78.931	0.891	0.109	0.000	0.00E+00	0.00E+00	2.94E-15	5.02E-15	9.51E-15
1.1	0.9	3.178	22.760	162.993	0.933	0.067	0.000	9.86E-15	3.25E-14	5.18E-14	5.24E-14	4.37E-14
1.2	0.2	2.578	3.660	5.198	0.339	0.599	0.061	7.21E-14	1.92E-13	3.63E-13	5.82E-13	1.57E-14
1.2	0.3	2.440	4.160	7.091	0.453	0.516	0.031	6.39E-15	8.75E-15	6.56E-15	7.53E-15	6.27E-15
1.2	0.4	2.397	4.954	10.238	0.561	0.424	0.015	2.46E-13	4.68E-13	8.19E-13	1.32E-12	7.27E-15
1.2	0.5	2.443	6.203	15.747	0.665	0.329	0.006	0.00E+00	6.52E-15	4.89E-15	3.91E-15	3.26E-15
1.2	0.6	2.574	8.166	25.907	0.757	0.241	0.002	0.00E+00	0.00E+00	3.84E-15	3.07E-15	5.90E-15
1.2	0.7	2.791	11.302	45.772	0.833	0.167	0.001	1.05E-14	1.10E-14	8.26E-15	6.61E-15	8.14E-15
1.2	0.8	3.100	16.445	87.232	0.891	0.109	0.000	0.00E+00	5.97E-15	8.84E-15	7.07E-15	9.12E-15
1.2	0.9	3.512	25.154	180.133	0.933	0.067	0.000	8.92E-15	4.42E-14	6.97E-14	7.04E-14	5.87E-14
1.3	0.2	2.855	4.054	5.755	0.344	0.596	0.060	5.93E-15	3.95E-15	5.97E-15	7.05E-15	1.34E-14
1.3	0.3	2.696	4.596	7.835	0.452	0.516	0.031	0.00E+00	7.35E-15	1.51E-14	1.82E-14	2.26E-14
1.3	0.4	2.648	5.474	11.313	0.561	0.424	0.015	1.12E-14	1.38E-14	1.39E-14	1.46E-14	1.52E-14
1.3	0.5	2.700	6.855	17.403	0.665	0.329	0.006	0.00E+00	0.00E+00	0.00E+00	3.40E-15	1.08E-14
1.3	0.6	2.845	9.025	28.632	0.757	0.241	0.002	0.00E+00	8.56E-15	9.27E-15	7.41E-15	8.20E-15
1.3	0.7	3.084	12.491	50.587	0.833	0.167	0.001	5.55E-15	3.70E-15	5.95E-15	8.74E-15	1.05E-14
1.3	0.8	3.426	18.174	96.406	0.891	0.109	0.000	1.43E-14	9.56E-15	1.04E-14	1.07E-14	1.28E-14
1.3	0.9	3.882	27.799	199.078	0.933	0.067	0.000	0.00E+00	0.00E+00	3.01E-15	4.87E-15	4.06E-15
1.4	0.2	3.149	4.470	6.347	0.339	0.599	0.062	1.07E-14	7.16E-15	5.37E-15	1.04E-14	4.19E-15
1.4	0.3	2.979	5.079	8.659	0.452	0.516	0.031	0.00E+00	6.02E-15	8.06E-15	1.05E-14	8.79E-15
1.4	0.4	2.928	6.051	12.506	0.562	0.424	0.015	1.01E-14	6.74E-15	5.05E-15	8.72E-15	1.10E-14
1.4	0.5	2.984	7.576	19.234	0.665	0.329	0.006	9.66E-15	1.52E-14	2.18E-14	1.97E-14	3.83E-14
1.4	0.6	3.144	9.974	31.644	0.757	0.241	0.002	0.00E+00	0.00E+00	0.00E+00	0.00E+00	2.46E-15
1.4	0.7	3.409	13.805	55.907	0.833	0.167	0.001	0.00E+00	0.00E+00	4.70E-15	3.76E-15	7.00E-15
1.4	0.8	3.786	20.086	106.546	0.891	0.109	0.000	7.95E-15	5.30E-15	8.76E-15	1.02E-14	8.52E-15
1.4	0.9	4.290	30.723	220.016	0.933	0.067	0.000	2.02E-14	4.19E-14	5.37E-14	5.29E-14	4.41E-14
1.5	0.2	3.489	4.953	7.032	0.345	0.595	0.060	9.71E-15	1.19E-14	1.88E-14	1.92E-14	1.05E-14
1.5	0.3	3.291	5.610	9.565	0.451	0.517	0.031	9.47E-15	1.12E-14	1.37E-14	1.92E-14	2.14E-14

Table 4.2. (continued)

μ	σ	x_1'	x_2'	x_3'	ω_1'	ω_2'	ω_3'	F.E. ¹	F.E. ²	F.E. ³	F.E. ⁴	F.E. ⁵
1.5	0.4	3.234	6.684	13.815	0.561	0.424	0.015	0.00E+00	4.28E-15	7.05E-15	8.78E-15	7.31E-15
1.5	0.5	3.298	8.372	21.256	0.665	0.329	0.006	1.43E-14	1.67E-14	1.25E-14	1.00E-14	3.50E-13
1.5	0.6	3.475	11.023	34.972	0.757	0.241	0.002	8.28E-15	1.70E-14	1.90E-14	1.52E-14	1.56E-14
1.5	0.7	3.767	15.256	61.786	0.833	0.167	0.001	7.76E-15	5.17E-15	3.88E-15	3.10E-15	2.59E-15
1.5	0.8	4.185	22.198	117.752	0.891	0.109	0.000	0.00E+00	6.56E-15	8.46E-15	1.54E-14	1.28E-14
1.5	0.9	4.741	33.954	243.156	0.933	0.067	0.000	1.22E-14	1.28E-14	9.58E-15	7.66E-15	6.39E-15
1.6	0.2	3.840	5.451	7.740	0.336	0.601	0.063	0.00E+00	0.00E+00	4.88E-15	3.91E-15	9.10E-15
1.6	0.3	3.638	6.203	10.575	0.452	0.517	0.031	8.57E-15	9.75E-15	1.12E-14	1.63E-14	1.69E-14
1.6	0.4	3.575	7.390	15.273	0.561	0.424	0.015	8.28E-15	5.52E-15	9.83E-15	7.86E-15	6.55E-15
1.6	0.5	3.645	9.253	23.492	0.665	0.329	0.006	7.91E-15	5.27E-15	1.15E-14	9.24E-15	1.13E-14
1.6	0.6	3.840	12.183	38.651	0.757	0.241	0.002	7.49E-15	4.99E-15	8.37E-15	6.70E-15	1.28E-14
1.6	0.7	4.163	16.861	68.284	0.833	0.167	0.001	7.02E-15	4.68E-15	3.51E-15	2.81E-15	5.19E-15
1.6	0.8	4.625	24.533	130.135	0.891	0.109	0.000	6.51E-15	4.34E-15	8.51E-15	6.81E-15	5.67E-15
1.6	0.9	5.240	37.525	268.730	0.933	0.067	0.000	0.00E+00	7.64E-15	1.06E-14	8.50E-15	7.08E-15
1.7	0.2	4.268	6.060	8.603	0.349	0.593	0.059	1.11E-14	1.47E-14	1.46E-14	1.54E-14	2.41E-15
1.7	0.3	4.020	6.853	11.684	0.452	0.517	0.031	7.76E-15	1.18E-14	8.83E-15	9.53E-15	9.94E-15
1.7	0.4	3.951	8.166	16.879	0.561	0.424	0.015	7.49E-15	2.22E-14	2.93E-14	3.75E-14	5.13E-14
1.7	0.5	4.028	10.227	25.966	0.665	0.328	0.006	3.97E-14	5.53E-14	6.68E-14	6.99E-14	7.12E-14
1.7	0.6	4.244	13.464	42.715	0.757	0.241	0.002	0.00E+00	0.00E+00	6.86E-15	7.76E-15	1.52E-14
1.7	0.7	4.601	18.634	75.466	0.833	0.167	0.001	5.55E-15	9.63E-15	7.23E-15	9.00E-15	1.10E-14
1.7	0.8	5.111	27.112	143.820	0.891	0.109	0.000	5.89E-15	8.32E-15	1.01E-14	8.11E-15	6.76E-15
1.7	0.9	5.791	41.472	296.991	0.933	0.067	0.000	1.08E-14	7.21E-15	1.27E-14	1.01E-14	8.44E-15
1.8	0.2	4.712	6.689	9.496	0.346	0.594	0.059	7.20E-15	4.80E-15	3.60E-15	5.34E-15	5.76E-15
1.8	0.3	4.445	7.577	12.918	0.452	0.516	0.031	0.00E+00	0.00E+00	0.00E+00	3.31E-15	5.18E-15
1.8	0.4	4.367	9.026	18.654	0.561	0.424	0.015	1.79E-14	1.66E-14	1.56E-14	1.62E-14	1.56E-14
1.8	0.5	4.452	11.302	28.695	0.665	0.329	0.006	0.00E+00	3.93E-15	7.11E-15	9.36E-15	1.04E-14
1.8	0.6	4.690	14.880	47.208	0.757	0.241	0.002	0.00E+00	6.30E-15	9.81E-15	1.09E-14	1.28E-14
1.8	0.7	5.085	20.594	83.402	0.833	0.167	0.001	0.00E+00	0.00E+00	2.83E-15	2.26E-15	1.89E-15
1.8	0.8	5.649	29.964	158.947	0.891	0.109	0.000	0.00E+00	7.20E-15	1.12E-14	8.93E-15	7.44E-15
1.8	0.9	6.400	45.833	328.226	0.933	0.067	0.000	1.53E-14	1.54E-14	1.15E-14	9.21E-15	7.68E-15
1.9	0.2	5.205	7.390	10.492	0.345	0.595	0.060	0.00E+00	0.00E+00	0.00E+00	0.00E+00	2.65E-15
1.9	0.3	4.913	8.375	14.279	0.452	0.516	0.031	5.55E-15	8.13E-15	6.09E-15	1.37E-14	1.14E-14
1.9	0.4	4.826	9.974	20.615	0.561	0.424	0.015	6.13E-15	4.09E-15	7.69E-15	1.88E-14	4.52E-14
1.9	0.5	4.920	12.491	31.712	0.665	0.329	0.006	5.86E-15	3.91E-15	2.93E-15	7.27E-15	6.06E-15
1.9	0.6	5.183	16.444	52.169	0.757	0.241	0.002	0.00E+00	5.16E-15	7.63E-15	1.02E-14	1.17E-14
1.9	0.7	5.620	22.760	92.175	0.833	0.167	0.001	0.00E+00	3.98E-15	7.18E-15	5.74E-15	4.78E-15
1.9	0.8	6.243	33.116	175.665	0.891	0.109	0.000	1.11E-14	7.40E-15	5.55E-15	4.44E-15	3.70E-15
1.9	0.9	7.073	50.654	362.745	0.933	0.067	0.000	8.86E-15	1.01E-14	1.16E-14	9.24E-15	7.70E-15
2.0	0.2	5.747	8.160	11.586	0.343	0.597	0.060	0.00E+00	4.00E-15	3.00E-15	1.13E-14	1.48E-14

Table 4.2. (continued)

μ	σ	x_1'	x_2'	x_3'	ω_1'	ω_2'	ω_3'	F.E. ¹	F.E. ²	F.E. ³	F.E. ⁴	F.E. ⁵
2.0	0.3	5.427	9.253	15.775	0.452	0.517	0.031	5.75E-15	1.11E-14	1.30E-14	1.63E-14	1.72E-14
2.0	0.4	5.334	11.025	22.787	0.562	0.424	0.015	0.00E+00	6.30E-15	1.16E-14	1.27E-14	1.65E-14
2.0	0.5	5.437	13.805	35.049	0.665	0.329	0.006	0.00E+00	5.26E-15	3.95E-15	3.16E-15	4.57E-15
2.0	0.6	5.729	18.175	57.659	0.757	0.241	0.002	1.56E-14	1.88E-14	1.69E-14	1.63E-14	1.36E-14
2.0	0.7	6.211	25.154	101.868	0.833	0.167	0.001	1.88E-14	5.16E-14	7.60E-14	8.02E-14	6.68E-14
2.0	0.8	6.899	36.598	194.139	0.891	0.109	0.000	8.73E-15	2.03E-14	3.74E-14	4.39E-14	3.66E-14
2.0	0.9	7.817	55.981	400.896	0.933	0.067	0.000	0.00E+00	0.00E+00	2.94E-15	2.36E-15	1.96E-15
2.1	0.2	6.361	9.031	12.821	0.346	0.594	0.059	1.07E-14	7.11E-15	9.69E-15	1.37E-14	1.05E-14
2.1	0.3	6.000	10.228	17.438	0.452	0.516	0.031	0.00E+00	0.00E+00	6.96E-15	1.75E-14	2.33E-14
2.1	0.4	5.895	12.185	25.184	0.562	0.424	0.015	0.00E+00	0.00E+00	0.00E+00	0.00E+00	0.00E+00
2.1	0.5	6.009	15.257	38.736	0.665	0.328	0.006	0.00E+00	4.31E-15	1.00E-14	1.24E-14	1.27E-14
2.1	0.6	6.331	20.085	63.720	0.757	0.241	0.002	5.55E-15	1.06E-14	1.21E-14	1.33E-14	1.11E-14
2.1	0.7	6.864	27.799	112.581	0.833	0.167	0.001	8.51E-15	1.63E-14	2.61E-14	2.86E-14	2.39E-14
2.1	0.8	7.625	40.447	214.557	0.891	0.109	0.000	7.90E-15	1.71E-14	2.22E-14	2.40E-14	2.00E-14
2.1	0.9	8.639	61.868	443.057	0.933	0.067	0.000	5.55E-15	3.70E-15	7.14E-15	5.71E-15	4.76E-15
2.2	0.2	7.026	9.975	14.163	0.345	0.595	0.060	9.65E-15	6.43E-15	4.82E-15	3.86E-15	5.67E-15
2.2	0.3	6.630	11.303	19.270	0.452	0.517	0.031	0.00E+00	4.86E-15	8.80E-15	7.04E-15	5.87E-15
2.2	0.4	6.514	13.463	27.825	0.561	0.424	0.015	9.08E-15	1.03E-14	1.90E-14	2.74E-14	3.60E-14
2.2	0.5	6.641	16.860	42.806	0.665	0.329	0.006	1.42E-14	1.65E-14	1.24E-14	1.29E-14	1.07E-14
2.2	0.6	6.997	22.199	70.427	0.757	0.241	0.002	2.47E-14	4.47E-14	6.42E-14	6.61E-14	5.51E-14
2.2	0.7	7.586	30.722	124.421	0.833	0.167	0.001	0.00E+00	0.00E+00	0.00E+00	0.00E+00	0.00E+00
2.2	0.8	8.427	44.702	237.126	0.891	0.109	0.000	7.15E-15	1.77E-14	2.72E-14	2.17E-14	1.81E-14
2.2	0.9	9.548	68.374	489.653	0.933	0.067	0.000	0.00E+00	0.00E+00	0.00E+00	0.00E+00	0.00E+00
2.3	0.2	7.794	11.066	15.711	0.353	0.589	0.057	8.73E-15	1.02E-14	1.24E-14	1.26E-14	7.36E-15
2.3	0.3	7.333	12.501	21.310	0.453	0.515	0.031	0.00E+00	0.00E+00	3.82E-15	3.06E-15	2.55E-15
2.3	0.4	7.198	14.876	30.746	0.561	0.424	0.015	0.00E+00	0.00E+00	0.00E+00	4.09E-15	8.73E-15
2.3	0.5	7.339	18.633	47.308	0.665	0.329	0.006	0.00E+00	5.78E-15	4.33E-15	3.47E-15	6.34E-15
2.3	0.6	7.733	24.533	77.832	0.757	0.241	0.002	7.44E-15	9.59E-15	1.17E-14	1.27E-14	1.06E-14
2.3	0.7	8.384	33.953	137.505	0.833	0.167	0.001	6.97E-15	1.18E-14	8.85E-15	7.08E-15	5.90E-15
2.3	0.8	9.313	49.403	262.064	0.891	0.109	0.000	0.00E+00	5.30E-15	9.12E-15	7.29E-15	6.08E-15
2.3	0.9	10.552	75.565	541.150	0.933	0.067	0.000	0.00E+00	1.13E-14	1.33E-14	1.06E-14	8.85E-15
2.4	0.2	8.574	12.171	17.278	0.343	0.596	0.061	7.90E-15	1.25E-14	1.64E-14	1.31E-14	6.23E-15
2.4	0.3	8.095	13.801	23.528	0.452	0.517	0.031	0.00E+00	1.30E-14	9.77E-15	1.02E-14	1.04E-14
2.4	0.4	7.958	16.448	33.993	0.562	0.424	0.015	0.00E+00	5.66E-15	4.25E-15	3.40E-15	2.83E-15
2.4	0.5	8.111	20.593	52.284	0.665	0.329	0.006	0.00E+00	0.00E+00	5.51E-15	9.74E-15	1.02E-14
2.4	0.6	8.546	27.112	86.014	0.757	0.241	0.002	6.73E-15	4.49E-15	6.72E-15	5.38E-15	4.48E-15
2.4	0.7	9.266	37.525	151.970	0.833	0.167	0.001	6.31E-15	4.20E-15	3.15E-15	2.52E-15	2.10E-15
2.4	0.8	10.293	54.598	289.622	0.891	0.109	0.000	1.14E-14	1.63E-14	1.60E-14	1.66E-14	1.38E-14
2.4	0.9	11.662	83.513	598.065	0.933	0.067	0.000	1.07E-14	1.33E-14	1.36E-14	1.08E-14	9.03E-15

Table 4.2. (continued)

μ	σ	x_1'	x_2'	x_3'	ω_1'	ω_2'	ω_3'	F.E. ¹	F.E. ²	F.E. ³	F.E. ⁴	F.E. ⁵
2.5	0.2	9.482	13.461	19.109	0.345	0.595	0.060	0.00E+00	1.18E-14	1.41E-14	1.37E-14	6.94E-15
2.5	0.3	8.943	15.247	25.994	0.451	0.518	0.032	6.97E-15	4.65E-15	3.48E-15	6.00E-15	5.00E-15
2.5	0.4	8.792	18.171	37.556	0.561	0.424	0.015	1.23E-14	8.19E-15	9.20E-15	1.10E-14	1.31E-14
2.5	0.5	8.965	22.760	57.783	0.665	0.329	0.006	6.43E-15	8.16E-15	1.02E-14	1.17E-14	9.78E-15
2.5	0.6	9.445	29.964	95.064	0.757	0.241	0.002	2.38E-14	2.21E-14	2.15E-14	1.72E-14	1.44E-14
2.5	0.7	10.240	41.472	167.956	0.833	0.167	0.001	5.71E-15	2.30E-14	3.94E-14	3.99E-14	3.33E-14
2.5	0.8	11.375	60.341	320.082	0.891	0.109	0.000	0.00E+00	0.00E+00	0.00E+00	0.00E+00	0.00E+00
2.5	0.9	12.888	92.296	660.966	0.933	0.067	0.000	0.00E+00	5.05E-15	3.79E-15	3.03E-15	2.53E-15
2.6	0.2	10.459	14.851	21.087	0.341	0.598	0.061	0.00E+00	0.00E+00	3.89E-15	3.11E-15	1.27E-14
2.6	0.3	9.889	16.859	28.743	0.452	0.517	0.031	1.74E-14	1.16E-14	8.70E-15	6.96E-15	5.80E-15
2.6	0.4	9.719	20.087	41.515	0.561	0.424	0.015	0.00E+00	0.00E+00	4.53E-15	3.63E-15	3.02E-15
2.6	0.5	9.907	25.153	63.861	0.665	0.329	0.006	0.00E+00	6.34E-15	7.78E-15	8.62E-15	7.18E-15
2.6	0.6	10.438	33.116	105.062	0.757	0.241	0.002	0.00E+00	5.09E-15	7.50E-15	6.00E-15	5.00E-15
2.6	0.7	11.317	45.834	185.618	0.833	0.167	0.001	1.03E-14	6.88E-15	5.16E-15	9.75E-15	8.13E-15
2.6	0.8	12.572	66.687	353.748	0.891	0.109	0.000	9.58E-15	1.22E-14	1.33E-14	1.07E-14	8.89E-15
2.6	0.9	14.244	102.003	730.479	0.933	0.067	0.000	0.00E+00	4.14E-15	3.10E-15	2.48E-15	2.07E-15
2.7	0.2	11.541	16.387	23.267	0.337	0.601	0.062	5.85E-15	3.90E-15	8.69E-15	1.13E-14	1.59E-14
2.7	0.3	10.924	18.623	31.749	0.451	0.517	0.032	0.00E+00	7.15E-15	9.96E-15	1.38E-14	1.15E-14
2.7	0.4	10.739	22.196	45.876	0.561	0.424	0.015	0.00E+00	6.21E-15	4.66E-15	3.73E-15	3.11E-15
2.7	0.5	10.950	27.801	70.583	0.665	0.328	0.006	0.00E+00	5.19E-15	8.37E-15	1.31E-14	1.09E-14
2.7	0.6	11.536	36.597	116.106	0.757	0.241	0.002	1.99E-14	3.41E-14	3.65E-14	3.72E-14	3.10E-14
2.7	0.7	12.508	50.654	205.140	0.833	0.167	0.001	9.34E-15	6.23E-15	7.72E-15	6.17E-15	5.14E-15
2.7	0.8	13.894	73.700	390.951	0.891	0.109	0.000	2.60E-14	3.16E-14	3.30E-14	2.64E-14	2.20E-14
2.7	0.9	15.741	112.728	807.297	0.933	0.067	0.000	7.96E-15	5.31E-15	3.98E-15	3.18E-15	2.65E-15
2.8	0.2	12.851	18.244	25.896	0.353	0.589	0.057	1.06E-14	7.06E-15	5.29E-15	1.00E-14	1.24E-14
2.8	0.3	12.083	20.597	35.111	0.452	0.516	0.031	0.00E+00	0.00E+00	3.41E-15	2.73E-15	4.37E-15
2.8	0.4	11.870	24.532	50.702	0.561	0.424	0.015	5.55E-15	8.79E-15	6.59E-15	5.27E-15	4.39E-15
2.8	0.5	12.100	30.720	77.993	0.665	0.329	0.006	2.06E-14	1.80E-14	1.68E-14	1.78E-14	1.48E-14
2.8	0.6	12.749	40.445	128.315	0.757	0.241	0.002	9.02E-15	1.28E-14	1.37E-14	1.45E-14	1.21E-14
2.8	0.7	13.823	55.980	226.710	0.833	0.167	0.001	1.11E-14	1.79E-14	1.79E-14	1.44E-14	1.20E-14
2.8	0.8	15.355	81.452	432.067	0.891	0.109	0.000	5.55E-15	3.70E-15	7.37E-15	5.89E-15	4.91E-15
2.8	0.9	17.397	124.586	892.208	0.933	0.067	0.000	1.28E-14	8.50E-15	6.38E-15	5.10E-15	4.25E-15
2.9	0.2	14.145	20.079	28.501	0.344	0.595	0.060	0.00E+00	0.00E+00	0.00E+00	3.87E-15	7.68E-15
2.9	0.3	13.357	22.770	38.817	0.453	0.516	0.031	5.55E-15	8.49E-15	1.14E-14	1.43E-14	1.19E-14
2.9	0.4	13.119	27.114	56.040	0.561	0.424	0.015	0.00E+00	0.00E+00	0.00E+00	0.00E+00	0.00E+00
2.9	0.5	13.374	33.955	86.207	0.665	0.329	0.006	0.00E+00	6.96E-15	1.01E-14	1.10E-14	9.17E-15
2.9	0.6	14.090	44.702	141.818	0.757	0.241	0.002	0.00E+00	0.00E+00	3.00E-15	2.40E-15	2.00E-15
2.9	0.7	15.277	61.868	250.554	0.833	0.167	0.001	0.00E+00	0.00E+00	3.34E-15	2.67E-15	2.23E-15
2.9	0.8	16.970	90.019	477.513	0.891	0.109	0.000	0.00E+00	0.00E+00	3.40E-15	2.72E-15	2.27E-15

Table 4.2. (continued)

μ	σ	x_1'	x_2'	x_3'	ω_1'	ω_2'	ω_3'	F.E. ¹	F.E. ²	F.E. ³	F.E. ⁴	F.E. ⁵
2.9	0.9	19.227	137.690	986.044	0.933	0.067	0.000	6.52E-15	4.35E-15	3.26E-15	2.61E-15	2.17E-15
3.0	0.2	15.647	22.215	31.539	0.347	0.594	0.059	0.00E+00	0.00E+00	4.69E-15	3.75E-15	5.05E-15
3.0	0.3	14.757	25.160	42.895	0.452	0.516	0.031	0.00E+00	0.00E+00	0.00E+00	3.48E-15	2.90E-15
3.0	0.4	14.496	29.960	61.922	0.561	0.424	0.015	0.00E+00	0.00E+00	0.00E+00	3.98E-15	3.31E-15
3.0	0.5	14.781	37.528	95.280	0.665	0.328	0.006	1.56E-14	1.04E-14	1.14E-14	9.16E-15	7.63E-15
3.0	0.6	15.572	49.402	156.732	0.757	0.241	0.002	1.85E-14	1.69E-14	1.71E-14	1.37E-14	1.14E-14
3.0	0.7	16.883	68.374	276.903	0.833	0.167	0.001	6.92E-15	4.61E-15	3.46E-15	2.77E-15	2.31E-15
3.0	0.8	18.755	99.486	527.733	0.891	0.109	0.000	1.28E-14	1.90E-14	2.43E-14	1.95E-14	1.62E-14
3.0	0.9	21.249	152.172	1089.760	0.933	0.067	0.000	5.90E-15	3.93E-15	2.95E-15	2.36E-15	1.97E-15
3.1	0.2	17.291	24.548	34.852	0.346	0.594	0.059	7.84E-15	1.23E-14	1.62E-14	1.30E-14	6.45E-15
3.1	0.3	16.305	27.796	47.386	0.452	0.517	0.031	7.65E-15	1.15E-14	1.42E-14	1.60E-14	1.33E-14
3.1	0.4	16.023	33.116	68.443	0.561	0.424	0.015	7.39E-15	4.92E-15	3.69E-15	5.62E-15	4.68E-15
3.1	0.5	16.336	41.474	105.298	0.665	0.328	0.006	1.26E-14	1.77E-14	1.87E-14	2.02E-14	1.68E-14
3.1	0.6	17.210	54.599	173.218	0.757	0.241	0.002	0.00E+00	0.00E+00	3.29E-15	2.63E-15	2.19E-15
3.1	0.7	18.659	75.565	306.029	0.833	0.167	0.001	6.26E-15	9.95E-15	7.46E-15	5.97E-15	4.97E-15
3.1	0.8	20.727	109.948	583.231	0.891	0.109	0.000	0.00E+00	4.28E-15	3.21E-15	2.57E-15	2.14E-15
3.1	0.9	23.483	168.173	1204.350	0.933	0.067	0.000	1.07E-14	7.12E-15	1.23E-14	9.83E-15	8.19E-15
3.2	0.2	19.129	27.162	38.565	0.349	0.593	0.059	0.00E+00	0.00E+00	5.15E-15	8.78E-15	7.74E-15
3.2	0.3	18.024	30.729	52.386	0.452	0.516	0.031	6.92E-15	4.61E-15	7.57E-15	6.06E-15	5.05E-15
3.2	0.4	17.708	36.597	75.638	0.561	0.424	0.015	0.00E+00	9.14E-15	6.86E-15	9.06E-15	7.55E-15
3.2	0.5	18.052	45.831	116.357	0.665	0.329	0.006	0.00E+00	0.00E+00	4.00E-15	6.68E-15	5.57E-15
3.2	0.6	19.020	60.341	191.436	0.757	0.241	0.002	2.37E-14	2.81E-14	2.59E-14	2.07E-14	1.73E-14
3.2	0.7	20.621	83.512	338.212	0.833	0.167	0.001	0.00E+00	0.00E+00	0.00E+00	0.00E+00	0.00E+00
3.2	0.8	22.907	121.510	644.564	0.891	0.109	0.000	0.00E+00	7.00E-15	1.08E-14	8.63E-15	7.19E-15
3.2	0.9	25.953	185.861	1331.030	0.933	0.067	0.000	0.00E+00	4.98E-15	3.74E-15	2.99E-15	2.49E-15
3.3	0.2	21.141	30.013	42.607	0.349	0.593	0.059	1.20E-14	2.23E-14	2.05E-14	2.27E-14	3.99E-15
3.3	0.3	19.929	33.977	57.928	0.453	0.516	0.031	1.25E-14	1.27E-14	1.25E-14	1.00E-14	8.36E-15
3.3	0.4	19.570	40.446	83.593	0.561	0.424	0.015	6.05E-15	7.78E-15	1.03E-14	8.22E-15	6.85E-15
3.3	0.5	19.949	50.649	128.593	0.665	0.329	0.006	1.71E-14	1.14E-14	1.15E-14	1.15E-14	9.62E-15
3.3	0.6	21.020	66.689	211.574	0.757	0.241	0.002	0.00E+00	5.02E-15	7.38E-15	5.90E-15	4.92E-15
3.3	0.7	22.790	92.294	373.780	0.833	0.167	0.001	0.00E+00	3.87E-15	2.90E-15	2.32E-15	1.93E-15
3.3	0.8	25.316	134.290	712.356	0.891	0.109	0.000	2.46E-14	3.36E-14	4.16E-14	3.33E-14	2.77E-14
3.3	0.9	28.683	205.409	1471.010	0.933	0.067	0.000	0.00E+00	4.08E-15	3.06E-15	2.45E-15	2.04E-15
3.4	0.2	23.391	33.220	47.177	0.351	0.591	0.058	0.00E+00	0.00E+00	0.00E+00	0.00E+00	3.83E-15
3.4	0.3	22.004	37.512	63.952	0.451	0.517	0.031	1.13E-14	1.46E-14	1.55E-14	1.52E-14	1.27E-14
3.4	0.4	21.628	44.700	92.385	0.561	0.424	0.015	1.11E-14	1.35E-14	1.01E-14	8.12E-15	6.77E-15
3.4	0.5	22.049	55.980	142.124	0.665	0.329	0.006	1.05E-14	1.21E-14	1.35E-14	1.08E-14	8.97E-15
3.4	0.6	23.229	73.697	233.810	0.757	0.241	0.002	0.00E+00	0.00E+00	5.35E-15	4.28E-15	3.57E-15
3.4	0.7	25.187	102.006	413.104	0.833	0.167	0.001	0.00E+00	0.00E+00	2.98E-15	2.39E-15	1.99E-15

Table 4.2. (continued)

μ	σ	x_1'	x_2'	x_3'	ω_1'	ω_2'	ω_3'	F.E. ¹	F.E. ²	F.E. ³	F.E. ⁴	F.E. ⁵
3.4	0.8	27.978	148.414	787.278	0.891	0.109	0.000	8.61E-15	1.04E-14	7.83E-15	6.26E-15	5.22E-15
3.4	0.9	31.700	227.014	1625.720	0.933	0.067	0.000	0.00E+00	0.00E+00	2.83E-15	2.26E-15	1.88E-15
3.5	0.2	25.760	36.577	51.937	0.344	0.596	0.060	1.61E-14	2.35E-14	2.18E-14	2.02E-14	3.51E-15
3.5	0.3	24.319	41.459	70.681	0.451	0.517	0.031	0.00E+00	5.77E-15	7.67E-15	6.14E-15	5.11E-15
3.5	0.4	23.907	49.412	102.125	0.562	0.424	0.015	0.00E+00	5.02E-15	8.64E-15	6.91E-15	5.76E-15
3.5	0.5	24.371	61.875	157.092	0.665	0.328	0.006	9.47E-15	1.47E-14	1.43E-14	1.14E-14	9.52E-15
3.5	0.6	25.674	81.454	258.418	0.757	0.241	0.002	5.55E-15	1.04E-14	7.82E-15	6.26E-15	5.21E-15
3.5	0.7	27.836	112.731	456.545	0.833	0.167	0.001	0.00E+00	5.19E-15	8.31E-15	6.65E-15	5.54E-15
3.5	0.8	30.921	164.023	870.076	0.891	0.109	0.000	5.55E-15	7.54E-15	5.66E-15	4.53E-15	3.77E-15
3.5	0.9	35.033	250.887	1796.690	0.933	0.067	0.000	7.16E-15	1.02E-14	1.19E-14	9.49E-15	7.91E-15
3.6	0.2	28.486	40.443	57.422	0.345	0.595	0.060	0.00E+00	5.22E-15	7.02E-15	5.61E-15	7.82E-15
3.6	0.3	26.883	45.830	78.130	0.452	0.517	0.031	9.28E-15	1.09E-14	1.31E-14	1.30E-14	1.09E-14
3.6	0.4	26.415	54.595	112.837	0.561	0.424	0.015	2.01E-14	1.75E-14	1.31E-14	1.05E-14	8.74E-15
3.6	0.5	26.931	68.377	173.600	0.665	0.329	0.006	8.57E-15	1.26E-14	9.43E-15	7.55E-15	6.29E-15
3.6	0.6	28.374	90.020	285.594	0.757	0.241	0.002	0.00E+00	5.51E-15	7.07E-15	5.65E-15	4.71E-15
3.6	0.7	30.764	124.588	504.559	0.833	0.167	0.001	5.55E-15	7.95E-15	1.25E-14	1.00E-14	8.34E-15
3.6	0.8	34.173	181.272	961.582	0.891	0.109	0.000	0.00E+00	6.29E-15	4.72E-15	3.78E-15	3.15E-15
3.6	0.9	38.718	277.273	1985.660	0.933	0.067	0.000	6.47E-15	8.80E-15	6.60E-15	5.28E-15	4.40E-15
3.7	0.2	31.500	44.719	63.482	0.346	0.595	0.060	0.00E+00	4.28E-15	3.21E-15	5.09E-15	1.85E-15
3.7	0.3	29.708	50.646	86.344	0.452	0.517	0.031	8.40E-15	1.33E-14	1.73E-14	1.39E-14	1.16E-14
3.7	0.4	29.191	60.331	124.692	0.561	0.424	0.015	0.00E+00	0.00E+00	0.00E+00	0.00E+00	0.00E+00
3.7	0.5	29.766	75.572	191.866	0.665	0.328	0.006	0.00E+00	0.00E+00	0.00E+00	0.00E+00	0.00E+00
3.7	0.6	31.358	99.485	315.623	0.757	0.241	0.002	7.34E-15	4.89E-15	3.67E-15	2.93E-15	2.45E-15
3.7	0.7	33.998	137.689	557.620	0.833	0.167	0.001	1.11E-14	7.40E-15	5.55E-15	4.44E-15	3.70E-15
3.7	0.8	37.766	200.335	1062.700	0.891	0.109	0.000	6.38E-15	4.25E-15	3.19E-15	2.55E-15	2.13E-15
3.7	0.9	42.790	306.435	2194.500	0.933	0.067	0.000	5.86E-15	1.12E-14	1.30E-14	1.04E-14	8.68E-15
3.8	0.2	34.939	49.621	70.463	0.354	0.589	0.057	7.79E-15	5.19E-15	3.90E-15	3.12E-15	4.86E-15
3.8	0.3	32.840	55.984	95.438	0.452	0.517	0.031	0.00E+00	0.00E+00	5.43E-15	4.35E-15	3.62E-15
3.8	0.4	32.272	66.703	137.864	0.562	0.424	0.015	0.00E+00	5.51E-15	4.13E-15	3.31E-15	2.75E-15
3.8	0.5	32.893	83.511	212.025	0.665	0.329	0.006	7.01E-15	4.68E-15	8.80E-15	7.04E-15	5.86E-15
3.8	0.6	34.656	109.948	348.818	0.757	0.241	0.002	6.64E-15	4.43E-15	6.54E-15	5.23E-15	4.36E-15
3.8	0.7	37.574	152.171	616.270	0.833	0.167	0.001	6.22E-15	4.15E-15	1.03E-14	8.24E-15	6.86E-15
3.8	0.8	41.738	221.405	1174.470	0.891	0.109	0.000	5.77E-15	8.07E-15	9.71E-15	7.77E-15	6.47E-15
3.8	0.9	47.290	338.657	2425.260	0.933	0.067	0.000	1.06E-14	7.07E-15	5.30E-15	4.24E-15	3.53E-15
3.9	0.2	38.599	54.816	77.836	0.353	0.590	0.057	0.00E+00	5.73E-15	9.34E-15	7.47E-15	0.00E+00
3.9	0.3	36.274	61.840	105.426	0.451	0.517	0.032	6.87E-15	9.77E-15	7.33E-15	5.86E-15	4.89E-15
3.9	0.4	35.663	73.711	152.347	0.561	0.424	0.015	6.64E-15	8.94E-15	6.70E-15	5.36E-15	4.47E-15
3.9	0.5	36.354	92.297	234.329	0.665	0.329	0.006	5.55E-15	3.70E-15	6.69E-15	5.36E-15	4.46E-15
3.9	0.6	38.302	121.516	385.518	0.757	0.241	0.002	0.00E+00	6.05E-15	4.53E-15	3.63E-15	3.02E-15

Table 4.2. (continued)

μ	σ	x_1'	x_2'	x_3'	ω_1'	ω_2'	ω_3'	F.E. ¹	F.E. ²	F.E. ³	F.E. ⁴	F.E. ⁵
3.9	0.7	41.527	168.179	681.099	0.833	0.167	0.001	5.63E-15	8.41E-15	1.16E-14	9.31E-15	7.76E-15
3.9	0.8	46.128	244.693	1298.000	0.891	0.109	0.000	1.04E-14	1.39E-14	1.04E-14	8.32E-15	6.94E-15
3.9	0.9	52.263	374.277	2680.340	0.933	0.067	0.000	0.00E+00	0.00E+00	0.00E+00	0.00E+00	0.00E+00
4.0	0.2	42.587	60.468	85.851	0.349	0.592	0.058	0.00E+00	0.00E+00	0.00E+00	0.00E+00	0.00E+00
4.0	0.3	40.131	68.418	116.637	0.453	0.516	0.031	0.00E+00	0.00E+00	2.98E-15	2.39E-15	1.99E-15
4.0	0.4	39.412	81.458	168.357	0.561	0.424	0.015	2.31E-14	1.54E-14	1.59E-14	1.27E-14	1.06E-14
4.0	0.5	40.176	102.001	258.966	0.665	0.329	0.006	1.15E-14	1.38E-14	1.91E-14	1.53E-14	1.27E-14
4.0	0.6	42.328	134.289	426.036	0.757	0.241	0.002	0.00E+00	4.95E-15	3.71E-15	2.97E-15	2.48E-15
4.0	0.7	45.894	185.865	752.724	0.833	0.167	0.001	1.02E-14	1.06E-14	1.19E-14	9.52E-15	7.93E-15
4.0	0.8	50.980	270.431	1434.530	0.891	0.109	0.000	9.45E-15	1.20E-14	8.97E-15	7.17E-15	5.98E-15
4.0	0.9	57.761	413.645	2962.250	0.933	0.067	0.000	0.00E+00	4.03E-15	3.02E-15	2.42E-15	3.70E-15
4.1	0.2	47.071	66.841	94.912	0.350	0.592	0.058	1.15E-14	1.15E-14	1.42E-14	1.13E-14	7.62E-15
4.1	0.3	44.331	75.579	128.852	0.452	0.516	0.031	5.63E-15	3.75E-15	2.81E-15	2.25E-15	1.88E-15
4.1	0.4	43.559	90.029	186.069	0.561	0.424	0.015	1.09E-14	7.25E-15	5.44E-15	4.35E-15	3.62E-15
4.1	0.5	44.402	112.730	286.206	0.665	0.329	0.006	0.00E+00	0.00E+00	0.00E+00	0.00E+00	0.00E+00
4.1	0.6	46.779	148.407	470.833	0.757	0.241	0.002	9.84E-15	1.47E-14	1.62E-14	1.30E-14	1.08E-14
4.1	0.7	50.720	205.411	831.882	0.833	0.167	0.001	9.22E-15	1.24E-14	1.51E-14	1.21E-14	1.01E-14
4.1	0.8	56.341	298.866	1585.370	0.891	0.109	0.000	8.55E-15	1.50E-14	1.42E-14	1.14E-14	9.46E-15
4.1	0.9	63.834	457.140	3273.770	0.933	0.067	0.000	0.00E+00	0.00E+00	0.00E+00	0.00E+00	0.00E+00
4.2	0.2	51.938	73.743	104.702	0.346	0.594	0.059	0.00E+00	0.00E+00	0.00E+00	0.00E+00	5.88E-15
4.2	0.3	48.981	83.504	142.360	0.452	0.517	0.031	0.00E+00	0.00E+00	3.27E-15	2.62E-15	2.18E-15
4.2	0.4	48.134	99.484	205.613	0.561	0.424	0.015	2.09E-14	1.40E-14	1.05E-14	8.38E-15	6.98E-15
4.2	0.5	49.072	124.588	316.312	0.665	0.329	0.006	0.00E+00	4.13E-15	6.29E-15	5.03E-15	4.19E-15
4.2	0.6	51.701	164.027	520.385	0.757	0.241	0.002	0.00E+00	6.64E-15	4.98E-15	3.98E-15	3.32E-15
4.2	0.7	56.055	227.014	919.370	0.833	0.167	0.001	0.00E+00	0.00E+00	0.00E+00	0.00E+00	0.00E+00
4.2	0.8	62.267	330.301	1752.110	0.891	0.109	0.000	2.10E-14	1.78E-14	1.34E-14	1.07E-14	8.90E-15
4.2	0.9	70.549	505.231	3618.140	0.933	0.067	0.000	0.00E+00	0.00E+00	0.00E+00	0.00E+00	0.00E+00
4.3	0.2	57.352	81.429	115.614	0.344	0.596	0.060	9.45E-15	1.15E-14	8.59E-15	6.87E-15	5.00E-15
4.3	0.3	54.128	92.280	157.322	0.452	0.517	0.031	9.22E-15	6.14E-15	4.61E-15	3.69E-15	3.07E-15
4.3	0.4	53.203	109.964	227.282	0.561	0.424	0.015	0.00E+00	4.05E-15	6.58E-15	5.26E-15	4.39E-15
4.3	0.5	54.234	137.693	349.583	0.665	0.329	0.006	0.00E+00	6.77E-15	5.08E-15	4.06E-15	3.39E-15
4.3	0.6	57.136	181.265	575.081	0.757	0.241	0.002	8.05E-15	5.37E-15	4.03E-15	3.22E-15	2.68E-15
4.3	0.7	61.950	250.888	1016.060	0.833	0.167	0.001	0.00E+00	0.00E+00	3.21E-15	2.56E-15	2.14E-15
4.3	0.8	68.815	365.039	1936.390	0.891	0.109	0.000	0.00E+00	0.00E+00	0.00E+00	0.00E+00	0
4.3	0.9	77.968	558.356	3998.580	0.933	0.067	0.000	0.00E+00	4.42E-15	3.31E-15	2.65E-15	2.21E-15
4.4	0.2	63.383	89.983	127.748	0.344	0.596	0.060	0.00E+00	0.00E+00	4.50E-15	3.60E-15	5.11E-15
4.4	0.3	59.841	102.018	173.919	0.452	0.516	0.031	8.34E-15	9.38E-15	1.06E-14	8.50E-15	7.08E-15
4.4	0.4	58.778	121.475	251.059	0.561	0.424	0.015	0.00E+00	0.00E+00	0.00E+00	0.00E+00	0.00E+00
4.4	0.5	59.938	152.173	386.345	0.665	0.329	0.006	7.70E-15	1.07E-14	8.01E-15	6.41E-15	5.34E-15

Table 4.2. (continued)

μ	σ	x_1'	x_2'	x_3'	ω_1'	ω_2'	ω_3'	F.E. ¹	F.E. ²	F.E. ³	F.E. ⁴	F.E. ⁵
4.4	0.6	63.147	200.337	635.581	0.757	0.241	0.002	0.00E+00	0.00E+00	0.00E+00	0.00E+00	0.00E+00
4.4	0.7	68.463	277.266	1122.900	0.833	0.167	0.001	1.24E-14	2.20E-14	1.65E-14	1.32E-14	1.10E-14
4.4	0.8	76.052	403.427	2140.040	0.891	0.109	0.000	6.33E-15	4.22E-15	3.17E-15	2.53E-15	2.11E-15
4.4	0.9	86.168	617.083	4419.160	0.933	0.067	0.000	0.00E+00	7.23E-15	5.43E-15	4.34E-15	3.62E-15
4.5	0.2	70.029	99.422	141.154	0.344	0.596	0.060	0.00E+00	0.00E+00	3.33E-15	2.67E-15	3.45E-15
4.5	0.3	66.175	112.826	192.353	0.453	0.516	0.031	7.55E-15	1.13E-14	8.46E-15	6.77E-15	5.64E-15
4.5	0.4	64.977	134.298	277.573	0.561	0.424	0.015	0.00E+00	0.00E+00	3.88E-15	3.11E-15	2.59E-15
4.5	0.5	66.246	168.189	427.003	0.665	0.328	0.006	1.11E-14	1.19E-14	8.96E-15	7.16E-15	5.97E-15
4.5	0.6	69.792	221.422	702.475	0.757	0.241	0.002	0.00E+00	7.28E-15	5.46E-15	4.37E-15	3.64E-15
4.5	0.7	75.666	306.437	1241.020	0.833	0.167	0.001	6.18E-15	9.74E-15	7.30E-15	5.84E-15	4.87E-15
4.5	0.8	84.051	445.855	2365.100	0.891	0.109	0.000	0.00E+00	4.16E-15	3.12E-15	2.50E-15	2.08E-15
4.5	0.9	95.231	681.982	4883.900	0.933	0.067	0.000	1.05E-14	7.02E-15	5.26E-15	4.21E-15	3.51E-15
4.6	0.2	77.619	110.196	156.438	0.350	0.592	0.058	0.00E+00	5.66E-15	4.24E-15	3.39E-15	6.12E-15
4.6	0.3	73.102	124.640	212.503	0.453	0.516	0.031	1.79E-14	1.20E-14	1.29E-14	1.03E-14	8.61E-15
4.6	0.4	71.804	148.404	306.721	0.561	0.424	0.015	0.00E+00	0.00E+00	0.00E+00	0.00E+00	0.00E+00
4.6	0.5	73.202	185.855	471.871	0.665	0.329	0.006	6.30E-15	7.92E-15	5.94E-15	4.75E-15	3.96E-15
4.6	0.6	77.126	244.690	776.307	0.757	0.241	0.002	5.97E-15	1.59E-14	1.19E-14	9.54E-15	7.95E-15
4.6	0.7	83.621	338.655	1371.520	0.833	0.167	0.001	1.11E-14	1.20E-14	9.02E-15	7.22E-15	6.01E-15
4.6	0.8	92.892	492.755	2613.860	0.891	0.109	0.000	0.00E+00	6.81E-15	5.11E-15	4.09E-15	3.41E-15
4.6	0.9	105.246	753.705	5397.560	0.933	0.067	0.000	0.00E+00	9.70E-15	7.27E-15	5.82E-15	4.85E-15
4.7	0.2	85.334	121.174	172.078	0.339	0.600	0.062	5.55E-15	3.70E-15	2.78E-15	2.22E-15	4.22E-15
4.7	0.3	80.824	137.790	234.898	0.453	0.516	0.031	1.17E-14	7.82E-15	1.17E-14	9.37E-15	7.80E-15
4.7	0.4	79.361	164.025	339.007	0.561	0.424	0.015	5.97E-15	1.13E-14	8.45E-15	6.76E-15	5.63E-15
4.7	0.5	80.898	205.396	521.497	0.665	0.329	0.006	5.70E-15	3.80E-15	5.70E-15	4.56E-15	3.80E-15
4.7	0.6	85.241	270.430	857.957	0.757	0.241	0.002	0.00E+00	4.88E-15	3.66E-15	2.93E-15	2.44E-15
4.7	0.7	92.417	374.273	1515.750	0.833	0.167	0.001	0.00E+00	3.76E-15	2.82E-15	2.26E-15	1.88E-15
4.7	0.8	102.660	544.574	2888.770	0.891	0.109	0.000	0.00E+00	5.58E-15	4.18E-15	3.35E-15	2.79E-15
4.7	0.9	116.315	832.971	5965.210	0.933	0.067	0.000	8.62E-15	1.37E-14	1.03E-14	8.21E-15	6.84E-15
4.8	0.2	94.666	134.422	190.868	0.347	0.594	0.059	5.73E-15	3.82E-15	2.87E-15	2.29E-15	1.90E-15
4.8	0.3	89.178	152.037	259.218	0.451	0.518	0.032	0.00E+00	0.00E+00	0.00E+00	0.00E+00	0.00E+00
4.8	0.4	87.719	181.296	374.700	0.561	0.424	0.015	5.55E-15	3.70E-15	2.78E-15	2.22E-15	1.85E-15
4.8	0.5	89.409	226.997	576.315	0.665	0.329	0.006	0.00E+00	0.00E+00	0.00E+00	0.00E+00	0.00E+00
4.8	0.6	94.199	298.854	948.140	0.757	0.241	0.002	0.00E+00	0.00E+00	0.00E+00	0.00E+00	0.00E+00
4.8	0.7	102.137	413.645	1675.220	0.833	0.167	0.001	0.00E+00	6.17E-15	4.62E-15	3.70E-15	3.08E-15
4.8	0.8	113.456	601.839	3192.530	0.891	0.109	0.000	5.55E-15	8.27E-15	6.20E-15	4.96E-15	4.13E-15
4.8	0.9	128.548	920.577	6592.570	0.933	0.067	0.000	0.00E+00	0.00E+00	0.00E+00	0.00E+00	0.00E+00
4.9	0.2	104.883	148.892	211.351	0.352	0.590	0.058	0.00E+00	6.21E-15	4.66E-15	3.72E-15	3.46E-15
4.9	0.3	98.667	168.208	286.760	0.452	0.516	0.031	1.01E-14	6.74E-15	5.06E-15	4.05E-15	3.37E-15
4.9	0.4	96.925	200.336	414.081	0.561	0.424	0.015	0.00E+00	4.88E-15	3.66E-15	2.93E-15	2.44E-15

Table 4.2. (continued)

μ	σ	x_1'	x_2'	x_3'	ω_1'	ω_2'	ω_3'	F.E. ¹	F.E. ²	F.E. ³	F.E. ⁴	F.E. ⁵
4.9	0.5	98.817	250.885	636.966	0.665	0.329	0.006	9.34E-15	6.23E-15	4.67E-15	3.74E-15	3.11E-15
4.9	0.6	104.111	330.296	1047.880	0.757	0.241	0.002	0.00E+00	0.00E+00	0.00E+00	0.00E+00	0.00E+00
4.9	0.7	112.880	457.152	1851.410	0.833	0.167	0.001	1.38E-14	1.93E-14	1.45E-14	1.16E-14	9.66E-15
4.9	0.8	125.389	665.142	3528.330	0.891	0.109	0.000	7.68E-15	8.86E-15	6.65E-15	5.32E-15	4.43E-15
4.9	0.9	142.067	1017.400	7285.960	0.933	0.067	0.000	1.82E-14	2.28E-14	1.71E-14	1.37E-14	1.14E-14
5.0	0.2	115.227	163.614	232.334	0.339	0.599	0.061	0.00E+00	5.08E-15	3.81E-15	3.05E-15	2.54E-15
5.0	0.3	108.991	185.823	316.819	0.452	0.517	0.031	0.00E+00	9.20E-15	6.90E-15	5.52E-15	4.60E-15
5.0	0.4	107.123	221.407	457.618	0.561	0.424	0.015	0.00E+00	8.00E-15	6.00E-15	4.80E-15	4.00E-15
5.0	0.5	109.214	277.283	703.987	0.665	0.328	0.006	0.00E+00	0.00E+00	0.00E+00	0.00E+00	0.00E+00
5.0	0.6	115.059	365.027	1158.070	0.757	0.241	0.002	0.00E+00	0.00E+00	0.00E+00	0.00E+00	0.00E+00
5.0	0.7	124.751	505.225	2046.100	0.833	0.167	0.001	1.11E-14	7.40E-15	5.55E-15	4.44E-15	3.70E-15
5.0	0.8	138.577	735.097	3899.410	0.891	0.109	0.000	0.00E+00	6.12E-15	4.59E-15	3.67E-15	3.06E-15
5.0	0.9	157.007	1124.380	8052.130	0.933	0.067	0.000	1.19E-14	1.23E-14	9.24E-15	7.39E-15	6.16E-15
5.1	0.2	127.557	181.144	257.247	0.343	0.597	0.060	8.49E-15	5.66E-15	4.25E-15	3.40E-15	2.83E-15
5.1	0.3	120.419	205.304	350.034	0.451	0.517	0.032	0.00E+00	0.00E+00	0.00E+00	0.00E+00	0.00E+00
5.1	0.4	118.402	244.711	505.762	0.561	0.424	0.015	0.00E+00	6.55E-15	4.91E-15	3.93E-15	3.27E-15
5.1	0.5	120.689	306.415	777.953	0.665	0.329	0.006	0.00E+00	0.00E+00	0.00E+00	0.00E+00	0.00E+00
5.1	0.6	127.163	403.434	1279.930	0.757	0.241	0.002	7.24E-15	9.21E-15	6.91E-15	5.53E-15	4.61E-15
5.1	0.7	137.871	558.356	2261.260	0.833	0.167	0.001	0.00E+00	0.00E+00	0.00E+00	0.00E+00	0.00E+00
5.1	0.8	153.151	812.409	4309.520	0.891	0.109	0.000	6.29E-15	9.21E-15	6.91E-15	5.52E-15	4.60E-15
5.1	0.9	173.521	1242.660	8899.090	0.933	0.067	0.000	5.78E-15	3.85E-15	2.89E-15	2.31E-15	1.93E-15
5.2	0.2	141.087	200.325	284.438	0.345	0.595	0.060	7.68E-15	1.19E-14	8.95E-15	7.16E-15	0.00E+00
5.2	0.3	133.204	227.092	387.156	0.452	0.516	0.031	0.00E+00	0.00E+00	0.00E+00	0.00E+00	0.00E+00
5.2	0.4	130.843	270.423	558.911	0.561	0.424	0.015	1.11E-14	1.22E-14	9.17E-15	7.34E-15	6.11E-15
5.2	0.5	133.380	338.633	859.759	0.665	0.329	0.006	1.25E-14	8.31E-15	6.23E-15	4.99E-15	4.16E-15
5.2	0.6	140.531	445.840	1414.450	0.757	0.241	0.002	6.55E-15	4.37E-15	3.27E-15	2.62E-15	2.18E-15
5.2	0.7	152.371	617.082	2499.090	0.833	0.167	0.001	6.14E-15	9.63E-15	7.22E-15	5.78E-15	4.82E-15
5.2	0.8	169.258	897.842	4762.710	0.891	0.109	0.000	0.00E+00	4.10E-15	3.08E-15	2.46E-15	2.05E-15
5.2	0.9	191.770	1373.330	9834.970	0.933	0.067	0.000	1.05E-14	6.97E-15	5.23E-15	4.18E-15	3.49E-15
5.3	0.2	155.977	221.472	314.475	0.345	0.595	0.060	6.95E-15	1.02E-14	7.66E-15	6.13E-15	6.02E-15
5.3	0.3	147.150	250.856	427.657	0.452	0.517	0.031	0.00E+00	0.00E+00	0.00E+00	0.00E+00	0.00E+00
5.3	0.4	144.572	298.795	617.547	0.561	0.424	0.015	0.00E+00	0.00E+00	0.00E+00	0.00E+00	0.00E+00
5.3	0.5	147.412	374.262	950.223	0.665	0.329	0.006	0.00E+00	7.33E-15	5.50E-15	4.40E-15	3.67E-15
5.3	0.6	155.319	492.758	1563.300	0.757	0.241	0.002	5.92E-15	9.83E-15	7.37E-15	5.90E-15	4.92E-15
5.3	0.7	168.392	681.958	2761.850	0.833	0.167	0.001	1.11E-14	7.40E-15	5.55E-15	4.44E-15	3.70E-15
5.3	0.8	187.054	992.241	5263.490	0.891	0.109	0.000	2.14E-14	2.10E-14	1.57E-14	1.26E-14	1.05E-14
5.3	0.9	211.938	1517.760	10869.200	0.933	0.067	0.000	2.06E-14	1.37E-14	1.03E-14	8.23E-15	6.85E-15
5.4	0.2	172.033	244.238	346.768	0.341	0.598	0.061	1.11E-14	1.20E-14	8.98E-15	7.18E-15	8.08E-15
5.4	0.3	162.574	277.162	472.523	0.451	0.517	0.031	6.14E-15	8.22E-15	6.17E-15	4.93E-15	4.11E-15

Table 4.2. (continued)

μ	σ	x_1'	x_2'	x_3'	ω_1'	ω_2'	ω_3'	F.E. ¹	F.E. ²	F.E. ³	F.E. ⁴	F.E. ⁵
5.4	0.4	159.805	330.276	682.601	0.561	0.424	0.015	1.15E-14	1.48E-14	1.11E-14	8.90E-15	7.42E-15
5.4	0.5	162.922	413.641	1050.190	0.665	0.329	0.006	1.68E-14	1.12E-14	8.38E-15	6.71E-15	5.59E-15
5.4	0.6	171.652	544.573	1727.690	0.757	0.241	0.002	0.00E+00	9.63E-15	7.22E-15	5.78E-15	4.82E-15
5.4	0.7	186.108	753.708	3052.420	0.833	0.167	0.001	0.00E+00	0.00E+00	0.00E+00	0.00E+00	0.00E+00
5.4	0.8	206.735	1096.650	5817.270	0.891	0.109	0.000	0.00E+00	1.10E-14	8.25E-15	6.60E-15	5.50E-15
5.4	0.9	234.228	1677.390	12012.400	0.933	0.067	0.000	1.11E-14	1.13E-14	8.49E-15	6.79E-15	5.66E-15
5.5	0.2	190.543	270.549	384.152	0.346	0.595	0.059	1.14E-14	1.13E-14	8.50E-15	6.80E-15	3.72E-15
5.5	0.3	179.827	306.575	522.648	0.453	0.516	0.031	5.55E-15	3.70E-15	2.78E-15	2.22E-15	1.85E-15
5.5	0.4	176.642	365.086	754.562	0.561	0.424	0.015	0.00E+00	5.88E-15	4.41E-15	3.53E-15	2.94E-15
5.5	0.5	180.056	457.145	1160.650	0.665	0.329	0.006	2.14E-14	1.42E-14	1.07E-14	8.54E-15	7.12E-15
5.5	0.6	189.709	601.867	1909.450	0.757	0.241	0.002	9.70E-15	1.04E-14	7.81E-15	6.25E-15	5.21E-15
5.5	0.7	205.684	832.995	3373.500	0.833	0.167	0.001	0.00E+00	0.00E+00	0.00E+00	0.00E+00	0.00E+00
5.5	0.8	228.473	1211.960	6428.960	0.891	0.109	0.000	5.55E-15	1.27E-14	9.53E-15	7.63E-15	6.36E-15
5.5	0.9	258.863	1853.820	13275.800	0.933	0.067	0.000	0.00E+00	0.00E+00	0.00E+00	0.00E+00	0.00E+00

Notably, x_2 and x_3 are significantly separated in table 4.2. In some cases, e.g., $\mu = 0.3\sim 5.5$ and $\sigma = 0.7\sim 0.9$, x_3 is much greater than its 99.5% percentile. Table 4.3 shows where x_1 , x_2 and x_3 locate in terms of percentile.

Table 4.3. Percentile locations for x_1 , x_2 and x_3

μ	σ	x_1	x_2	x_3
0.3~5.5	0.2~0.3	5%~35%	65%~95%	95%~99.5%
0.3~5.5	0.4~0.9	35%~65%	65%~95%	>99.5%
0.3~5.5	0.7~0.9	35%~65%	95%~99.5%	>99.5%

The common remedy for the numerical moment matching is to apply 10%, 50%, and 90% percentile locations as x_1 , x_2 and x_3 . For the weights, 0.3, 0.4 and 0.3 are applied. Table

4.4 represents the result. The average F.E. is 26.07%. In order to obtain a simple and more accurate remedy, x_1 , x_2 and x_3 should be relocated properly, and the weights remain unmoved. Table 4.5 shows the method to relocate x_1 , x_2 and x_3 . The average F.E. is decreased to 13.86%, and F.E. is decreased for each case (Table 4.6).

Table 4.4. The result of common remedy

μ	σ	x_1'	x_2'	x_3'	ω_1'	ω_2'	ω_3'	F.E. ¹	F.E. ²	F.E. ³	F.E. ⁴	F.E. ⁵
0.3	0.2	1.045	1.350	1.744	0.300	0.400	0.300	1.89E-02	9.60E-02	3.00E-01	7.22E-01	1.46E+00
0.3	0.3	0.919	1.350	1.983	0.300	0.400	0.300	5.42E-02	3.40E-01	1.15E+00	2.81E+00	5.51E+00
0.3	0.4	0.808	1.350	2.254	0.300	0.400	0.300	1.25E-01	8.87E-01	3.02E+00	7.01E+00	1.28E+01
0.3	0.5	0.711	1.350	2.562	0.300	0.400	0.300	2.51E-01	1.88E+00	6.16E+00	1.32E+01	2.20E+01
0.3	0.6	0.626	1.350	2.912	0.300	0.400	0.300	4.56E-01	3.45E+00	1.06E+01	2.07E+01	3.12E+01
0.3	0.7	0.550	1.350	3.310	0.300	0.400	0.300	7.66E-01	5.64E+00	1.59E+01	2.82E+01	3.92E+01
0.3	0.8	0.484	1.350	3.763	0.300	0.400	0.300	1.20E+00	8.46E+00	2.16E+01	3.51E+01	4.56E+01
0.3	0.9	0.426	1.350	4.278	0.300	0.400	0.300	1.80E+00	1.18E+01	2.74E+01	4.10E+01	5.07E+01
0.4	0.2	1.155	1.492	1.928	0.300	0.400	0.300	1.89E-02	9.60E-02	3.00E-01	7.22E-01	1.46E+00
0.4	0.3	1.016	1.492	2.191	0.300	0.400	0.300	5.42E-02	3.40E-01	1.15E+00	2.81E+00	5.51E+00
0.4	0.4	0.893	1.492	2.491	0.300	0.400	0.300	1.25E-01	8.87E-01	3.02E+00	7.01E+00	1.28E+01
0.4	0.5	0.786	1.492	2.831	0.300	0.400	0.300	2.51E-01	1.88E+00	6.16E+00	1.32E+01	2.20E+01
0.4	0.6	0.691	1.492	3.219	0.300	0.400	0.300	4.56E-01	3.45E+00	1.06E+01	2.07E+01	3.12E+01
0.4	0.7	0.608	1.492	3.659	0.300	0.400	0.300	7.66E-01	5.64E+00	1.59E+01	2.82E+01	3.92E+01
0.4	0.8	0.535	1.492	4.159	0.300	0.400	0.300	1.20E+00	8.46E+00	2.16E+01	3.51E+01	4.56E+01
0.4	0.9	0.471	1.492	4.727	0.300	0.400	0.300	1.80E+00	1.18E+01	2.74E+01	4.10E+01	5.07E+01
0.5	0.2	1.276	1.649	2.130	0.300	0.400	0.300	1.89E-02	9.60E-02	3.00E-01	7.22E-01	1.46E+00
0.5	0.3	1.122	1.649	2.422	0.300	0.400	0.300	5.42E-02	3.40E-01	1.15E+00	2.81E+00	5.51E+00
0.5	0.4	0.987	1.649	2.753	0.300	0.400	0.300	1.25E-01	8.87E-01	3.02E+00	7.01E+00	1.28E+01
0.5	0.5	0.869	1.649	3.129	0.300	0.400	0.300	2.51E-01	1.88E+00	6.16E+00	1.32E+01	2.20E+01
0.5	0.6	0.764	1.649	3.557	0.300	0.400	0.300	4.56E-01	3.45E+00	1.06E+01	2.07E+01	3.12E+01
0.5	0.7	0.672	1.649	4.043	0.300	0.400	0.300	7.66E-01	5.64E+00	1.59E+01	2.82E+01	3.92E+01
0.5	0.8	0.591	1.649	4.596	0.300	0.400	0.300	1.20E+00	8.46E+00	2.16E+01	3.51E+01	4.56E+01
0.5	0.9	0.520	1.649	5.225	0.300	0.400	0.300	1.80E+00	1.18E+01	2.74E+01	4.10E+01	5.07E+01
0.6	0.2	1.410	1.822	2.354	0.300	0.400	0.300	1.89E-02	9.60E-02	3.00E-01	7.22E-01	1.46E+00
0.6	0.3	1.241	1.822	2.676	0.300	0.400	0.300	5.42E-02	3.40E-01	1.15E+00	2.81E+00	5.51E+00
0.6	0.4	1.091	1.822	3.042	0.300	0.400	0.300	1.25E-01	8.87E-01	3.02E+00	7.01E+00	1.28E+01
0.6	0.5	0.960	1.822	3.458	0.300	0.400	0.300	2.51E-01	1.88E+00	6.16E+00	1.32E+01	2.20E+01
0.6	0.6	0.845	1.822	3.931	0.300	0.400	0.300	4.56E-01	3.45E+00	1.06E+01	2.07E+01	3.12E+01

Table 4.4. (continued)

μ	σ	x_1'	x_2'	x_3'	ω_1'	ω_2'	ω_3'	F.E. ¹	F.E. ²	F.E. ³	F.E. ⁴	F.E. ⁵
0.6	0.7	0.743	1.822	4.469	0.300	0.400	0.300	7.66E-01	5.64E+00	1.59E+01	2.82E+01	3.92E+01
0.6	0.8	0.654	1.822	5.080	0.300	0.400	0.300	1.20E+00	8.46E+00	2.16E+01	3.51E+01	4.56E+01
0.6	0.9	0.575	1.822	5.774	0.300	0.400	0.300	1.80E+00	1.18E+01	2.74E+01	4.10E+01	5.07E+01
0.7	0.2	1.558	2.014	2.602	0.300	0.400	0.300	1.89E-02	9.60E-02	3.00E-01	7.22E-01	1.46E+00
0.7	0.3	1.371	2.014	2.958	0.300	0.400	0.300	5.42E-02	3.40E-01	1.15E+00	2.81E+00	5.51E+00
0.7	0.4	1.206	2.014	3.362	0.300	0.400	0.300	1.25E-01	8.87E-01	3.02E+00	7.01E+00	1.28E+01
0.7	0.5	1.061	2.014	3.822	0.300	0.400	0.300	2.51E-01	1.88E+00	6.16E+00	1.32E+01	2.20E+01
0.7	0.6	0.933	2.014	4.345	0.300	0.400	0.300	4.56E-01	3.45E+00	1.06E+01	2.07E+01	3.12E+01
0.7	0.7	0.821	2.014	4.939	0.300	0.400	0.300	7.66E-01	5.64E+00	1.59E+01	2.82E+01	3.92E+01
0.7	0.8	0.722	2.014	5.614	0.300	0.400	0.300	1.20E+00	8.46E+00	2.16E+01	3.51E+01	4.56E+01
0.7	0.9	0.635	2.014	6.381	0.300	0.400	0.300	1.80E+00	1.18E+01	2.74E+01	4.10E+01	5.07E+01
0.8	0.2	1.722	2.226	2.876	0.300	0.400	0.300	1.89E-02	9.60E-02	3.00E-01	7.22E-01	1.46E+00
0.8	0.3	1.515	2.226	3.269	0.300	0.400	0.300	5.42E-02	3.40E-01	1.15E+00	2.81E+00	5.51E+00
0.8	0.4	1.333	2.226	3.716	0.300	0.400	0.300	1.25E-01	8.87E-01	3.02E+00	7.01E+00	1.28E+01
0.8	0.5	1.173	2.226	4.224	0.300	0.400	0.300	2.51E-01	1.88E+00	6.16E+00	1.32E+01	2.20E+01
0.8	0.6	1.032	2.226	4.802	0.300	0.400	0.300	4.56E-01	3.45E+00	1.06E+01	2.07E+01	3.12E+01
0.8	0.7	0.907	2.226	5.458	0.300	0.400	0.300	7.66E-01	5.64E+00	1.59E+01	2.82E+01	3.92E+01
0.8	0.8	0.798	2.226	6.204	0.300	0.400	0.300	1.20E+00	8.46E+00	2.16E+01	3.51E+01	4.56E+01
0.8	0.9	0.702	2.226	7.053	0.300	0.400	0.300	1.80E+00	1.18E+01	2.74E+01	4.10E+01	5.07E+01
0.9	0.2	1.903	2.460	3.178	0.300	0.400	0.300	1.89E-02	9.60E-02	3.00E-01	7.22E-01	1.46E+00
0.9	0.3	1.675	2.460	3.613	0.300	0.400	0.300	5.42E-02	3.40E-01	1.15E+00	2.81E+00	5.51E+00
0.9	0.4	1.473	2.460	4.107	0.300	0.400	0.300	1.25E-01	8.87E-01	3.02E+00	7.01E+00	1.28E+01
0.9	0.5	1.296	2.460	4.668	0.300	0.400	0.300	2.51E-01	1.88E+00	6.16E+00	1.32E+01	2.20E+01
0.9	0.6	1.140	2.460	5.306	0.300	0.400	0.300	4.56E-01	3.45E+00	1.06E+01	2.07E+01	3.12E+01
0.9	0.7	1.003	2.460	6.032	0.300	0.400	0.300	7.66E-01	5.64E+00	1.59E+01	2.82E+01	3.92E+01
0.9	0.8	0.882	2.460	6.857	0.300	0.400	0.300	1.20E+00	8.46E+00	2.16E+01	3.51E+01	4.56E+01
0.9	0.9	0.776	2.460	7.794	0.300	0.400	0.300	1.80E+00	1.18E+01	2.74E+01	4.10E+01	5.07E+01
1.0	0.2	2.104	2.718	3.512	0.300	0.400	0.300	1.89E-02	9.60E-02	3.00E-01	7.22E-01	1.46E+00
1.0	0.3	1.851	2.718	3.993	0.300	0.400	0.300	5.42E-02	3.40E-01	1.15E+00	2.81E+00	5.51E+00
1.0	0.4	1.628	2.718	4.539	0.300	0.400	0.300	1.25E-01	8.87E-01	3.02E+00	7.01E+00	1.28E+01
1.0	0.5	1.432	2.718	5.159	0.300	0.400	0.300	2.51E-01	1.88E+00	6.16E+00	1.32E+01	2.20E+01
1.0	0.6	1.260	2.718	5.865	0.300	0.400	0.300	4.56E-01	3.45E+00	1.06E+01	2.07E+01	3.12E+01
1.0	0.7	1.108	2.718	6.666	0.300	0.400	0.300	7.66E-01	5.64E+00	1.59E+01	2.82E+01	3.92E+01
1.0	0.8	0.975	2.718	7.578	0.300	0.400	0.300	1.20E+00	8.46E+00	2.16E+01	3.51E+01	4.56E+01
1.0	0.9	0.858	2.718	8.614	0.300	0.400	0.300	1.80E+00	1.18E+01	2.74E+01	4.10E+01	5.07E+01
1.1	0.2	2.325	3.004	3.882	0.300	0.400	0.300	1.89E-02	9.60E-02	3.00E-01	7.22E-01	1.46E+00
1.1	0.3	2.045	3.004	4.413	0.300	0.400	0.300	5.42E-02	3.40E-01	1.15E+00	2.81E+00	5.51E+00
1.1	0.4	1.799	3.004	5.016	0.300	0.400	0.300	1.25E-01	8.87E-01	3.02E+00	7.01E+00	1.28E+01
1.1	0.5	1.583	3.004	5.702	0.300	0.400	0.300	2.51E-01	1.88E+00	6.16E+00	1.32E+01	2.20E+01

Table 4.4. (continued)

μ	σ	x_1'	x_2'	x_3'	ω_1'	ω_2'	ω_3'	F.E. ¹	F.E. ²	F.E. ³	F.E. ⁴	F.E. ⁵
1.1	0.6	1.392	3.004	6.481	0.300	0.400	0.300	4.56E-01	3.45E+00	1.06E+01	2.07E+01	3.12E+01
1.1	0.7	1.225	3.004	7.368	0.300	0.400	0.300	7.66E-01	5.64E+00	1.59E+01	2.82E+01	3.92E+01
1.1	0.8	1.078	3.004	8.375	0.300	0.400	0.300	1.20E+00	8.46E+00	2.16E+01	3.51E+01	4.56E+01
1.1	0.9	0.948	3.004	9.520	0.300	0.400	0.300	1.80E+00	1.18E+01	2.74E+01	4.10E+01	5.07E+01
1.2	0.2	2.569	3.320	4.290	0.300	0.400	0.300	1.89E-02	9.60E-02	3.00E-01	7.22E-01	1.46E+00
1.2	0.3	2.260	3.320	4.877	0.300	0.400	0.300	5.42E-02	3.40E-01	1.15E+00	2.81E+00	5.51E+00
1.2	0.4	1.988	3.320	5.543	0.300	0.400	0.300	1.25E-01	8.87E-01	3.02E+00	7.01E+00	1.28E+01
1.2	0.5	1.749	3.320	6.301	0.300	0.400	0.300	2.51E-01	1.88E+00	6.16E+00	1.32E+01	2.20E+01
1.2	0.6	1.539	3.320	7.163	0.300	0.400	0.300	4.56E-01	3.45E+00	1.06E+01	2.07E+01	3.12E+01
1.2	0.7	1.354	3.320	8.142	0.300	0.400	0.300	7.66E-01	5.64E+00	1.59E+01	2.82E+01	3.92E+01
1.2	0.8	1.191	3.320	9.256	0.300	0.400	0.300	1.20E+00	8.46E+00	2.16E+01	3.51E+01	4.56E+01
1.2	0.9	1.048	3.320	10.521	0.300	0.400	0.300	1.80E+00	1.18E+01	2.74E+01	4.10E+01	5.07E+01
1.3	0.2	2.840	3.669	4.741	0.300	0.400	0.300	1.89E-02	9.60E-02	3.00E-01	7.22E-01	1.46E+00
1.3	0.3	2.498	3.669	5.390	0.300	0.400	0.300	5.42E-02	3.40E-01	1.15E+00	2.81E+00	5.51E+00
1.3	0.4	2.198	3.669	6.126	0.300	0.400	0.300	1.25E-01	8.87E-01	3.02E+00	7.01E+00	1.28E+01
1.3	0.5	1.933	3.669	6.964	0.300	0.400	0.300	2.51E-01	1.88E+00	6.16E+00	1.32E+01	2.20E+01
1.3	0.6	1.701	3.669	7.916	0.300	0.400	0.300	4.56E-01	3.45E+00	1.06E+01	2.07E+01	3.12E+01
1.3	0.7	1.496	3.669	8.999	0.300	0.400	0.300	7.66E-01	5.64E+00	1.59E+01	2.82E+01	3.92E+01
1.3	0.8	1.316	3.669	10.229	0.300	0.400	0.300	1.20E+00	8.46E+00	2.16E+01	3.51E+01	4.56E+01
1.3	0.9	1.158	3.669	11.628	0.300	0.400	0.300	1.80E+00	1.18E+01	2.74E+01	4.10E+01	5.07E+01
1.4	0.2	3.138	4.055	5.240	0.300	0.400	0.300	1.89E-02	9.60E-02	3.00E-01	7.22E-01	1.46E+00
1.4	0.3	2.761	4.055	5.956	0.300	0.400	0.300	5.42E-02	3.40E-01	1.15E+00	2.81E+00	5.51E+00
1.4	0.4	2.429	4.055	6.771	0.300	0.400	0.300	1.25E-01	8.87E-01	3.02E+00	7.01E+00	1.28E+01
1.4	0.5	2.137	4.055	7.697	0.300	0.400	0.300	2.51E-01	1.88E+00	6.16E+00	1.32E+01	2.20E+01
1.4	0.6	1.880	4.055	8.749	0.300	0.400	0.300	4.56E-01	3.45E+00	1.06E+01	2.07E+01	3.12E+01
1.4	0.7	1.654	4.055	9.945	0.300	0.400	0.300	7.66E-01	5.64E+00	1.59E+01	2.82E+01	3.92E+01
1.4	0.8	1.455	4.055	11.305	0.300	0.400	0.300	1.20E+00	8.46E+00	2.16E+01	3.51E+01	4.56E+01
1.4	0.9	1.280	4.055	12.851	0.300	0.400	0.300	1.80E+00	1.18E+01	2.74E+01	4.10E+01	5.07E+01
1.5	0.2	3.468	4.482	5.791	0.300	0.400	0.300	1.89E-02	9.60E-02	3.00E-01	7.22E-01	1.46E+00
1.5	0.3	3.051	4.482	6.583	0.300	0.400	0.300	5.42E-02	3.40E-01	1.15E+00	2.81E+00	5.51E+00
1.5	0.4	2.684	4.482	7.483	0.300	0.400	0.300	1.25E-01	8.87E-01	3.02E+00	7.01E+00	1.28E+01
1.5	0.5	2.361	4.482	8.506	0.300	0.400	0.300	2.51E-01	1.88E+00	6.16E+00	1.32E+01	2.20E+01
1.5	0.6	2.077	4.482	9.669	0.300	0.400	0.300	4.56E-01	3.45E+00	1.06E+01	2.07E+01	3.12E+01
1.5	0.7	1.827	4.482	10.991	0.300	0.400	0.300	7.66E-01	5.64E+00	1.59E+01	2.82E+01	3.92E+01
1.5	0.8	1.608	4.482	12.494	0.300	0.400	0.300	1.20E+00	8.46E+00	2.16E+01	3.51E+01	4.56E+01
1.5	0.9	1.414	4.482	14.202	0.300	0.400	0.300	1.80E+00	1.18E+01	2.74E+01	4.10E+01	5.07E+01
1.6	0.2	3.833	4.953	6.400	0.300	0.400	0.300	1.89E-02	9.60E-02	3.00E-01	7.22E-01	1.46E+00
1.6	0.3	3.372	4.953	7.275	0.300	0.400	0.300	5.42E-02	3.40E-01	1.15E+00	2.81E+00	5.51E+00
1.6	0.4	2.966	4.953	8.270	0.300	0.400	0.300	1.25E-01	8.87E-01	3.02E+00	7.01E+00	1.28E+01

Table 4.4. (continued)

μ	σ	x_1'	x_2'	x_3'	ω_1'	ω_2'	ω_3'	F.E. ¹	F.E. ²	F.E. ³	F.E. ⁴	F.E. ⁵
1.6	0.5	2.610	4.953	9.401	0.300	0.400	0.300	2.51E-01	1.88E+00	6.16E+00	1.32E+01	2.20E+01
1.6	0.6	2.296	4.953	10.686	0.300	0.400	0.300	4.56E-01	3.45E+00	1.06E+01	2.07E+01	3.12E+01
1.6	0.7	2.020	4.953	12.147	0.300	0.400	0.300	7.66E-01	5.64E+00	1.59E+01	2.82E+01	3.92E+01
1.6	0.8	1.777	4.953	13.808	0.300	0.400	0.300	1.20E+00	8.46E+00	2.16E+01	3.51E+01	4.56E+01
1.6	0.9	1.563	4.953	15.696	0.300	0.400	0.300	1.80E+00	1.18E+01	2.74E+01	4.10E+01	5.07E+01
1.7	0.2	4.236	5.474	7.073	0.300	0.400	0.300	1.89E-02	9.60E-02	3.00E-01	7.22E-01	1.46E+00
1.7	0.3	3.727	5.474	8.040	0.300	0.400	0.300	5.42E-02	3.40E-01	1.15E+00	2.81E+00	5.51E+00
1.7	0.4	3.278	5.474	9.140	0.300	0.400	0.300	1.25E-01	8.87E-01	3.02E+00	7.01E+00	1.28E+01
1.7	0.5	2.884	5.474	10.389	0.300	0.400	0.300	2.51E-01	1.88E+00	6.16E+00	1.32E+01	2.20E+01
1.7	0.6	2.537	5.474	11.810	0.300	0.400	0.300	4.56E-01	3.45E+00	1.06E+01	2.07E+01	3.12E+01
1.7	0.7	2.232	5.474	13.425	0.300	0.400	0.300	7.66E-01	5.64E+00	1.59E+01	2.82E+01	3.92E+01
1.7	0.8	1.964	5.474	15.260	0.300	0.400	0.300	1.20E+00	8.46E+00	2.16E+01	3.51E+01	4.56E+01
1.7	0.9	1.727	5.474	17.347	0.300	0.400	0.300	1.80E+00	1.18E+01	2.74E+01	4.10E+01	5.07E+01
1.8	0.2	4.682	6.050	7.817	0.300	0.400	0.300	1.89E-02	9.60E-02	3.00E-01	7.22E-01	1.46E+00
1.8	0.3	4.119	6.050	8.886	0.300	0.400	0.300	5.42E-02	3.40E-01	1.15E+00	2.81E+00	5.51E+00
1.8	0.4	3.623	6.050	10.101	0.300	0.400	0.300	1.25E-01	8.87E-01	3.02E+00	7.01E+00	1.28E+01
1.8	0.5	3.187	6.050	11.482	0.300	0.400	0.300	2.51E-01	1.88E+00	6.16E+00	1.32E+01	2.20E+01
1.8	0.6	2.804	6.050	13.052	0.300	0.400	0.300	4.56E-01	3.45E+00	1.06E+01	2.07E+01	3.12E+01
1.8	0.7	2.467	6.050	14.836	0.300	0.400	0.300	7.66E-01	5.64E+00	1.59E+01	2.82E+01	3.92E+01
1.8	0.8	2.170	6.050	16.865	0.300	0.400	0.300	1.20E+00	8.46E+00	2.16E+01	3.51E+01	4.56E+01
1.8	0.9	1.909	6.050	19.171	0.300	0.400	0.300	1.80E+00	1.18E+01	2.74E+01	4.10E+01	5.07E+01
1.9	0.2	5.174	6.686	8.639	0.300	0.400	0.300	1.89E-02	9.60E-02	3.00E-01	7.22E-01	1.46E+00
1.9	0.3	4.552	6.686	9.820	0.300	0.400	0.300	5.42E-02	3.40E-01	1.15E+00	2.81E+00	5.51E+00
1.9	0.4	4.004	6.686	11.163	0.300	0.400	0.300	1.25E-01	8.87E-01	3.02E+00	7.01E+00	1.28E+01
1.9	0.5	3.523	6.686	12.690	0.300	0.400	0.300	2.51E-01	1.88E+00	6.16E+00	1.32E+01	2.20E+01
1.9	0.6	3.099	6.686	14.425	0.300	0.400	0.300	4.56E-01	3.45E+00	1.06E+01	2.07E+01	3.12E+01
1.9	0.7	2.726	6.686	16.397	0.300	0.400	0.300	7.66E-01	5.64E+00	1.59E+01	2.82E+01	3.92E+01
1.9	0.8	2.398	6.686	18.639	0.300	0.400	0.300	1.20E+00	8.46E+00	2.16E+01	3.51E+01	4.56E+01
1.9	0.9	2.110	6.686	21.187	0.300	0.400	0.300	1.80E+00	1.18E+01	2.74E+01	4.10E+01	5.07E+01
2.0	0.2	5.718	7.389	9.548	0.300	0.400	0.300	1.89E-02	9.60E-02	3.00E-01	7.22E-01	1.46E+00
2.0	0.3	5.031	7.389	10.853	0.300	0.400	0.300	5.42E-02	3.40E-01	1.15E+00	2.81E+00	5.51E+00
2.0	0.4	4.425	7.389	12.337	0.300	0.400	0.300	1.25E-01	8.87E-01	3.02E+00	7.01E+00	1.28E+01
2.0	0.5	3.893	7.389	14.024	0.300	0.400	0.300	2.51E-01	1.88E+00	6.16E+00	1.32E+01	2.20E+01
2.0	0.6	3.425	7.389	15.942	0.300	0.400	0.300	4.56E-01	3.45E+00	1.06E+01	2.07E+01	3.12E+01
2.0	0.7	3.013	7.389	18.121	0.300	0.400	0.300	7.66E-01	5.64E+00	1.59E+01	2.82E+01	3.92E+01
2.0	0.8	2.651	7.389	20.599	0.300	0.400	0.300	1.20E+00	8.46E+00	2.16E+01	3.51E+01	4.56E+01
2.0	0.9	2.332	7.389	23.415	0.300	0.400	0.300	1.80E+00	1.18E+01	2.74E+01	4.10E+01	5.07E+01
2.1	0.2	6.320	8.166	10.552	0.300	0.400	0.300	1.89E-02	9.60E-02	3.00E-01	7.22E-01	1.46E+00
2.1	0.3	5.560	8.166	11.995	0.300	0.400	0.300	5.42E-02	3.40E-01	1.15E+00	2.81E+00	5.51E+00

Table 4.4. (continued)

μ	σ	x_1'	x_2'	x_3'	ω_1'	ω_2'	ω_3'	F.E. ¹	F.E. ²	F.E. ³	F.E. ⁴	F.E. ⁵
2.1	0.4	4.891	8.166	13.635	0.300	0.400	0.300	1.25E-01	8.87E-01	3.02E+00	7.01E+00	1.28E+01
2.1	0.5	4.303	8.166	15.499	0.300	0.400	0.300	2.51E-01	1.88E+00	6.16E+00	1.32E+01	2.20E+01
2.1	0.6	3.785	8.166	17.618	0.300	0.400	0.300	4.56E-01	3.45E+00	1.06E+01	2.07E+01	3.12E+01
2.1	0.7	3.330	8.166	20.027	0.300	0.400	0.300	7.66E-01	5.64E+00	1.59E+01	2.82E+01	3.92E+01
2.1	0.8	2.929	8.166	22.765	0.300	0.400	0.300	1.20E+00	8.46E+00	2.16E+01	3.51E+01	4.56E+01
2.1	0.9	2.577	8.166	25.878	0.300	0.400	0.300	1.80E+00	1.18E+01	2.74E+01	4.10E+01	5.07E+01
2.2	0.2	6.984	9.025	11.662	0.300	0.400	0.300	1.89E-02	9.60E-02	3.00E-01	7.22E-01	1.46E+00
2.2	0.3	6.144	9.025	13.256	0.300	0.400	0.300	5.42E-02	3.40E-01	1.15E+00	2.81E+00	5.51E+00
2.2	0.4	5.405	9.025	15.069	0.300	0.400	0.300	1.25E-01	8.87E-01	3.02E+00	7.01E+00	1.28E+01
2.2	0.5	4.755	9.025	17.129	0.300	0.400	0.300	2.51E-01	1.88E+00	6.16E+00	1.32E+01	2.20E+01
2.2	0.6	4.183	9.025	19.471	0.300	0.400	0.300	4.56E-01	3.45E+00	1.06E+01	2.07E+01	3.12E+01
2.2	0.7	3.680	9.025	22.133	0.300	0.400	0.300	7.66E-01	5.64E+00	1.59E+01	2.82E+01	3.92E+01
2.2	0.8	3.237	9.025	25.160	0.300	0.400	0.300	1.20E+00	8.46E+00	2.16E+01	3.51E+01	4.56E+01
2.2	0.9	2.848	9.025	28.600	0.300	0.400	0.300	1.80E+00	1.18E+01	2.74E+01	4.10E+01	5.07E+01
2.3	0.2	7.719	9.974	12.888	0.300	0.400	0.300	1.89E-02	9.60E-02	3.00E-01	7.22E-01	1.46E+00
2.3	0.3	6.791	9.974	14.650	0.300	0.400	0.300	5.42E-02	3.40E-01	1.15E+00	2.81E+00	5.51E+00
2.3	0.4	5.974	9.974	16.654	0.300	0.400	0.300	1.25E-01	8.87E-01	3.02E+00	7.01E+00	1.28E+01
2.3	0.5	5.255	9.974	18.931	0.300	0.400	0.300	2.51E-01	1.88E+00	6.16E+00	1.32E+01	2.20E+01
2.3	0.6	4.623	9.974	21.519	0.300	0.400	0.300	4.56E-01	3.45E+00	1.06E+01	2.07E+01	3.12E+01
2.3	0.7	4.067	9.974	24.461	0.300	0.400	0.300	7.66E-01	5.64E+00	1.59E+01	2.82E+01	3.92E+01
2.3	0.8	3.578	9.974	27.806	0.300	0.400	0.300	1.20E+00	8.46E+00	2.16E+01	3.51E+01	4.56E+01
2.3	0.9	3.147	9.974	31.608	0.300	0.400	0.300	1.80E+00	1.18E+01	2.74E+01	4.10E+01	5.07E+01
2.4	0.2	8.531	11.023	14.244	0.300	0.400	0.300	1.89E-02	9.60E-02	3.00E-01	7.22E-01	1.46E+00
2.4	0.3	7.505	11.023	16.191	0.300	0.400	0.300	5.42E-02	3.40E-01	1.15E+00	2.81E+00	5.51E+00
2.4	0.4	6.602	11.023	18.405	0.300	0.400	0.300	1.25E-01	8.87E-01	3.02E+00	7.01E+00	1.28E+01
2.4	0.5	5.808	11.023	20.921	0.300	0.400	0.300	2.51E-01	1.88E+00	6.16E+00	1.32E+01	2.20E+01
2.4	0.6	5.109	11.023	23.782	0.300	0.400	0.300	4.56E-01	3.45E+00	1.06E+01	2.07E+01	3.12E+01
2.4	0.7	4.495	11.023	27.034	0.300	0.400	0.300	7.66E-01	5.64E+00	1.59E+01	2.82E+01	3.92E+01
2.4	0.8	3.954	11.023	30.730	0.300	0.400	0.300	1.20E+00	8.46E+00	2.16E+01	3.51E+01	4.56E+01
2.4	0.9	3.479	11.023	34.932	0.300	0.400	0.300	1.80E+00	1.18E+01	2.74E+01	4.10E+01	5.07E+01
2.5	0.2	9.428	12.182	15.742	0.300	0.400	0.300	1.89E-02	9.60E-02	3.00E-01	7.22E-01	1.46E+00
2.5	0.3	8.294	12.182	17.894	0.300	0.400	0.300	5.42E-02	3.40E-01	1.15E+00	2.81E+00	5.51E+00
2.5	0.4	7.296	12.182	20.341	0.300	0.400	0.300	1.25E-01	8.87E-01	3.02E+00	7.01E+00	1.28E+01
2.5	0.5	6.419	12.182	23.122	0.300	0.400	0.300	2.51E-01	1.88E+00	6.16E+00	1.32E+01	2.20E+01
2.5	0.6	5.647	12.182	26.283	0.300	0.400	0.300	4.56E-01	3.45E+00	1.06E+01	2.07E+01	3.12E+01
2.5	0.7	4.967	12.182	29.877	0.300	0.400	0.300	7.66E-01	5.64E+00	1.59E+01	2.82E+01	3.92E+01
2.5	0.8	4.370	12.182	33.962	0.300	0.400	0.300	1.20E+00	8.46E+00	2.16E+01	3.51E+01	4.56E+01
2.5	0.9	3.844	12.182	38.606	0.300	0.400	0.300	1.80E+00	1.18E+01	2.74E+01	4.10E+01	5.07E+01
2.6	0.2	10.420	13.464	17.397	0.300	0.400	0.300	1.89E-02	9.60E-02	3.00E-01	7.22E-01	1.46E+00

Table 4.4. (continued)

μ	σ	x_1'	x_2'	x_3'	ω_1'	ω_2'	ω_3'	F.E. ¹	F.E. ²	F.E. ³	F.E. ⁴	F.E. ⁵
2.6	0.3	9.166	13.464	19.776	0.300	0.400	0.300	5.42E-02	3.40E-01	1.15E+00	2.81E+00	5.51E+00
2.6	0.4	8.064	13.464	22.480	0.300	0.400	0.300	1.25E-01	8.87E-01	3.02E+00	7.01E+00	1.28E+01
2.6	0.5	7.094	13.464	25.554	0.300	0.400	0.300	2.51E-01	1.88E+00	6.16E+00	1.32E+01	2.20E+01
2.6	0.6	6.241	13.464	29.047	0.300	0.400	0.300	4.56E-01	3.45E+00	1.06E+01	2.07E+01	3.12E+01
2.6	0.7	5.490	13.464	33.019	0.300	0.400	0.300	7.66E-01	5.64E+00	1.59E+01	2.82E+01	3.92E+01
2.6	0.8	4.830	13.464	37.534	0.300	0.400	0.300	1.20E+00	8.46E+00	2.16E+01	3.51E+01	4.56E+01
2.6	0.9	4.249	13.464	42.666	0.300	0.400	0.300	1.80E+00	1.18E+01	2.74E+01	4.10E+01	5.07E+01
2.7	0.2	11.515	14.880	19.227	0.300	0.400	0.300	1.89E-02	9.60E-02	3.00E-01	7.22E-01	1.46E+00
2.7	0.3	10.130	14.880	21.856	0.300	0.400	0.300	5.42E-02	3.40E-01	1.15E+00	2.81E+00	5.51E+00
2.7	0.4	8.912	14.880	24.844	0.300	0.400	0.300	1.25E-01	8.87E-01	3.02E+00	7.01E+00	1.28E+01
2.7	0.5	7.840	14.880	28.241	0.300	0.400	0.300	2.51E-01	1.88E+00	6.16E+00	1.32E+01	2.20E+01
2.7	0.6	6.897	14.880	32.102	0.300	0.400	0.300	4.56E-01	3.45E+00	1.06E+01	2.07E+01	3.12E+01
2.7	0.7	6.067	14.880	36.492	0.300	0.400	0.300	7.66E-01	5.64E+00	1.59E+01	2.82E+01	3.92E+01
2.7	0.8	5.338	14.880	41.481	0.300	0.400	0.300	1.20E+00	8.46E+00	2.16E+01	3.51E+01	4.56E+01
2.7	0.9	4.695	14.880	47.153	0.300	0.400	0.300	1.80E+00	1.18E+01	2.74E+01	4.10E+01	5.07E+01
2.8	0.2	12.727	16.445	21.249	0.300	0.400	0.300	1.89E-02	9.60E-02	3.00E-01	7.22E-01	1.46E+00
2.8	0.3	11.196	16.445	24.154	0.300	0.400	0.300	5.42E-02	3.40E-01	1.15E+00	2.81E+00	5.51E+00
2.8	0.4	9.849	16.445	27.457	0.300	0.400	0.300	1.25E-01	8.87E-01	3.02E+00	7.01E+00	1.28E+01
2.8	0.5	8.664	16.445	31.211	0.300	0.400	0.300	2.51E-01	1.88E+00	6.16E+00	1.32E+01	2.20E+01
2.8	0.6	7.622	16.445	35.479	0.300	0.400	0.300	4.56E-01	3.45E+00	1.06E+01	2.07E+01	3.12E+01
2.8	0.7	6.705	16.445	40.330	0.300	0.400	0.300	7.66E-01	5.64E+00	1.59E+01	2.82E+01	3.92E+01
2.8	0.8	5.899	16.445	45.844	0.300	0.400	0.300	1.20E+00	8.46E+00	2.16E+01	3.51E+01	4.56E+01
2.8	0.9	5.189	16.445	52.112	0.300	0.400	0.300	1.80E+00	1.18E+01	2.74E+01	4.10E+01	5.07E+01
2.9	0.2	14.065	18.174	23.484	0.300	0.400	0.300	1.89E-02	9.60E-02	3.00E-01	7.22E-01	1.46E+00
2.9	0.3	12.373	18.174	26.695	0.300	0.400	0.300	5.42E-02	3.40E-01	1.15E+00	2.81E+00	5.51E+00
2.9	0.4	10.885	18.174	30.345	0.300	0.400	0.300	1.25E-01	8.87E-01	3.02E+00	7.01E+00	1.28E+01
2.9	0.5	9.576	18.174	34.494	0.300	0.400	0.300	2.51E-01	1.88E+00	6.16E+00	1.32E+01	2.20E+01
2.9	0.6	8.424	18.174	39.210	0.300	0.400	0.300	4.56E-01	3.45E+00	1.06E+01	2.07E+01	3.12E+01
2.9	0.7	7.411	18.174	44.571	0.300	0.400	0.300	7.66E-01	5.64E+00	1.59E+01	2.82E+01	3.92E+01
2.9	0.8	6.519	18.174	50.665	0.300	0.400	0.300	1.20E+00	8.46E+00	2.16E+01	3.51E+01	4.56E+01
2.9	0.9	5.735	18.174	57.593	0.300	0.400	0.300	1.80E+00	1.18E+01	2.74E+01	4.10E+01	5.07E+01
3.0	0.2	15.544	20.086	25.954	0.300	0.400	0.300	1.89E-02	9.60E-02	3.00E-01	7.22E-01	1.46E+00
3.0	0.3	13.675	20.086	29.502	0.300	0.400	0.300	5.42E-02	3.40E-01	1.15E+00	2.81E+00	5.51E+00
3.0	0.4	12.030	20.086	33.536	0.300	0.400	0.300	1.25E-01	8.87E-01	3.02E+00	7.01E+00	1.28E+01
3.0	0.5	10.583	20.086	38.121	0.300	0.400	0.300	2.51E-01	1.88E+00	6.16E+00	1.32E+01	2.20E+01
3.0	0.6	9.310	20.086	43.334	0.300	0.400	0.300	4.56E-01	3.45E+00	1.06E+01	2.07E+01	3.12E+01
3.0	0.7	8.190	20.086	49.259	0.300	0.400	0.300	7.66E-01	5.64E+00	1.59E+01	2.82E+01	3.92E+01
3.0	0.8	7.205	20.086	55.994	0.300	0.400	0.300	1.20E+00	8.46E+00	2.16E+01	3.51E+01	4.56E+01
3.0	0.9	6.338	20.086	63.650	0.300	0.400	0.300	1.80E+00	1.18E+01	2.74E+01	4.10E+01	5.07E+01

Table 4.4. (continued)

μ	σ	x_1'	x_2'	x_3'	ω_1'	ω_2'	ω_3'	F.E. ¹	F.E. ²	F.E. ³	F.E. ⁴	F.E. ⁵
3.1	0.2	17.179	22.198	28.683	0.300	0.400	0.300	1.89E-02	9.60E-02	3.00E-01	7.22E-01	1.46E+00
3.1	0.3	15.113	22.198	32.605	0.300	0.400	0.300	5.42E-02	3.40E-01	1.15E+00	2.81E+00	5.51E+00
3.1	0.4	13.295	22.198	37.063	0.300	0.400	0.300	1.25E-01	8.87E-01	3.02E+00	7.01E+00	1.28E+01
3.1	0.5	11.696	22.198	42.131	0.300	0.400	0.300	2.51E-01	1.88E+00	6.16E+00	1.32E+01	2.20E+01
3.1	0.6	10.289	22.198	47.891	0.300	0.400	0.300	4.56E-01	3.45E+00	1.06E+01	2.07E+01	3.12E+01
3.1	0.7	9.051	22.198	54.439	0.300	0.400	0.300	7.66E-01	5.64E+00	1.59E+01	2.82E+01	3.92E+01
3.1	0.8	7.963	22.198	61.883	0.300	0.400	0.300	1.20E+00	8.46E+00	2.16E+01	3.51E+01	4.56E+01
3.1	0.9	7.005	22.198	70.344	0.300	0.400	0.300	1.80E+00	1.18E+01	2.74E+01	4.10E+01	5.07E+01
3.2	0.2	18.986	24.533	31.700	0.300	0.400	0.300	1.89E-02	9.60E-02	3.00E-01	7.22E-01	1.46E+00
3.2	0.3	16.702	24.533	36.034	0.300	0.400	0.300	5.42E-02	3.40E-01	1.15E+00	2.81E+00	5.51E+00
3.2	0.4	14.693	24.533	40.961	0.300	0.400	0.300	1.25E-01	8.87E-01	3.02E+00	7.01E+00	1.28E+01
3.2	0.5	12.926	24.533	46.562	0.300	0.400	0.300	2.51E-01	1.88E+00	6.16E+00	1.32E+01	2.20E+01
3.2	0.6	11.371	24.533	52.928	0.300	0.400	0.300	4.56E-01	3.45E+00	1.06E+01	2.07E+01	3.12E+01
3.2	0.7	10.003	24.533	60.165	0.300	0.400	0.300	7.66E-01	5.64E+00	1.59E+01	2.82E+01	3.92E+01
3.2	0.8	8.800	24.533	68.391	0.300	0.400	0.300	1.20E+00	8.46E+00	2.16E+01	3.51E+01	4.56E+01
3.2	0.9	7.742	24.533	77.742	0.300	0.400	0.300	1.80E+00	1.18E+01	2.74E+01	4.10E+01	5.07E+01
3.3	0.2	20.983	27.113	35.034	0.300	0.400	0.300	1.89E-02	9.60E-02	3.00E-01	7.22E-01	1.46E+00
3.3	0.3	18.459	27.113	39.824	0.300	0.400	0.300	5.42E-02	3.40E-01	1.15E+00	2.81E+00	5.51E+00
3.3	0.4	16.238	27.113	45.269	0.300	0.400	0.300	1.25E-01	8.87E-01	3.02E+00	7.01E+00	1.28E+01
3.3	0.5	14.285	27.113	51.459	0.300	0.400	0.300	2.51E-01	1.88E+00	6.16E+00	1.32E+01	2.20E+01
3.3	0.6	12.567	27.113	58.494	0.300	0.400	0.300	4.56E-01	3.45E+00	1.06E+01	2.07E+01	3.12E+01
3.3	0.7	11.055	27.113	66.492	0.300	0.400	0.300	7.66E-01	5.64E+00	1.59E+01	2.82E+01	3.92E+01
3.3	0.8	9.726	27.113	75.584	0.300	0.400	0.300	1.20E+00	8.46E+00	2.16E+01	3.51E+01	4.56E+01
3.3	0.9	8.556	27.113	85.918	0.300	0.400	0.300	1.80E+00	1.18E+01	2.74E+01	4.10E+01	5.07E+01
3.4	0.2	23.189	29.964	38.718	0.300	0.400	0.300	1.89E-02	9.60E-02	3.00E-01	7.22E-01	1.46E+00
3.4	0.3	20.400	29.964	44.012	0.300	0.400	0.300	5.42E-02	3.40E-01	1.15E+00	2.81E+00	5.51E+00
3.4	0.4	17.946	29.964	50.030	0.300	0.400	0.300	1.25E-01	8.87E-01	3.02E+00	7.01E+00	1.28E+01
3.4	0.5	15.788	29.964	56.870	0.300	0.400	0.300	2.51E-01	1.88E+00	6.16E+00	1.32E+01	2.20E+01
3.4	0.6	13.889	29.964	64.646	0.300	0.400	0.300	4.56E-01	3.45E+00	1.06E+01	2.07E+01	3.12E+01
3.4	0.7	12.218	29.964	73.485	0.300	0.400	0.300	7.66E-01	5.64E+00	1.59E+01	2.82E+01	3.92E+01
3.4	0.8	10.748	29.964	83.533	0.300	0.400	0.300	1.20E+00	8.46E+00	2.16E+01	3.51E+01	4.56E+01
3.4	0.9	9.456	29.964	94.954	0.300	0.400	0.300	1.80E+00	1.18E+01	2.74E+01	4.10E+01	5.07E+01
3.5	0.2	25.628	33.115	42.790	0.300	0.400	0.300	1.89E-02	9.60E-02	3.00E-01	7.22E-01	1.46E+00
3.5	0.3	22.545	33.115	48.641	0.300	0.400	0.300	5.42E-02	3.40E-01	1.15E+00	2.81E+00	5.51E+00
3.5	0.4	19.834	33.115	55.292	0.300	0.400	0.300	1.25E-01	8.87E-01	3.02E+00	7.01E+00	1.28E+01
3.5	0.5	17.448	33.115	62.852	0.300	0.400	0.300	2.51E-01	1.88E+00	6.16E+00	1.32E+01	2.20E+01
3.5	0.6	15.349	33.115	71.445	0.300	0.400	0.300	4.56E-01	3.45E+00	1.06E+01	2.07E+01	3.12E+01
3.5	0.7	13.503	33.115	81.214	0.300	0.400	0.300	7.66E-01	5.64E+00	1.59E+01	2.82E+01	3.92E+01
3.5	0.8	11.879	33.115	92.318	0.300	0.400	0.300	1.20E+00	8.46E+00	2.16E+01	3.51E+01	4.56E+01

Table 4.4. (continued)

μ	σ	x_1'	x_2'	x_3'	ω_1'	ω_2'	ω_3'	F.E. ¹	F.E. ²	F.E. ³	F.E. ⁴	F.E. ⁵
3.5	0.9	10.450	33.115	104.941	0.300	0.400	0.300	1.80E+00	1.18E+01	2.74E+01	4.10E+01	5.07E+01
3.6	0.2	28.323	36.598	47.291	0.300	0.400	0.300	1.89E-02	9.60E-02	3.00E-01	7.22E-01	1.46E+00
3.6	0.3	24.917	36.598	53.757	0.300	0.400	0.300	5.42E-02	3.40E-01	1.15E+00	2.81E+00	5.51E+00
3.6	0.4	21.920	36.598	61.107	0.300	0.400	0.300	1.25E-01	8.87E-01	3.02E+00	7.01E+00	1.28E+01
3.6	0.5	19.283	36.598	69.462	0.300	0.400	0.300	2.51E-01	1.88E+00	6.16E+00	1.32E+01	2.20E+01
3.6	0.6	16.964	36.598	78.959	0.300	0.400	0.300	4.56E-01	3.45E+00	1.06E+01	2.07E+01	3.12E+01
3.6	0.7	14.923	36.598	89.755	0.300	0.400	0.300	7.66E-01	5.64E+00	1.59E+01	2.82E+01	3.92E+01
3.6	0.8	13.128	36.598	102.027	0.300	0.400	0.300	1.20E+00	8.46E+00	2.16E+01	3.51E+01	4.56E+01
3.6	0.9	11.549	36.598	115.978	0.300	0.400	0.300	1.80E+00	1.18E+01	2.74E+01	4.10E+01	5.07E+01
3.7	0.2	31.302	40.447	52.264	0.300	0.400	0.300	1.89E-02	9.60E-02	3.00E-01	7.22E-01	1.46E+00
3.7	0.3	27.537	40.447	59.410	0.300	0.400	0.300	5.42E-02	3.40E-01	1.15E+00	2.81E+00	5.51E+00
3.7	0.4	24.225	40.447	67.533	0.300	0.400	0.300	1.25E-01	8.87E-01	3.02E+00	7.01E+00	1.28E+01
3.7	0.5	21.311	40.447	76.767	0.300	0.400	0.300	2.51E-01	1.88E+00	6.16E+00	1.32E+01	2.20E+01
3.7	0.6	18.748	40.447	87.263	0.300	0.400	0.300	4.56E-01	3.45E+00	1.06E+01	2.07E+01	3.12E+01
3.7	0.7	16.493	40.447	99.195	0.300	0.400	0.300	7.66E-01	5.64E+00	1.59E+01	2.82E+01	3.92E+01
3.7	0.8	14.509	40.447	112.758	0.300	0.400	0.300	1.20E+00	8.46E+00	2.16E+01	3.51E+01	4.56E+01
3.7	0.9	12.764	40.447	128.175	0.300	0.400	0.300	1.80E+00	1.18E+01	2.74E+01	4.10E+01	5.07E+01
3.8	0.2	34.594	44.701	57.761	0.300	0.400	0.300	1.89E-02	9.60E-02	3.00E-01	7.22E-01	1.46E+00
3.8	0.3	30.433	44.701	65.658	0.300	0.400	0.300	5.42E-02	3.40E-01	1.15E+00	2.81E+00	5.51E+00
3.8	0.4	26.773	44.701	74.636	0.300	0.400	0.300	1.25E-01	8.87E-01	3.02E+00	7.01E+00	1.28E+01
3.8	0.5	23.552	44.701	84.841	0.300	0.400	0.300	2.51E-01	1.88E+00	6.16E+00	1.32E+01	2.20E+01
3.8	0.6	20.719	44.701	96.441	0.300	0.400	0.300	4.56E-01	3.45E+00	1.06E+01	2.07E+01	3.12E+01
3.8	0.7	18.227	44.701	109.627	0.300	0.400	0.300	7.66E-01	5.64E+00	1.59E+01	2.82E+01	3.92E+01
3.8	0.8	16.035	44.701	124.617	0.300	0.400	0.300	1.20E+00	8.46E+00	2.16E+01	3.51E+01	4.56E+01
3.8	0.9	14.106	44.701	141.655	0.300	0.400	0.300	1.80E+00	1.18E+01	2.74E+01	4.10E+01	5.07E+01
3.9	0.2	38.233	49.402	63.836	0.300	0.400	0.300	1.89E-02	9.60E-02	3.00E-01	7.22E-01	1.46E+00
3.9	0.3	33.634	49.402	72.564	0.300	0.400	0.300	5.42E-02	3.40E-01	1.15E+00	2.81E+00	5.51E+00
3.9	0.4	29.588	49.402	82.485	0.300	0.400	0.300	1.25E-01	8.87E-01	3.02E+00	7.01E+00	1.28E+01
3.9	0.5	26.029	49.402	93.764	0.300	0.400	0.300	2.51E-01	1.88E+00	6.16E+00	1.32E+01	2.20E+01
3.9	0.6	22.898	49.402	106.584	0.300	0.400	0.300	4.56E-01	3.45E+00	1.06E+01	2.07E+01	3.12E+01
3.9	0.7	20.144	49.402	121.157	0.300	0.400	0.300	7.66E-01	5.64E+00	1.59E+01	2.82E+01	3.92E+01
3.9	0.8	17.721	49.402	137.723	0.300	0.400	0.300	1.20E+00	8.46E+00	2.16E+01	3.51E+01	4.56E+01
3.9	0.9	15.590	49.402	156.553	0.300	0.400	0.300	1.80E+00	1.18E+01	2.74E+01	4.10E+01	5.07E+01
4.0	0.2	42.254	54.598	70.549	0.300	0.400	0.300	1.89E-02	9.60E-02	3.00E-01	7.22E-01	1.46E+00
4.0	0.3	37.171	54.598	80.195	0.300	0.400	0.300	5.42E-02	3.40E-01	1.15E+00	2.81E+00	5.51E+00
4.0	0.4	32.700	54.598	91.160	0.300	0.400	0.300	1.25E-01	8.87E-01	3.02E+00	7.01E+00	1.28E+01
4.0	0.5	28.767	54.598	103.625	0.300	0.400	0.300	2.51E-01	1.88E+00	6.16E+00	1.32E+01	2.20E+01
4.0	0.6	25.307	54.598	117.793	0.300	0.400	0.300	4.56E-01	3.45E+00	1.06E+01	2.07E+01	3.12E+01
4.0	0.7	22.263	54.598	133.899	0.300	0.400	0.300	7.66E-01	5.64E+00	1.59E+01	2.82E+01	3.92E+01

Table 4.4. (continued)

μ	σ	x_1'	x_2'	x_3'	ω_1'	ω_2'	ω_3'	F.E. ¹	F.E. ²	F.E. ³	F.E. ⁴	F.E. ⁵
4.0	0.8	19.585	54.598	152.207	0.300	0.400	0.300	1.20E+00	8.46E+00	2.16E+01	3.51E+01	4.56E+01
4.0	0.9	17.229	54.598	173.018	0.300	0.400	0.300	1.80E+00	1.18E+01	2.74E+01	4.10E+01	5.07E+01
4.1	0.2	46.697	60.340	77.969	0.300	0.400	0.300	1.89E-02	9.60E-02	3.00E-01	7.22E-01	1.46E+00
4.1	0.3	41.081	60.340	88.630	0.300	0.400	0.300	5.42E-02	3.40E-01	1.15E+00	2.81E+00	5.51E+00
4.1	0.4	36.139	60.340	100.748	0.300	0.400	0.300	1.25E-01	8.87E-01	3.02E+00	7.01E+00	1.28E+01
4.1	0.5	31.792	60.340	114.523	0.300	0.400	0.300	2.51E-01	1.88E+00	6.16E+00	1.32E+01	2.20E+01
4.1	0.6	27.968	60.340	130.182	0.300	0.400	0.300	4.56E-01	3.45E+00	1.06E+01	2.07E+01	3.12E+01
4.1	0.7	24.604	60.340	147.981	0.300	0.400	0.300	7.66E-01	5.64E+00	1.59E+01	2.82E+01	3.92E+01
4.1	0.8	21.645	60.340	168.215	0.300	0.400	0.300	1.20E+00	8.46E+00	2.16E+01	3.51E+01	4.56E+01
4.1	0.9	19.041	60.340	191.215	0.300	0.400	0.300	1.80E+00	1.18E+01	2.74E+01	4.10E+01	5.07E+01
4.2	0.2	51.609	66.686	86.169	0.300	0.400	0.300	1.89E-02	9.60E-02	3.00E-01	7.22E-01	1.46E+00
4.2	0.3	45.401	66.686	97.951	0.300	0.400	0.300	5.42E-02	3.40E-01	1.15E+00	2.81E+00	5.51E+00
4.2	0.4	39.940	66.686	111.344	0.300	0.400	0.300	1.25E-01	8.87E-01	3.02E+00	7.01E+00	1.28E+01
4.2	0.5	35.136	66.686	126.568	0.300	0.400	0.300	2.51E-01	1.88E+00	6.16E+00	1.32E+01	2.20E+01
4.2	0.6	30.910	66.686	143.873	0.300	0.400	0.300	4.56E-01	3.45E+00	1.06E+01	2.07E+01	3.12E+01
4.2	0.7	27.192	66.686	163.545	0.300	0.400	0.300	7.66E-01	5.64E+00	1.59E+01	2.82E+01	3.92E+01
4.2	0.8	23.921	66.686	185.906	0.300	0.400	0.300	1.20E+00	8.46E+00	2.16E+01	3.51E+01	4.56E+01
4.2	0.9	21.044	66.686	211.325	0.300	0.400	0.300	1.80E+00	1.18E+01	2.74E+01	4.10E+01	5.07E+01
4.3	0.2	57.036	73.700	95.231	0.300	0.400	0.300	1.89E-02	9.60E-02	3.00E-01	7.22E-01	1.46E+00
4.3	0.3	50.176	73.700	108.252	0.300	0.400	0.300	5.42E-02	3.40E-01	1.15E+00	2.81E+00	5.51E+00
4.3	0.4	44.141	73.700	123.054	0.300	0.400	0.300	1.25E-01	8.87E-01	3.02E+00	7.01E+00	1.28E+01
4.3	0.5	38.831	73.700	139.879	0.300	0.400	0.300	2.51E-01	1.88E+00	6.16E+00	1.32E+01	2.20E+01
4.3	0.6	34.160	73.700	159.004	0.300	0.400	0.300	4.56E-01	3.45E+00	1.06E+01	2.07E+01	3.12E+01
4.3	0.7	30.052	73.700	180.745	0.300	0.400	0.300	7.66E-01	5.64E+00	1.59E+01	2.82E+01	3.92E+01
4.3	0.8	26.437	73.700	205.458	0.300	0.400	0.300	1.20E+00	8.46E+00	2.16E+01	3.51E+01	4.56E+01
4.3	0.9	23.257	73.700	233.550	0.300	0.400	0.300	1.80E+00	1.18E+01	2.74E+01	4.10E+01	5.07E+01
4.4	0.2	63.035	81.451	105.247	0.300	0.400	0.300	1.89E-02	9.60E-02	3.00E-01	7.22E-01	1.46E+00
4.4	0.3	55.453	81.451	119.637	0.300	0.400	0.300	5.42E-02	3.40E-01	1.15E+00	2.81E+00	5.51E+00
4.4	0.4	48.783	81.451	135.995	0.300	0.400	0.300	1.25E-01	8.87E-01	3.02E+00	7.01E+00	1.28E+01
4.4	0.5	42.915	81.451	154.590	0.300	0.400	0.300	2.51E-01	1.88E+00	6.16E+00	1.32E+01	2.20E+01
4.4	0.6	37.753	81.451	175.727	0.300	0.400	0.300	4.56E-01	3.45E+00	1.06E+01	2.07E+01	3.12E+01
4.4	0.7	33.212	81.451	199.754	0.300	0.400	0.300	7.66E-01	5.64E+00	1.59E+01	2.82E+01	3.92E+01
4.4	0.8	29.217	81.451	227.066	0.300	0.400	0.300	1.20E+00	8.46E+00	2.16E+01	3.51E+01	4.56E+01
4.4	0.9	25.703	81.451	258.113	0.300	0.400	0.300	1.80E+00	1.18E+01	2.74E+01	4.10E+01	5.07E+01
4.5	0.2	69.664	90.017	116.316	0.300	0.400	0.300	1.89E-02	9.60E-02	3.00E-01	7.22E-01	1.46E+00
4.5	0.3	61.285	90.017	132.220	0.300	0.400	0.300	5.42E-02	3.40E-01	1.15E+00	2.81E+00	5.51E+00
4.5	0.4	53.913	90.017	150.298	0.300	0.400	0.300	1.25E-01	8.87E-01	3.02E+00	7.01E+00	1.28E+01
4.5	0.5	47.429	90.017	170.848	0.300	0.400	0.300	2.51E-01	1.88E+00	6.16E+00	1.32E+01	2.20E+01
4.5	0.6	41.724	90.017	194.208	0.300	0.400	0.300	4.56E-01	3.45E+00	1.06E+01	2.07E+01	3.12E+01

Table 4.4. (continued)

μ	σ	x_1'	x_2'	x_3'	ω_1'	ω_2'	ω_3'	F.E. ¹	F.E. ²	F.E. ³	F.E. ⁴	F.E. ⁵
4.5	0.7	36.705	90.017	220.762	0.300	0.400	0.300	7.66E-01	5.64E+00	1.59E+01	2.82E+01	3.92E+01
4.5	0.8	32.290	90.017	250.947	0.300	0.400	0.300	1.20E+00	8.46E+00	2.16E+01	3.51E+01	4.56E+01
4.5	0.9	28.406	90.017	285.259	0.300	0.400	0.300	1.80E+00	1.18E+01	2.74E+01	4.10E+01	5.07E+01
4.6	0.2	76.991	99.484	128.549	0.300	0.400	0.300	1.89E-02	9.60E-02	3.00E-01	7.22E-01	1.46E+00
4.6	0.3	67.730	99.484	146.125	0.300	0.400	0.300	5.42E-02	3.40E-01	1.15E+00	2.81E+00	5.51E+00
4.6	0.4	59.584	99.484	166.105	0.300	0.400	0.300	1.25E-01	8.87E-01	3.02E+00	7.01E+00	1.28E+01
4.6	0.5	52.417	99.484	188.817	0.300	0.400	0.300	2.51E-01	1.88E+00	6.16E+00	1.32E+01	2.20E+01
4.6	0.6	46.112	99.484	214.633	0.300	0.400	0.300	4.56E-01	3.45E+00	1.06E+01	2.07E+01	3.12E+01
4.6	0.7	40.565	99.484	243.980	0.300	0.400	0.300	7.66E-01	5.64E+00	1.59E+01	2.82E+01	3.92E+01
4.6	0.8	35.686	99.484	277.339	0.300	0.400	0.300	1.20E+00	8.46E+00	2.16E+01	3.51E+01	4.56E+01
4.6	0.9	31.394	99.484	315.260	0.300	0.400	0.300	1.80E+00	1.18E+01	2.74E+01	4.10E+01	5.07E+01
4.7	0.2	85.088	109.947	142.069	0.300	0.400	0.300	1.89E-02	9.60E-02	3.00E-01	7.22E-01	1.46E+00
4.7	0.3	74.854	109.947	161.494	0.300	0.400	0.300	5.42E-02	3.40E-01	1.15E+00	2.81E+00	5.51E+00
4.7	0.4	65.850	109.947	183.575	0.300	0.400	0.300	1.25E-01	8.87E-01	3.02E+00	7.01E+00	1.28E+01
4.7	0.5	57.929	109.947	208.675	0.300	0.400	0.300	2.51E-01	1.88E+00	6.16E+00	1.32E+01	2.20E+01
4.7	0.6	50.961	109.947	237.206	0.300	0.400	0.300	4.56E-01	3.45E+00	1.06E+01	2.07E+01	3.12E+01
4.7	0.7	44.832	109.947	269.640	0.300	0.400	0.300	7.66E-01	5.64E+00	1.59E+01	2.82E+01	3.92E+01
4.7	0.8	39.439	109.947	306.507	0.300	0.400	0.300	1.20E+00	8.46E+00	2.16E+01	3.51E+01	4.56E+01
4.7	0.9	34.695	109.947	348.416	0.300	0.400	0.300	1.80E+00	1.18E+01	2.74E+01	4.10E+01	5.07E+01
4.8	0.2	94.037	121.510	157.010	0.300	0.400	0.300	1.89E-02	9.60E-02	3.00E-01	7.22E-01	1.46E+00
4.8	0.3	82.726	121.510	178.478	0.300	0.400	0.300	5.42E-02	3.40E-01	1.15E+00	2.81E+00	5.51E+00
4.8	0.4	72.776	121.510	202.881	0.300	0.400	0.300	1.25E-01	8.87E-01	3.02E+00	7.01E+00	1.28E+01
4.8	0.5	64.022	121.510	230.621	0.300	0.400	0.300	2.51E-01	1.88E+00	6.16E+00	1.32E+01	2.20E+01
4.8	0.6	56.321	121.510	262.154	0.300	0.400	0.300	4.56E-01	3.45E+00	1.06E+01	2.07E+01	3.12E+01
4.8	0.7	49.547	121.510	297.998	0.300	0.400	0.300	7.66E-01	5.64E+00	1.59E+01	2.82E+01	3.92E+01
4.8	0.8	43.587	121.510	338.743	0.300	0.400	0.300	1.20E+00	8.46E+00	2.16E+01	3.51E+01	4.56E+01
4.8	0.9	38.344	121.510	385.059	0.300	0.400	0.300	1.80E+00	1.18E+01	2.74E+01	4.10E+01	5.07E+01
4.9	0.2	103.927	134.290	173.523	0.300	0.400	0.300	1.89E-02	9.60E-02	3.00E-01	7.22E-01	1.46E+00
4.9	0.3	91.426	134.290	197.249	0.300	0.400	0.300	5.42E-02	3.40E-01	1.15E+00	2.81E+00	5.51E+00
4.9	0.4	80.429	134.290	224.218	0.300	0.400	0.300	1.25E-01	8.87E-01	3.02E+00	7.01E+00	1.28E+01
4.9	0.5	70.755	134.290	254.876	0.300	0.400	0.300	2.51E-01	1.88E+00	6.16E+00	1.32E+01	2.20E+01
4.9	0.6	62.244	134.290	289.725	0.300	0.400	0.300	4.56E-01	3.45E+00	1.06E+01	2.07E+01	3.12E+01
4.9	0.7	54.757	134.290	329.338	0.300	0.400	0.300	7.66E-01	5.64E+00	1.59E+01	2.82E+01	3.92E+01
4.9	0.8	48.171	134.290	374.369	0.300	0.400	0.300	1.20E+00	8.46E+00	2.16E+01	3.51E+01	4.56E+01
4.9	0.9	42.377	134.290	425.556	0.300	0.400	0.300	1.80E+00	1.18E+01	2.74E+01	4.10E+01	5.07E+01
5.0	0.2	114.857	148.413	191.773	0.300	0.400	0.300	1.89E-02	9.60E-02	3.00E-01	7.22E-01	1.46E+00
5.0	0.3	101.042	148.413	217.994	0.300	0.400	0.300	5.42E-02	3.40E-01	1.15E+00	2.81E+00	5.51E+00
5.0	0.4	88.888	148.413	247.800	0.300	0.400	0.300	1.25E-01	8.87E-01	3.02E+00	7.01E+00	1.28E+01
5.0	0.5	78.196	148.413	281.681	0.300	0.400	0.300	2.51E-01	1.88E+00	6.16E+00	1.32E+01	2.20E+01

Table 4.4. (continued)

μ	σ	x_1'	x_2'	x_3'	ω_1'	ω_2'	ω_3'	F.E. ¹	F.E. ²	F.E. ³	F.E. ⁴	F.E. ⁵
5.0	0.6	68.791	148.413	320.195	0.300	0.400	0.300	4.56E-01	3.45E+00	1.06E+01	2.07E+01	3.12E+01
5.0	0.7	60.516	148.413	363.975	0.300	0.400	0.300	7.66E-01	5.64E+00	1.59E+01	2.82E+01	3.92E+01
5.0	0.8	53.237	148.413	413.741	0.300	0.400	0.300	1.20E+00	8.46E+00	2.16E+01	3.51E+01	4.56E+01
5.0	0.9	46.834	148.413	470.312	0.300	0.400	0.300	1.80E+00	1.18E+01	2.74E+01	4.10E+01	5.07E+01
5.1	0.2	126.937	164.022	211.942	0.300	0.400	0.300	1.89E-02	9.60E-02	3.00E-01	7.22E-01	1.46E+00
5.1	0.3	111.668	164.022	240.920	0.300	0.400	0.300	5.42E-02	3.40E-01	1.15E+00	2.81E+00	5.51E+00
5.1	0.4	98.237	164.022	273.861	0.300	0.400	0.300	1.25E-01	8.87E-01	3.02E+00	7.01E+00	1.28E+01
5.1	0.5	86.420	164.022	311.306	0.300	0.400	0.300	2.51E-01	1.88E+00	6.16E+00	1.32E+01	2.20E+01
5.1	0.6	76.026	164.022	353.870	0.300	0.400	0.300	4.56E-01	3.45E+00	1.06E+01	2.07E+01	3.12E+01
5.1	0.7	66.881	164.022	402.255	0.300	0.400	0.300	7.66E-01	5.64E+00	1.59E+01	2.82E+01	3.92E+01
5.1	0.8	58.836	164.022	457.255	0.300	0.400	0.300	1.20E+00	8.46E+00	2.16E+01	3.51E+01	4.56E+01
5.1	0.9	51.759	164.022	519.775	0.300	0.400	0.300	1.80E+00	1.18E+01	2.74E+01	4.10E+01	5.07E+01
5.2	0.2	140.287	181.272	234.232	0.300	0.400	0.300	1.89E-02	9.60E-02	3.00E-01	7.22E-01	1.46E+00
5.2	0.3	123.413	181.272	266.258	0.300	0.400	0.300	5.42E-02	3.40E-01	1.15E+00	2.81E+00	5.51E+00
5.2	0.4	108.568	181.272	302.663	0.300	0.400	0.300	1.25E-01	8.87E-01	3.02E+00	7.01E+00	1.28E+01
5.2	0.5	95.509	181.272	344.046	0.300	0.400	0.300	2.51E-01	1.88E+00	6.16E+00	1.32E+01	2.20E+01
5.2	0.6	84.021	181.272	391.087	0.300	0.400	0.300	4.56E-01	3.45E+00	1.06E+01	2.07E+01	3.12E+01
5.2	0.7	73.915	181.272	444.560	0.300	0.400	0.300	7.66E-01	5.64E+00	1.59E+01	2.82E+01	3.92E+01
5.2	0.8	65.024	181.272	505.345	0.300	0.400	0.300	1.20E+00	8.46E+00	2.16E+01	3.51E+01	4.56E+01
5.2	0.9	57.203	181.272	574.440	0.300	0.400	0.300	1.80E+00	1.18E+01	2.74E+01	4.10E+01	5.07E+01
5.3	0.2	155.041	200.337	258.866	0.300	0.400	0.300	1.89E-02	9.60E-02	3.00E-01	7.22E-01	1.46E+00
5.3	0.3	136.392	200.337	294.261	0.300	0.400	0.300	5.42E-02	3.40E-01	1.15E+00	2.81E+00	5.51E+00
5.3	0.4	119.987	200.337	334.495	0.300	0.400	0.300	1.25E-01	8.87E-01	3.02E+00	7.01E+00	1.28E+01
5.3	0.5	105.554	200.337	380.230	0.300	0.400	0.300	2.51E-01	1.88E+00	6.16E+00	1.32E+01	2.20E+01
5.3	0.6	92.858	200.337	432.218	0.300	0.400	0.300	4.56E-01	3.45E+00	1.06E+01	2.07E+01	3.12E+01
5.3	0.7	81.689	200.337	491.315	0.300	0.400	0.300	7.66E-01	5.64E+00	1.59E+01	2.82E+01	3.92E+01
5.3	0.8	71.863	200.337	558.493	0.300	0.400	0.300	1.20E+00	8.46E+00	2.16E+01	3.51E+01	4.56E+01
5.3	0.9	63.219	200.337	634.855	0.300	0.400	0.300	1.80E+00	1.18E+01	2.74E+01	4.10E+01	5.07E+01
5.4	0.2	171.347	221.406	286.091	0.300	0.400	0.300	1.89E-02	9.60E-02	3.00E-01	7.22E-01	1.46E+00
5.4	0.3	150.737	221.406	325.208	0.300	0.400	0.300	5.42E-02	3.40E-01	1.15E+00	2.81E+00	5.51E+00
5.4	0.4	132.606	221.406	369.674	0.300	0.400	0.300	1.25E-01	8.87E-01	3.02E+00	7.01E+00	1.28E+01
5.4	0.5	116.655	221.406	420.219	0.300	0.400	0.300	2.51E-01	1.88E+00	6.16E+00	1.32E+01	2.20E+01
5.4	0.6	102.624	221.406	477.675	0.300	0.400	0.300	4.56E-01	3.45E+00	1.06E+01	2.07E+01	3.12E+01
5.4	0.7	90.280	221.406	542.987	0.300	0.400	0.300	7.66E-01	5.64E+00	1.59E+01	2.82E+01	3.92E+01
5.4	0.8	79.421	221.406	617.230	0.300	0.400	0.300	1.20E+00	8.46E+00	2.16E+01	3.51E+01	4.56E+01
5.4	0.9	69.868	221.406	701.623	0.300	0.400	0.300	1.80E+00	1.18E+01	2.74E+01	4.10E+01	5.07E+01
5.5	0.2	189.368	244.692	316.180	0.300	0.400	0.300	1.89E-02	9.60E-02	3.00E-01	7.22E-01	1.46E+00
5.5	0.3	166.590	244.692	359.411	0.300	0.400	0.300	5.42E-02	3.40E-01	1.15E+00	2.81E+00	5.51E+00
5.5	0.4	146.552	244.692	408.553	0.300	0.400	0.300	1.25E-01	8.87E-01	3.02E+00	7.01E+00	1.28E+01

Table 4.4. (continued)

μ	σ	x_1'	x_2'	x_3'	ω_1'	ω_2'	ω_3'	F.E. ¹	F.E. ²	F.E. ³	F.E. ⁴	F.E. ⁵
5.5	0.5	128.924	244.692	464.414	0.300	0.400	0.300	2.51E-01	1.88E+00	6.16E+00	1.32E+01	2.20E+01
5.5	0.6	113.417	244.692	527.913	0.300	0.400	0.300	4.56E-01	3.45E+00	1.06E+01	2.07E+01	3.12E+01
5.5	0.7	99.775	244.692	600.094	0.300	0.400	0.300	7.66E-01	5.64E+00	1.59E+01	2.82E+01	3.92E+01
5.5	0.8	87.773	244.692	682.144	0.300	0.400	0.300	1.20E+00	8.46E+00	2.16E+01	3.51E+01	4.56E+01
5.5	0.9	77.216	244.692	775.413	0.300	0.400	0.300	1.80E+00	1.18E+01	2.74E+01	4.10E+01	5.07E+01

Table 4.5. Relocation of x_1 , x_2 and x_3 ; P_k represents k -th percentile location

σ	x_1'	x_2'	x_3'
0.2	x_1	x_2	x_3
0.3	x_1	x_2	x_3
0.4	x_1	x_2	$P_{99.5}$
0.5	x_1	x_2	$P_{99.5}$
0.6	x_1	P_{95}	$P_{99.5}$
0.7	x_1	P_{97}	$P_{99.5}$
0.8	x_1	P_{98}	$P_{99.5}$
0.9	x_1	P_{99}	$P_{99.5}$

The following Table 4.6 shows the solution with applying adjusted remedy. For more practical real-world use, the locations are relocated without adjusting their corresponding weights. Notably, the error rate drops dramatically for each case compared to the result of applying the common remedy.

Table 4.6. Results of GANMM with x_1' , x_2' and x_3'

μ	σ	x_1'	x_2'	x_3'	ω_1'	ω_2'	ω_3'	F.E. ¹	F.E. ²	F.E. ³	F.E. ⁴	F.E. ⁵
0.3	0.2	1.050	1.491	2.116	0.344	0.596	0.060	1.04E-06	5.02E-05	1.22E-04	1.56E-04	1.83E-04
0.3	0.3	0.992	1.691	2.883	0.452	0.516	0.031	1.69E-05	1.56E-05	5.21E-05	7.28E-05	1.01E-04
0.3	0.4	0.974	2.013	3.782	0.561	0.424	0.015	1.93E-01	7.25E-01	1.87E+00	3.87E+00	6.78E+00
0.3	0.5	0.993	2.522	4.894	0.665	0.329	0.006	3.11E-01	1.40E+00	4.07E+00	8.95E+00	1.57E+01
0.3	0.6	1.046	3.622	6.331	0.757	0.241	0.002	1.94E+00	4.29E+00	4.16E+00	7.74E+00	1.59E+01
0.3	0.7	1.135	5.036	8.191	0.833	0.167	0.001	1.90E+00	4.65E+00	4.17E+00	9.95E+00	2.03E+01
0.3	0.8	1.260	6.980	10.598	0.891	0.109	0.000	7.19E-01	1.47E+00	3.80E+00	1.36E+01	2.57E+01
0.3	0.9	1.428	10.954	13.712	0.933	0.067	0.000	1.14E+00	3.58E+00	3.44E+00	1.37E+01	2.65E+01
0.4	0.2	1.160	1.647	2.338	0.342	0.597	0.061	1.60E-04	2.58E-04	3.83E-04	4.92E-04	5.95E-04
0.4	0.3	1.095	1.867	3.183	0.451	0.517	0.032	6.55E-05	1.96E-04	2.66E-04	3.84E-04	4.45E-04
0.4	0.4	1.077	2.225	4.180	0.561	0.424	0.015	1.93E-01	7.25E-01	1.87E+00	3.87E+00	6.78E+00
0.4	0.5	1.098	2.787	5.408	0.665	0.328	0.006	3.11E-01	1.40E+00	4.07E+00	8.95E+00	1.57E+01
0.4	0.6	1.157	4.002	6.997	0.757	0.241	0.002	1.94E+00	4.29E+00	4.16E+00	7.74E+00	1.59E+01
0.4	0.7	1.254	5.565	9.053	0.833	0.167	0.001	1.90E+00	4.65E+00	4.17E+00	9.95E+00	2.03E+01
0.4	0.8	1.393	7.714	11.713	0.891	0.109	0.000	7.19E-01	1.47E+00	3.80E+00	1.35E+01	2.57E+01
0.4	0.9	1.578	12.106	15.154	0.933	0.067	0.000	1.14E+00	3.59E+00	3.44E+00	1.37E+01	2.65E+01
0.5	0.2	1.283	1.822	2.586	0.345	0.595	0.060	8.55E-05	7.83E-05	9.23E-05	1.42E-04	1.23E-04
0.5	0.3	1.212	2.066	3.522	0.453	0.516	0.031	2.72E-06	6.79E-05	6.32E-05	5.47E-05	7.71E-05
0.5	0.4	1.190	2.460	4.620	0.561	0.424	0.015	1.93E-01	7.25E-01	1.87E+00	3.87E+00	6.78E+00
0.5	0.5	1.213	3.080	5.977	0.665	0.328	0.006	3.11E-01	1.40E+00	4.07E+00	8.95E+00	1.57E+01
0.5	0.6	1.278	4.423	7.733	0.757	0.241	0.002	1.94E+00	4.29E+00	4.16E+00	7.74E+00	1.59E+01
0.5	0.7	1.386	6.151	10.005	0.833	0.167	0.001	1.90E+00	4.65E+00	4.17E+00	9.95E+00	2.03E+01
0.5	0.8	1.539	8.525	12.944	0.891	0.109	0.000	7.19E-01	1.47E+00	3.80E+00	1.35E+01	2.57E+01
0.5	0.9	1.744	13.379	16.747	0.933	0.067	0.000	1.14E+00	3.58E+00	3.44E+00	1.37E+01	2.65E+01
0.6	0.2	1.420	2.016	2.862	0.347	0.594	0.059	1.13E-04	1.57E-04	1.96E-04	2.24E-04	3.13E-04
0.6	0.3	1.339	2.282	3.890	0.452	0.516	0.031	6.00E-05	1.06E-04	1.65E-04	2.10E-04	2.76E-04
0.6	0.4	1.315	2.718	5.106	0.561	0.424	0.015	1.93E-01	7.25E-01	1.87E+00	3.87E+00	6.78E+00
0.6	0.5	1.341	3.404	6.606	0.665	0.329	0.006	3.11E-01	1.40E+00	4.07E+00	8.95E+00	1.57E+01
0.6	0.6	1.413	4.889	8.546	0.757	0.241	0.002	1.94E+00	4.29E+00	4.17E+00	7.74E+00	1.59E+01
0.6	0.7	1.532	6.798	11.057	0.833	0.167	0.001	1.90E+00	4.65E+00	4.17E+00	9.95E+00	2.03E+01
0.6	0.8	1.701	9.422	14.306	0.891	0.109	0.000	7.20E-01	1.47E+00	3.80E+00	1.35E+01	2.57E+01
0.6	0.9	1.928	14.786	18.509	0.933	0.067	0.000	1.14E+00	3.59E+00	3.44E+00	1.37E+01	2.65E+01
0.7	0.2	1.564	2.221	3.153	0.340	0.599	0.061	1.75E-06	1.59E-04	2.62E-04	3.79E-04	4.85E-04
0.7	0.3	1.480	2.523	4.302	0.453	0.516	0.031	1.11E-04	1.19E-04	1.06E-04	1.65E-04	1.64E-04
0.7	0.4	1.454	3.005	5.643	0.561	0.424	0.015	1.93E-01	7.26E-01	1.87E+00	3.88E+00	6.79E+00
0.7	0.5	1.482	3.763	7.300	0.665	0.328	0.006	3.11E-01	1.40E+00	4.07E+00	8.95E+00	1.57E+01
0.7	0.6	1.561	5.403	9.445	0.757	0.241	0.002	1.94E+00	4.29E+00	4.16E+00	7.74E+00	1.59E+01

Table 4.6. (continued)

μ	σ	x_1'	x_2'	x_3'	ω_1'	ω_2'	ω_3'	F.E. ¹	F.E. ²	F.E. ³	F.E. ⁴	F.E. ⁵
0.7	0.7	1.693	7.512	12.220	0.833	0.167	0.001	1.90E+00	4.65E+00	4.17E+00	9.95E+00	2.03E+01
0.7	0.8	1.880	10.412	15.810	0.891	0.109	0.000	7.19E-01	1.47E+00	3.80E+00	1.35E+01	2.57E+01
0.7	0.9	2.130	16.342	20.455	0.933	0.067	0.000	1.14E+00	3.58E+00	3.44E+00	1.37E+01	2.65E+01
0.8	0.2	1.727	2.451	3.481	0.338	0.600	0.062	4.80E-05	7.51E-05	2.02E-04	2.53E-04	2.94E-04
0.8	0.3	1.635	2.788	4.753	0.452	0.516	0.031	3.12E-05	2.63E-05	2.07E-05	6.94E-05	9.64E-05
0.8	0.4	1.606	3.320	6.236	0.561	0.424	0.015	1.93E-01	7.25E-01	1.87E+00	3.87E+00	6.79E+00
0.8	0.5	1.638	4.158	8.068	0.665	0.328	0.006	3.11E-01	1.40E+00	4.07E+00	8.95E+00	1.57E+01
0.8	0.6	1.725	5.971	10.438	0.757	0.241	0.002	1.94E+00	4.29E+00	4.17E+00	7.74E+00	1.59E+01
0.8	0.7	1.871	8.302	13.505	0.833	0.167	0.001	1.90E+00	4.65E+00	4.16E+00	9.95E+00	2.03E+01
0.8	0.8	2.078	11.508	17.473	0.891	0.109	0.000	7.19E-01	1.47E+00	3.80E+00	1.35E+01	2.57E+01
0.8	0.9	2.354	18.060	22.607	0.933	0.067	0.000	1.14E+00	3.58E+00	3.44E+00	1.37E+01	2.65E+01
0.9	0.2	1.919	2.725	3.870	0.350	0.591	0.058	2.20E-05	5.28E-05	7.04E-05	7.43E-05	7.48E-05
0.9	0.3	1.806	3.080	5.250	0.452	0.517	0.031	1.28E-04	1.44E-04	1.50E-04	1.25E-04	1.11E-04
0.9	0.4	1.775	3.669	6.892	0.561	0.424	0.015	1.93E-01	7.25E-01	1.87E+00	3.87E+00	6.78E+00
0.9	0.5	1.810	4.595	8.917	0.665	0.328	0.006	3.11E-01	1.40E+00	4.07E+00	8.95E+00	1.57E+01
0.9	0.6	1.907	6.599	11.536	0.757	0.241	0.002	1.94E+00	4.29E+00	4.16E+00	7.74E+00	1.59E+01
0.9	0.7	2.067	9.176	14.926	0.833	0.167	0.001	1.90E+00	4.65E+00	4.17E+00	9.95E+00	2.03E+01
0.9	0.8	2.297	12.718	19.311	0.891	0.109	0.000	7.19E-01	1.47E+00	3.80E+00	1.36E+01	2.57E+01
0.9	0.9	2.602	19.960	24.984	0.933	0.067	0.000	1.14E+00	3.58E+00	3.44E+00	1.37E+01	2.65E+01
1.0	0.2	2.118	3.008	4.271	0.347	0.594	0.059	2.64E-05	9.56E-05	1.94E-04	2.14E-04	2.37E-04
1.0	0.3	1.997	3.405	5.805	0.452	0.516	0.031	3.44E-05	5.79E-05	7.80E-05	1.36E-04	1.25E-04
1.0	0.4	1.962	4.054	7.617	0.561	0.424	0.015	1.93E-01	7.25E-01	1.87E+00	3.87E+00	6.78E+00
1.0	0.5	2.000	5.078	9.854	0.665	0.329	0.006	3.11E-01	1.40E+00	4.07E+00	8.95E+00	1.57E+01
1.0	0.6	2.107	7.293	12.750	0.757	0.241	0.002	1.94E+00	4.29E+00	4.16E+00	7.74E+00	1.59E+01
1.0	0.7	2.285	10.141	16.495	0.833	0.167	0.001	1.90E+00	4.65E+00	4.17E+00	9.95E+00	2.03E+01
1.0	0.8	2.538	14.055	21.342	0.891	0.109	0.000	7.19E-01	1.47E+00	3.80E+00	1.35E+01	2.57E+01
1.0	0.9	2.876	22.059	27.612	0.933	0.067	0.000	1.14E+00	3.58E+00	3.44E+00	1.37E+01	2.65E+01
1.1	0.2	2.338	3.320	4.714	0.344	0.596	0.060	1.33E-04	1.64E-04	2.10E-04	2.74E-04	2.66E-04
1.1	0.3	2.207	3.762	6.414	0.452	0.517	0.031	5.25E-05	1.10E-04	1.38E-04	1.42E-04	1.76E-04
1.1	0.4	2.168	4.482	8.418	0.561	0.424	0.015	1.93E-01	7.25E-01	1.87E+00	3.87E+00	6.78E+00
1.1	0.5	2.211	5.613	10.891	0.665	0.328	0.006	3.11E-01	1.40E+00	4.07E+00	8.95E+00	1.57E+01
1.1	0.6	2.329	8.060	14.090	0.757	0.241	0.002	1.94E+00	4.29E+00	4.16E+00	7.74E+00	1.59E+01
1.1	0.7	2.525	11.207	18.230	0.833	0.167	0.001	1.90E+00	4.66E+00	4.17E+00	9.95E+00	2.03E+01
1.1	0.8	2.805	15.534	23.586	0.891	0.109	0.000	7.19E-01	1.47E+00	3.80E+00	1.36E+01	2.57E+01
1.1	0.9	3.178	24.379	30.516	0.933	0.067	0.000	1.14E+00	3.58E+00	3.44E+00	1.37E+01	2.65E+01
1.2	0.2	2.578	3.660	5.198	0.339	0.599	0.061	3.16E-06	5.82E-05	1.11E-04	1.75E-04	1.77E-04
1.2	0.3	2.440	4.160	7.091	0.453	0.516	0.031	7.78E-05	1.34E-04	1.13E-04	1.15E-04	1.52E-04
1.2	0.4	2.397	4.954	9.303	0.561	0.424	0.015	1.93E-01	7.26E-01	1.87E+00	3.88E+00	6.79E+00
1.2	0.5	2.443	6.203	12.036	0.665	0.329	0.006	3.11E-01	1.40E+00	4.07E+00	8.95E+00	1.57E+01

Table 4.6. (continued)

μ	σ	x_1'	x_2'	x_3'	ω_1'	ω_2'	ω_3'	F.E. ¹	F.E. ²	F.E. ³	F.E. ⁴	F.E. ⁵
1.2	0.6	2.574	8.908	15.572	0.757	0.241	0.002	1.94E+00	4.29E+00	4.17E+00	7.74E+00	1.59E+01
1.2	0.7	2.791	12.386	20.148	0.833	0.167	0.001	1.90E+00	4.66E+00	4.17E+00	9.95E+00	2.03E+01
1.2	0.8	3.100	17.167	26.067	0.891	0.109	0.000	7.19E-01	1.47E+00	3.80E+00	1.36E+01	2.57E+01
1.2	0.9	3.512	26.943	33.725	0.933	0.067	0.000	1.14E+00	3.58E+00	3.44E+00	1.37E+01	2.65E+01
1.3	0.2	2.855	4.054	5.755	0.344	0.596	0.060	1.50E-05	3.90E-05	6.29E-05	7.41E-05	7.76E-05
1.3	0.3	2.696	4.596	7.835	0.452	0.516	0.031	9.52E-05	7.61E-05	1.05E-04	1.47E-04	1.60E-04
1.3	0.4	2.648	5.474	10.281	0.561	0.424	0.015	1.93E-01	7.25E-01	1.87E+00	3.87E+00	6.78E+00
1.3	0.5	2.700	6.855	13.302	0.665	0.329	0.006	3.11E-01	1.40E+00	4.07E+00	8.95E+00	1.57E+01
1.3	0.6	2.845	9.844	17.210	0.757	0.241	0.002	1.94E+00	4.29E+00	4.16E+00	7.74E+00	1.59E+01
1.3	0.7	3.084	13.688	22.266	0.833	0.167	0.001	1.90E+00	4.65E+00	4.17E+00	9.95E+00	2.03E+01
1.3	0.8	3.426	18.973	28.808	0.891	0.109	0.000	7.19E-01	1.47E+00	3.80E+00	1.36E+01	2.57E+01
1.3	0.9	3.882	29.776	37.272	0.933	0.067	0.000	1.14E+00	3.58E+00	3.44E+00	1.37E+01	2.65E+01
1.4	0.2	3.149	4.470	6.347	0.339	0.599	0.062	3.38E-06	4.93E-05	5.42E-05	4.95E-05	7.42E-05
1.4	0.3	2.979	5.079	8.659	0.452	0.516	0.031	3.28E-05	7.08E-05	7.51E-05	8.38E-05	7.50E-05
1.4	0.4	2.928	6.051	11.363	0.562	0.424	0.015	1.93E-01	7.26E-01	1.87E+00	3.88E+00	6.79E+00
1.4	0.5	2.984	7.576	14.701	0.665	0.329	0.006	3.11E-01	1.40E+00	4.07E+00	8.95E+00	1.57E+01
1.4	0.6	3.144	10.880	19.020	0.757	0.241	0.002	1.94E+00	4.29E+00	4.16E+00	7.74E+00	1.59E+01
1.4	0.7	3.409	15.128	24.608	0.833	0.167	0.001	1.90E+00	4.65E+00	4.17E+00	9.95E+00	2.03E+01
1.4	0.8	3.786	20.968	31.838	0.891	0.109	0.000	7.19E-01	1.47E+00	3.80E+00	1.36E+01	2.57E+01
1.4	0.9	4.290	32.908	41.192	0.933	0.067	0.000	1.14E+00	3.58E+00	3.44E+00	1.37E+01	2.65E+01
1.5	0.2	3.489	4.953	7.032	0.345	0.595	0.060	5.74E-05	4.38E-05	3.88E-05	4.24E-05	5.69E-05
1.5	0.3	3.291	5.610	9.565	0.451	0.517	0.031	3.63E-06	7.69E-05	8.56E-05	9.40E-05	8.70E-05
1.5	0.4	3.234	6.684	12.558	0.561	0.424	0.015	1.93E-01	7.24E-01	1.87E+00	3.87E+00	6.78E+00
1.5	0.5	3.298	8.372	16.247	0.665	0.329	0.006	3.11E-01	1.40E+00	4.07E+00	8.95E+00	1.57E+01
1.5	0.6	3.475	12.024	21.020	0.757	0.241	0.002	1.94E+00	4.29E+00	4.16E+00	7.74E+00	1.59E+01
1.5	0.7	3.767	16.719	27.196	0.833	0.167	0.001	1.90E+00	4.65E+00	4.17E+00	9.95E+00	2.03E+01
1.5	0.8	4.185	23.173	35.187	0.891	0.109	0.000	7.19E-01	1.47E+00	3.80E+00	1.36E+01	2.57E+01
1.5	0.9	4.741	36.369	45.524	0.933	0.067	0.000	1.14E+00	3.58E+00	3.44E+00	1.37E+01	2.65E+01
1.6	0.2	3.840	5.451	7.740	0.336	0.601	0.063	8.61E-06	2.46E-05	1.13E-04	1.15E-04	1.34E-04
1.6	0.3	3.638	6.203	10.575	0.452	0.517	0.031	5.17E-06	2.98E-05	2.45E-05	5.59E-05	8.76E-05
1.6	0.4	3.575	7.390	13.878	0.561	0.424	0.015	1.93E-01	7.25E-01	1.87E+00	3.87E+00	6.79E+00
1.6	0.5	3.645	9.253	17.956	0.665	0.329	0.006	3.11E-01	1.40E+00	4.07E+00	8.95E+00	1.57E+01
1.6	0.6	3.840	13.289	23.231	0.757	0.241	0.002	1.94E+00	4.29E+00	4.16E+00	7.74E+00	1.59E+01
1.6	0.7	4.163	18.478	30.057	0.833	0.167	0.001	1.90E+00	4.65E+00	4.17E+00	9.95E+00	2.03E+01
1.6	0.8	4.625	25.610	38.887	0.891	0.109	0.000	7.19E-01	1.47E+00	3.80E+00	1.35E+01	2.57E+01
1.6	0.9	5.240	40.194	50.312	0.933	0.067	0.000	1.14E+00	3.58E+00	3.44E+00	1.37E+01	2.65E+01
1.7	0.2	4.268	6.060	8.603	0.349	0.593	0.059	3.63E-05	2.42E-05	5.50E-05	5.44E-05	4.95E-05
1.7	0.3	4.020	6.853	11.684	0.452	0.517	0.031	2.38E-05	4.42E-05	4.20E-05	1.37E-04	2.81E-04
1.7	0.4	3.951	8.166	15.338	0.561	0.424	0.015	1.93E-01	7.25E-01	1.87E+00	3.87E+00	6.79E+00

Table 4.6. (continued)

μ	σ	x_1'	x_2'	x_3'	ω_1'	ω_2'	ω_3'	F.E. ¹	F.E. ²	F.E. ³	F.E. ⁴	F.E. ⁵
1.7	0.5	4.028	10.227	19.844	0.665	0.328	0.006	3.11E-01	1.40E+00	4.07E+00	8.95E+00	1.57E+01
1.7	0.6	4.244	14.686	25.674	0.757	0.241	0.002	1.94E+00	4.29E+00	4.16E+00	7.74E+00	1.59E+01
1.7	0.7	4.601	20.421	33.218	0.833	0.167	0.001	1.90E+00	4.65E+00	4.17E+00	9.95E+00	2.03E+01
1.7	0.8	5.111	28.304	42.977	0.891	0.109	0.000	7.19E-01	1.47E+00	3.80E+00	1.35E+01	2.57E+01
1.7	0.9	5.791	44.421	55.604	0.933	0.067	0.000	1.14E+00	3.58E+00	3.44E+00	1.37E+01	2.65E+01
1.8	0.2	4.712	6.689	9.496	0.346	0.594	0.059	6.95E-06	1.41E-05	5.72E-05	8.79E-05	9.11E-05
1.8	0.3	4.445	7.577	12.918	0.452	0.516	0.031	8.64E-06	1.80E-05	4.32E-05	1.03E-04	2.29E-04
1.8	0.4	4.367	9.026	16.951	0.561	0.424	0.015	1.93E-01	7.25E-01	1.87E+00	3.87E+00	6.79E+00
1.8	0.5	4.452	11.302	21.931	0.665	0.329	0.006	3.11E-01	1.40E+00	4.07E+00	8.95E+00	1.57E+01
1.8	0.6	4.690	16.231	28.375	0.757	0.241	0.002	1.94E+00	4.29E+00	4.16E+00	7.74E+00	1.59E+01
1.8	0.7	5.085	22.569	36.711	0.833	0.167	0.001	1.90E+00	4.65E+00	4.17E+00	9.95E+00	2.03E+01
1.8	0.8	5.649	31.281	47.497	0.891	0.109	0.000	7.19E-01	1.47E+00	3.80E+00	1.35E+01	2.57E+01
1.8	0.9	6.400	49.093	61.451	0.933	0.067	0.000	1.14E+00	3.58E+00	3.44E+00	1.37E+01	2.65E+01
1.9	0.2	5.205	7.390	10.492	0.345	0.595	0.060	4.10E-05	7.42E-05	1.21E-04	1.99E-04	3.31E-04
1.9	0.3	4.913	8.375	14.279	0.452	0.516	0.031	1.98E-05	4.41E-05	3.66E-05	5.38E-05	5.94E-05
1.9	0.4	4.826	9.974	18.734	0.561	0.424	0.015	1.93E-01	7.25E-01	1.87E+00	3.87E+00	6.79E+00
1.9	0.5	4.920	12.491	24.238	0.665	0.329	0.006	3.11E-01	1.40E+00	4.07E+00	8.95E+00	1.57E+01
1.9	0.6	5.183	17.938	31.359	0.757	0.241	0.002	1.94E+00	4.29E+00	4.17E+00	7.74E+00	1.59E+01
1.9	0.7	5.620	24.942	40.572	0.833	0.167	0.001	1.90E+00	4.65E+00	4.17E+00	9.95E+00	2.03E+01
1.9	0.8	6.243	34.570	52.492	0.891	0.109	0.000	7.19E-01	1.47E+00	3.80E+00	1.36E+01	2.57E+01
1.9	0.9	7.073	54.256	67.914	0.933	0.067	0.000	1.14E+00	3.58E+00	3.44E+00	1.37E+01	2.65E+01
2.0	0.2	5.747	8.160	11.586	0.343	0.597	0.060	4.20E-05	3.29E-05	6.23E-05	1.12E-04	1.81E-04
2.0	0.3	5.427	9.253	15.775	0.452	0.517	0.031	2.77E-05	3.33E-05	6.61E-05	1.18E-04	1.89E-04
2.0	0.4	5.334	11.025	20.704	0.562	0.424	0.015	1.93E-01	7.26E-01	1.87E+00	3.88E+00	6.79E+00
2.0	0.5	5.437	13.805	26.787	0.665	0.329	0.006	3.11E-01	1.40E+00	4.07E+00	8.95E+00	1.57E+01
2.0	0.6	5.729	19.824	34.657	0.757	0.241	0.002	1.94E+00	4.29E+00	4.16E+00	7.74E+00	1.59E+01
2.0	0.7	6.211	27.565	44.839	0.833	0.167	0.001	1.90E+00	4.65E+00	4.17E+00	9.95E+00	2.03E+01
2.0	0.8	6.899	38.206	58.013	0.891	0.109	0.000	7.19E-01	1.47E+00	3.80E+00	1.36E+01	2.57E+01
2.0	0.9	7.817	59.962	75.057	0.933	0.067	0.000	1.14E+00	3.58E+00	3.44E+00	1.37E+01	2.65E+01
2.1	0.2	6.361	9.031	12.821	0.346	0.594	0.059	4.60E-05	4.65E-05	5.27E-05	8.19E-05	1.47E-04
2.1	0.3	6.000	10.228	17.438	0.452	0.516	0.031	6.75E-05	1.39E-04	1.95E-04	2.53E-04	2.47E-04
2.1	0.4	5.895	12.185	22.882	0.562	0.424	0.015	1.93E-01	7.26E-01	1.87E+00	3.88E+00	6.79E+00
2.1	0.5	6.009	15.257	29.604	0.665	0.328	0.006	3.11E-01	1.40E+00	4.07E+00	8.95E+00	1.57E+01
2.1	0.6	6.331	21.909	38.302	0.757	0.241	0.002	1.94E+00	4.29E+00	4.17E+00	7.74E+00	1.59E+01
2.1	0.7	6.864	30.464	49.555	0.833	0.167	0.001	1.90E+00	4.65E+00	4.17E+00	9.95E+00	2.03E+01
2.1	0.8	7.625	42.224	64.114	0.891	0.109	0.000	7.19E-01	1.47E+00	3.80E+00	1.36E+01	2.57E+01
2.1	0.9	8.639	66.268	82.951	0.933	0.067	0.000	1.14E+00	3.58E+00	3.44E+00	1.37E+01	2.65E+01
2.2	0.2	7.026	9.975	14.163	0.345	0.595	0.060	1.37E-05	4.90E-05	8.77E-05	1.26E-04	1.86E-04
2.2	0.3	6.630	11.303	19.270	0.452	0.517	0.031	1.63E-04	2.95E-04	4.16E-04	4.92E-04	5.13E-04

Table 4.6. (continued)

μ	σ	x_1'	x_2'	x_3'	ω_1'	ω_2'	ω_3'	F.E. ¹	F.E. ²	F.E. ³	F.E. ⁴	F.E. ⁵
2.2	0.4	6.514	13.463	25.288	0.561	0.424	0.015	1.93E-01	7.25E-01	1.87E+00	3.87E+00	6.78E+00
2.2	0.5	6.641	16.860	32.718	0.665	0.329	0.006	3.11E-01	1.40E+00	4.07E+00	8.95E+00	1.57E+01
2.2	0.6	6.997	24.214	42.330	0.757	0.241	0.002	1.94E+00	4.29E+00	4.16E+00	7.74E+00	1.59E+01
2.2	0.7	7.586	33.668	54.767	0.833	0.167	0.001	1.90E+00	4.65E+00	4.17E+00	9.95E+00	2.03E+01
2.2	0.8	8.427	46.665	70.857	0.891	0.109	0.000	7.19E-01	1.47E+00	3.80E+00	1.36E+01	2.57E+01
2.2	0.9	9.548	73.238	91.675	0.933	0.067	0.000	1.14E+00	3.58E+00	3.44E+00	1.37E+01	2.65E+01
2.3	0.2	7.794	11.066	15.711	0.353	0.589	0.057	2.44E-04	2.91E-04	4.10E-04	4.66E-04	5.47E-04
2.3	0.3	7.333	12.501	21.310	0.453	0.515	0.031	1.07E-04	1.95E-04	1.64E-04	1.41E-04	1.47E-04
2.3	0.4	7.198	14.876	27.948	0.561	0.424	0.015	1.93E-01	7.24E-01	1.87E+00	3.87E+00	6.78E+00
2.3	0.5	7.339	18.633	36.159	0.665	0.329	0.006	3.11E-01	1.40E+00	4.07E+00	8.95E+00	1.57E+01
2.3	0.6	7.733	26.760	46.782	0.757	0.241	0.002	1.94E+00	4.29E+00	4.16E+00	7.74E+00	1.59E+01
2.3	0.7	8.384	37.209	60.526	0.833	0.167	0.001	1.90E+00	4.66E+00	4.17E+00	9.95E+00	2.03E+01
2.3	0.8	9.313	51.573	78.309	0.891	0.109	0.000	7.19E-01	1.47E+00	3.80E+00	1.36E+01	2.57E+01
2.3	0.9	10.552	80.940	101.316	0.933	0.067	0.000	1.14E+00	3.58E+00	3.44E+00	1.37E+01	2.65E+01
2.4	0.2	8.574	12.171	17.278	0.343	0.596	0.061	1.17E-04	8.94E-05	1.68E-04	2.22E-04	2.81E-04
2.4	0.3	8.095	13.801	23.528	0.452	0.517	0.031	9.02E-05	1.40E-04	2.68E-04	4.32E-04	5.37E-04
2.4	0.4	7.958	16.448	30.887	0.562	0.424	0.015	1.93E-01	7.25E-01	1.87E+00	3.88E+00	6.79E+00
2.4	0.5	8.111	20.593	39.961	0.665	0.329	0.006	3.11E-01	1.40E+00	4.07E+00	8.95E+00	1.57E+01
2.4	0.6	8.546	29.574	51.702	0.757	0.241	0.002	1.94E+00	4.29E+00	4.17E+00	7.74E+00	1.59E+01
2.4	0.7	9.266	41.123	66.892	0.833	0.167	0.001	1.90E+00	4.65E+00	4.17E+00	9.95E+00	2.03E+01
2.4	0.8	10.293	56.997	86.545	0.891	0.109	0.000	7.19E-01	1.47E+00	3.80E+00	1.36E+01	2.57E+01
2.4	0.9	11.662	89.453	111.972	0.933	0.067	0.000	1.14E+00	3.58E+00	3.44E+00	1.37E+01	2.65E+01
2.5	0.2	9.482	13.461	19.109	0.345	0.595	0.060	7.69E-05	1.94E-04	2.83E-04	3.29E-04	3.95E-04
2.5	0.3	8.943	15.247	25.994	0.451	0.518	0.032	6.33E-05	1.28E-04	1.12E-04	1.02E-04	1.06E-04
2.5	0.4	8.792	18.171	34.135	0.561	0.424	0.015	1.93E-01	7.25E-01	1.87E+00	3.87E+00	6.78E+00
2.5	0.5	8.965	22.760	44.164	0.665	0.329	0.006	3.11E-01	1.40E+00	4.07E+00	8.95E+00	1.57E+01
2.5	0.6	9.445	32.685	57.140	0.757	0.241	0.002	1.94E+00	4.29E+00	4.16E+00	7.74E+00	1.59E+01
2.5	0.7	10.240	45.447	73.927	0.833	0.167	0.001	1.90E+00	4.65E+00	4.17E+00	9.95E+00	2.03E+01
2.5	0.8	11.375	62.991	95.647	0.891	0.109	0.000	7.19E-01	1.47E+00	3.80E+00	1.36E+01	2.57E+01
2.5	0.9	12.888	98.861	123.748	0.933	0.067	0.000	1.14E+00	3.58E+00	3.44E+00	1.37E+01	2.65E+01
2.6	0.2	10.459	14.851	21.087	0.341	0.598	0.061	9.77E-05	8.08E-05	6.33E-05	8.21E-05	1.15E-04
2.6	0.3	9.889	16.859	28.743	0.452	0.517	0.031	1.79E-04	1.73E-04	1.50E-04	1.49E-04	1.59E-04
2.6	0.4	9.719	20.087	37.725	0.561	0.424	0.015	1.93E-01	7.25E-01	1.87E+00	3.87E+00	6.79E+00
2.6	0.5	9.907	25.153	48.809	0.665	0.329	0.006	3.11E-01	1.40E+00	4.07E+00	8.95E+00	1.57E+01
2.6	0.6	10.438	36.122	63.149	0.757	0.241	0.002	1.94E+00	4.29E+00	4.16E+00	7.74E+00	1.59E+01
2.6	0.7	11.317	50.227	81.702	0.833	0.167	0.001	1.90E+00	4.65E+00	4.17E+00	9.95E+00	2.03E+01
2.6	0.8	12.572	69.616	105.706	0.891	0.109	0.000	7.19E-01	1.47E+00	3.80E+00	1.36E+01	2.57E+01
2.6	0.9	14.244	109.258	136.763	0.933	0.067	0.000	1.14E+00	3.58E+00	3.44E+00	1.37E+01	2.65E+01
2.7	0.2	11.541	16.387	23.267	0.337	0.601	0.062	2.44E-05	1.94E-04	2.72E-04	3.74E-04	4.07E-04

Table 4.6. (continued)

μ	σ	x_1'	x_2'	x_3'	ω_1'	ω_2'	ω_3'	F.E. ¹	F.E. ²	F.E. ³	F.E. ⁴	F.E. ⁵
2.7	0.3	10.924	18.623	31.749	0.451	0.517	0.032	4.55E-05	1.48E-04	1.38E-04	1.58E-04	1.72E-04
2.7	0.4	10.739	22.196	41.693	0.561	0.424	0.015	1.93E-01	7.25E-01	1.87E+00	3.87E+00	6.78E+00
2.7	0.5	10.950	27.801	53.942	0.665	0.328	0.006	3.11E-01	1.40E+00	4.07E+00	8.95E+00	1.57E+01
2.7	0.6	11.536	39.921	69.790	0.757	0.241	0.002	1.94E+00	4.29E+00	4.17E+00	7.74E+00	1.59E+01
2.7	0.7	12.508	55.510	90.295	0.833	0.167	0.001	1.90E+00	4.65E+00	4.17E+00	9.95E+00	2.03E+01
2.7	0.8	13.894	76.938	116.823	0.891	0.109	0.000	7.19E-01	1.47E+00	3.80E+00	1.36E+01	2.57E+01
2.7	0.9	15.741	120.749	151.146	0.933	0.067	0.000	1.14E+00	3.59E+00	3.44E+00	1.37E+01	2.65E+01
2.8	0.2	12.851	18.244	25.896	0.353	0.589	0.057	1.81E-04	1.32E-04	2.06E-04	2.78E-04	3.60E-04
2.8	0.3	12.083	20.597	35.111	0.452	0.516	0.031	1.47E-04	1.10E-04	1.29E-04	2.03E-04	2.14E-04
2.8	0.4	11.870	24.532	46.078	0.561	0.424	0.015	1.93E-01	7.25E-01	1.87E+00	3.87E+00	6.78E+00
2.8	0.5	12.100	30.720	59.615	0.665	0.329	0.006	3.11E-01	1.40E+00	4.07E+00	8.95E+00	1.57E+01
2.8	0.6	12.749	44.120	77.130	0.757	0.241	0.002	1.94E+00	4.29E+00	4.17E+00	7.74E+00	1.59E+01
2.8	0.7	13.823	61.348	99.791	0.833	0.167	0.001	1.90E+00	4.65E+00	4.17E+00	9.95E+00	2.03E+01
2.8	0.8	15.355	85.030	129.110	0.891	0.109	0.000	7.19E-01	1.47E+00	3.80E+00	1.36E+01	2.57E+01
2.8	0.9	17.397	133.448	167.042	0.933	0.067	0.000	1.14E+00	3.58E+00	3.44E+00	1.37E+01	2.65E+01
2.9	0.2	14.145	20.079	28.501	0.344	0.595	0.060	4.40E-05	3.20E-05	5.42E-05	1.30E-04	1.52E-04
2.9	0.3	13.357	22.770	38.817	0.453	0.516	0.031	3.98E-05	1.40E-04	2.00E-04	2.63E-04	2.97E-04
2.9	0.4	13.119	27.114	50.924	0.561	0.424	0.015	1.93E-01	7.25E-01	1.87E+00	3.87E+00	6.79E+00
2.9	0.5	13.374	33.955	65.885	0.665	0.329	0.006	3.11E-01	1.40E+00	4.07E+00	8.95E+00	1.57E+01
2.9	0.6	14.090	48.760	85.242	0.757	0.241	0.002	1.94E+00	4.29E+00	4.16E+00	7.74E+00	1.59E+01
2.9	0.7	15.277	67.800	110.286	0.833	0.167	0.001	1.90E+00	4.65E+00	4.17E+00	9.95E+00	2.03E+01
2.9	0.8	16.970	93.972	142.688	0.891	0.109	0.000	7.19E-01	1.47E+00	3.80E+00	1.36E+01	2.57E+01
2.9	0.9	19.227	147.483	184.610	0.933	0.067	0.000	1.14E+00	3.58E+00	3.44E+00	1.37E+01	2.65E+01
3.0	0.2	15.647	22.215	31.539	0.347	0.594	0.059	1.22E-05	4.39E-05	7.39E-05	1.14E-04	1.35E-04
3.0	0.3	14.757	25.160	42.895	0.452	0.516	0.031	1.22E-04	1.26E-04	9.90E-05	1.20E-04	1.21E-04
3.0	0.4	14.496	29.960	56.280	0.561	0.424	0.015	1.93E-01	7.25E-01	1.87E+00	3.87E+00	6.78E+00
3.0	0.5	14.781	37.528	72.814	0.665	0.328	0.006	3.11E-01	1.40E+00	4.07E+00	8.95E+00	1.57E+01
3.0	0.6	15.572	53.888	94.207	0.757	0.241	0.002	1.94E+00	4.29E+00	4.16E+00	7.74E+00	1.59E+01
3.0	0.7	16.883	74.930	121.885	0.833	0.167	0.001	1.90E+00	4.66E+00	4.17E+00	9.95E+00	2.03E+01
3.0	0.8	18.755	103.855	157.695	0.891	0.109	0.000	7.19E-01	1.47E+00	3.80E+00	1.36E+01	2.57E+01
3.0	0.9	21.249	162.994	204.026	0.933	0.067	0.000	1.14E+00	3.58E+00	3.44E+00	1.37E+01	2.65E+01
3.1	0.2	17.291	24.548	34.852	0.346	0.594	0.059	6.36E-05	8.65E-05	1.11E-04	1.12E-04	9.85E-05
3.1	0.3	16.305	27.796	47.386	0.452	0.517	0.031	9.51E-05	1.34E-04	1.56E-04	1.84E-04	1.58E-04
3.1	0.4	16.023	33.116	62.199	0.561	0.424	0.015	1.93E-01	7.25E-01	1.87E+00	3.87E+00	6.78E+00
3.1	0.5	16.336	41.474	80.472	0.665	0.328	0.006	3.11E-01	1.40E+00	4.07E+00	8.95E+00	1.57E+01
3.1	0.6	17.210	59.556	104.115	0.757	0.241	0.002	1.94E+00	4.29E+00	4.16E+00	7.74E+00	1.59E+01
3.1	0.7	18.659	82.811	134.704	0.833	0.167	0.001	1.90E+00	4.65E+00	4.17E+00	9.95E+00	2.03E+01
3.1	0.8	20.727	114.778	174.280	0.891	0.109	0.000	7.19E-01	1.47E+00	3.80E+00	1.36E+01	2.57E+01
3.1	0.9	23.483	180.136	225.483	0.933	0.067	0.000	1.14E+00	3.59E+00	3.44E+00	1.37E+01	2.65E+01

Table 4.6. (continued)

μ	σ	x_1'	x_2'	x_3'	ω_1'	ω_2'	ω_3'	F.E. ¹	F.E. ²	F.E. ³	F.E. ⁴	F.E. ⁵
3.2	0.2	19.129	27.162	38.565	0.349	0.593	0.059	1.79E-05	4.70E-05	1.35E-04	1.48E-04	1.28E-04
3.2	0.3	18.024	30.729	52.386	0.452	0.516	0.031	3.10E-05	7.68E-05	1.65E-04	2.18E-04	2.19E-04
3.2	0.4	17.708	36.597	68.740	0.561	0.424	0.015	1.93E-01	7.25E-01	1.87E+00	3.87E+00	6.78E+00
3.2	0.5	18.052	45.831	88.936	0.665	0.329	0.006	3.11E-01	1.40E+00	4.07E+00	8.95E+00	1.57E+01
3.2	0.6	19.020	65.819	115.065	0.757	0.241	0.002	1.94E+00	4.29E+00	4.16E+00	7.74E+00	1.59E+01
3.2	0.7	20.621	91.520	148.871	0.833	0.167	0.001	1.90E+00	4.65E+00	4.17E+00	9.95E+00	2.03E+01
3.2	0.8	22.907	126.849	192.609	0.891	0.109	0.000	7.19E-01	1.47E+00	3.80E+00	1.35E+01	2.57E+01
3.2	0.9	25.953	199.081	249.198	0.933	0.067	0.000	1.14E+00	3.58E+00	3.44E+00	1.37E+01	2.65E+01
3.3	0.2	21.141	30.013	42.607	0.349	0.593	0.059	1.40E-04	1.43E-04	1.77E-04	2.04E-04	2.48E-04
3.3	0.3	19.929	33.977	57.928	0.453	0.516	0.031	2.67E-05	8.88E-05	1.15E-04	2.45E-04	2.82E-04
3.3	0.4	19.570	40.446	75.969	0.561	0.424	0.015	1.93E-01	7.25E-01	1.87E+00	3.87E+00	6.78E+00
3.3	0.5	19.949	50.649	98.289	0.665	0.329	0.006	3.11E-01	1.40E+00	4.07E+00	8.95E+00	1.57E+01
3.3	0.6	21.020	72.742	127.167	0.757	0.241	0.002	1.94E+00	4.29E+00	4.16E+00	7.74E+00	1.59E+01
3.3	0.7	22.790	101.145	164.528	0.833	0.167	0.001	1.90E+00	4.66E+00	4.17E+00	9.95E+00	2.03E+01
3.3	0.8	25.316	140.190	212.866	0.891	0.109	0.000	7.19E-01	1.47E+00	3.80E+00	1.36E+01	2.57E+01
3.3	0.9	28.683	220.019	275.406	0.933	0.067	0.000	1.14E+00	3.58E+00	3.44E+00	1.37E+01	2.65E+01
3.4	0.2	23.391	33.220	47.177	0.351	0.591	0.058	4.42E-05	7.33E-05	6.60E-05	1.68E-04	1.90E-04
3.4	0.3	22.004	37.512	63.952	0.451	0.517	0.031	7.81E-05	1.59E-04	1.68E-04	1.92E-04	2.11E-04
3.4	0.4	21.628	44.700	83.959	0.561	0.424	0.015	1.93E-01	7.25E-01	1.87E+00	3.87E+00	6.78E+00
3.4	0.5	22.049	55.980	108.626	0.665	0.329	0.006	3.11E-01	1.40E+00	4.07E+00	8.95E+00	1.57E+01
3.4	0.6	23.229	80.392	140.541	0.757	0.241	0.002	1.94E+00	4.29E+00	4.17E+00	7.74E+00	1.59E+01
3.4	0.7	25.187	111.783	181.832	0.833	0.167	0.001	1.90E+00	4.65E+00	4.17E+00	9.95E+00	2.03E+01
3.4	0.8	27.978	154.934	235.253	0.891	0.109	0.000	7.19E-01	1.47E+00	3.80E+00	1.36E+01	2.57E+01
3.4	0.9	31.700	243.158	304.371	0.933	0.067	0.000	1.14E+00	3.58E+00	3.44E+00	1.37E+01	2.65E+01
3.5	0.2	25.760	36.577	51.937	0.344	0.596	0.060	6.38E-05	6.14E-05	5.32E-05	5.63E-05	4.83E-05
3.5	0.3	24.319	41.459	70.681	0.451	0.517	0.031	2.00E-05	7.39E-05	7.75E-05	1.03E-04	1.36E-04
3.5	0.4	23.907	49.412	92.789	0.562	0.424	0.015	1.93E-01	7.26E-01	1.87E+00	3.88E+00	6.79E+00
3.5	0.5	24.371	61.875	120.051	0.665	0.328	0.006	3.11E-01	1.40E+00	4.07E+00	8.95E+00	1.57E+01
3.5	0.6	25.674	88.847	155.322	0.757	0.241	0.002	1.94E+00	4.29E+00	4.16E+00	7.74E+00	1.59E+01
3.5	0.7	27.836	123.539	200.955	0.833	0.167	0.001	1.90E+00	4.65E+00	4.17E+00	9.95E+00	2.03E+01
3.5	0.8	30.921	171.229	259.995	0.891	0.109	0.000	7.19E-01	1.47E+00	3.80E+00	1.36E+01	2.57E+01
3.5	0.9	35.033	268.732	336.382	0.933	0.067	0.000	1.14E+00	3.58E+00	3.44E+00	1.37E+01	2.65E+01
3.6	0.2	28.486	40.443	57.422	0.345	0.595	0.060	3.19E-05	7.39E-05	8.90E-05	8.66E-05	9.18E-05
3.6	0.3	26.883	45.830	78.130	0.452	0.517	0.031	5.79E-05	5.75E-05	4.67E-05	5.59E-05	4.84E-05
3.6	0.4	26.415	54.595	102.548	0.561	0.424	0.015	1.93E-01	7.25E-01	1.87E+00	3.87E+00	6.78E+00
3.6	0.5	26.931	68.377	132.677	0.665	0.329	0.006	3.11E-01	1.40E+00	4.07E+00	8.95E+00	1.57E+01
3.6	0.6	28.374	98.191	171.657	0.757	0.241	0.002	1.94E+00	4.29E+00	4.16E+00	7.74E+00	1.59E+01
3.6	0.7	30.764	136.532	222.090	0.833	0.167	0.001	1.90E+00	4.65E+00	4.17E+00	9.95E+00	2.03E+01
3.6	0.8	34.173	189.237	287.339	0.891	0.109	0.000	7.19E-01	1.47E+00	3.80E+00	1.35E+01	2.57E+01

Table 4.6. (continued)

μ	σ	x_1'	x_2'	x_3'	ω_1'	ω_2'	ω_3'	F.E. ¹	F.E. ²	F.E. ³	F.E. ⁴	F.E. ⁵
3.6	0.9	38.718	296.994	371.759	0.933	0.067	0.000	1.14E+00	3.58E+00	3.44E+00	1.37E+01	2.65E+01
3.7	0.2	31.500	44.719	63.482	0.346	0.595	0.060	1.24E-05	1.09E-05	3.75E-05	6.81E-05	6.27E-05
3.7	0.3	29.708	50.646	86.344	0.452	0.517	0.031	5.34E-07	4.09E-05	6.12E-05	8.05E-05	8.80E-05
3.7	0.4	29.191	60.331	113.333	0.561	0.424	0.015	1.93E-01	7.25E-01	1.87E+00	3.87E+00	6.78E+00
3.7	0.5	29.766	75.572	146.630	0.665	0.328	0.006	3.11E-01	1.40E+00	4.07E+00	8.95E+00	1.57E+01
3.7	0.6	31.358	108.518	189.710	0.757	0.241	0.002	1.94E+00	4.29E+00	4.16E+00	7.74E+00	1.59E+01
3.7	0.7	33.998	150.891	245.447	0.833	0.167	0.001	1.90E+00	4.65E+00	4.17E+00	9.95E+00	2.03E+01
3.7	0.8	37.766	209.139	317.559	0.891	0.109	0.000	7.19E-01	1.47E+00	3.80E+00	1.35E+01	2.57E+01
3.7	0.9	42.790	328.230	410.857	0.933	0.067	0.000	1.14E+00	3.58E+00	3.44E+00	1.37E+01	2.65E+01
3.8	0.2	34.939	49.621	70.463	0.354	0.589	0.057	5.41E-05	9.71E-05	2.37E-04	2.41E-04	2.59E-04
3.8	0.3	32.840	55.984	95.438	0.452	0.517	0.031	2.29E-05	8.61E-05	1.30E-04	1.30E-04	1.30E-04
3.8	0.4	32.272	66.703	125.253	0.562	0.424	0.015	1.93E-01	7.26E-01	1.87E+00	3.88E+00	6.79E+00
3.8	0.5	32.893	83.511	162.052	0.665	0.329	0.006	3.11E-01	1.40E+00	4.07E+00	8.95E+00	1.57E+01
3.8	0.6	34.656	119.930	209.662	0.757	0.241	0.002	1.94E+00	4.29E+00	4.16E+00	7.74E+00	1.59E+01
3.8	0.7	37.574	166.760	271.261	0.833	0.167	0.001	1.90E+00	4.65E+00	4.17E+00	9.95E+00	2.03E+01
3.8	0.8	41.738	231.134	350.957	0.891	0.109	0.000	7.19E-01	1.47E+00	3.80E+00	1.35E+01	2.57E+01
3.8	0.9	47.290	362.750	454.068	0.933	0.067	0.000	1.14E+00	3.59E+00	3.44E+00	1.37E+01	2.65E+01
3.9	0.2	38.599	54.816	77.836	0.353	0.590	0.057	9.20E-05	1.45E-04	1.35E-04	1.68E-04	1.96E-04
3.9	0.3	36.274	61.840	105.426	0.451	0.517	0.032	4.17E-05	4.66E-05	1.32E-04	1.95E-04	2.86E-04
3.9	0.4	35.663	73.711	138.425	0.561	0.424	0.015	1.93E-01	7.26E-01	1.87E+00	3.88E+00	6.79E+00
3.9	0.5	36.354	92.297	179.095	0.665	0.329	0.006	3.11E-01	1.40E+00	4.07E+00	8.95E+00	1.57E+01
3.9	0.6	38.302	132.544	231.713	0.757	0.241	0.002	1.94E+00	4.29E+00	4.16E+00	7.74E+00	1.59E+01
3.9	0.7	41.527	184.298	299.789	0.833	0.167	0.001	1.90E+00	4.65E+00	4.17E+00	9.95E+00	2.03E+01
3.9	0.8	46.128	255.443	387.867	0.891	0.109	0.000	7.19E-01	1.47E+00	3.80E+00	1.36E+01	2.57E+01
3.9	0.9	52.263	400.900	501.822	0.933	0.067	0.000	1.14E+00	3.59E+00	3.44E+00	1.37E+01	2.65E+01
4.0	0.2	42.587	60.468	85.851	0.349	0.592	0.058	3.36E-05	9.12E-05	8.50E-05	1.13E-04	1.22E-04
4.0	0.3	40.131	68.418	116.637	0.453	0.516	0.031	2.72E-05	6.29E-05	5.19E-05	1.34E-04	2.76E-04
4.0	0.4	39.412	81.458	152.984	0.561	0.424	0.015	1.93E-01	7.26E-01	1.87E+00	3.87E+00	6.79E+00
4.0	0.5	40.176	102.001	197.930	0.665	0.329	0.006	3.11E-01	1.40E+00	4.07E+00	8.95E+00	1.57E+01
4.0	0.6	42.328	146.483	256.082	0.757	0.241	0.002	1.94E+00	4.29E+00	4.16E+00	7.74E+00	1.59E+01
4.0	0.7	45.894	203.681	331.319	0.833	0.167	0.001	1.90E+00	4.65E+00	4.17E+00	9.95E+00	2.03E+01
4.0	0.8	50.980	282.308	428.660	0.891	0.109	0.000	7.19E-01	1.47E+00	3.80E+00	1.36E+01	2.57E+01
4.0	0.9	57.761	443.063	554.600	0.933	0.067	0.000	1.14E+00	3.58E+00	3.44E+00	1.37E+01	2.65E+01
4.1	0.2	47.071	66.841	94.912	0.350	0.592	0.058	8.08E-05	1.40E-04	1.40E-04	1.84E-04	1.59E-04
4.1	0.3	44.331	75.579	128.852	0.452	0.516	0.031	8.39E-06	8.62E-06	2.03E-05	1.00E-04	1.88E-04
4.1	0.4	43.559	90.029	169.073	0.561	0.424	0.015	1.93E-01	7.26E-01	1.87E+00	3.88E+00	6.79E+00
4.1	0.5	44.402	112.730	218.747	0.665	0.329	0.006	3.11E-01	1.40E+00	4.07E+00	8.95E+00	1.57E+01
4.1	0.6	46.779	161.889	283.014	0.757	0.241	0.002	1.94E+00	4.29E+00	4.17E+00	7.74E+00	1.59E+01
4.1	0.7	50.720	225.102	366.164	0.833	0.167	0.001	1.90E+00	4.65E+00	4.17E+00	9.95E+00	2.03E+01

Table 4.6. (continued)

μ	σ	x_1'	x_2'	x_3'	ω_1'	ω_2'	ω_3'	F.E. ¹	F.E. ²	F.E. ³	F.E. ⁴	F.E. ⁵
4.1	0.8	56.341	311.999	473.742	0.891	0.109	0.000	7.19E-01	1.47E+00	3.80E+00	1.35E+01	2.57E+01
4.1	0.9	63.834	489.661	612.927	0.933	0.067	0.000	1.14E+00	3.59E+00	3.44E+00	1.37E+01	2.65E+01
4.2	0.2	51.938	73.743	104.702	0.346	0.594	0.059	2.03E-05	4.67E-05	8.93E-05	1.36E-04	2.41E-04
4.2	0.3	48.981	83.504	142.360	0.452	0.517	0.031	3.68E-06	1.85E-05	1.97E-05	2.11E-05	2.27E-05
4.2	0.4	48.134	99.484	186.855	0.561	0.424	0.015	1.93E-01	7.25E-01	1.87E+00	3.87E+00	6.78E+00
4.2	0.5	49.072	124.588	241.753	0.665	0.329	0.006	3.11E-01	1.40E+00	4.07E+00	8.95E+00	1.57E+01
4.2	0.6	51.701	178.915	312.779	0.757	0.241	0.002	1.94E+00	4.29E+00	4.16E+00	7.74E+00	1.59E+01
4.2	0.7	56.055	248.777	404.673	0.833	0.167	0.001	1.90E+00	4.65E+00	4.17E+00	9.95E+00	2.03E+01
4.2	0.8	62.267	344.812	523.566	0.891	0.109	0.000	7.19E-01	1.47E+00	3.80E+00	1.36E+01	2.57E+01
4.2	0.9	70.549	541.159	677.389	0.933	0.067	0.000	1.14E+00	3.58E+00	3.44E+00	1.37E+01	2.65E+01
4.3	0.2	57.352	81.429	115.614	0.344	0.596	0.060	1.24E-05	5.25E-05	9.82E-05	1.45E-04	2.00E-04
4.3	0.3	54.128	92.280	157.322	0.452	0.517	0.031	2.61E-05	3.54E-05	3.67E-05	5.51E-05	1.01E-04
4.3	0.4	53.203	109.964	206.506	0.561	0.424	0.015	1.93E-01	7.26E-01	1.87E+00	3.88E+00	6.79E+00
4.3	0.5	54.234	137.693	267.178	0.665	0.329	0.006	3.11E-01	1.40E+00	4.07E+00	8.95E+00	1.57E+01
4.3	0.6	57.136	197.732	345.675	0.757	0.241	0.002	1.94E+00	4.29E+00	4.17E+00	7.74E+00	1.59E+01
4.3	0.7	61.950	274.941	447.233	0.833	0.167	0.001	1.90E+00	4.65E+00	4.17E+00	9.95E+00	2.03E+01
4.3	0.8	68.815	381.076	578.630	0.891	0.109	0.000	7.19E-01	1.47E+00	3.80E+00	1.36E+01	2.57E+01
4.3	0.9	77.968	598.073	748.631	0.933	0.067	0.000	1.14E+00	3.58E+00	3.44E+00	1.37E+01	2.65E+01
4.4	0.2	63.383	89.983	127.748	0.344	0.596	0.060	3.79E-06	3.55E-05	8.23E-05	1.23E-04	1.86E-04
4.4	0.3	59.841	102.018	173.919	0.452	0.516	0.031	6.74E-05	1.71E-04	2.49E-04	3.33E-04	4.31E-04
4.4	0.4	58.778	121.475	228.225	0.561	0.424	0.015	1.93E-01	7.24E-01	1.87E+00	3.87E+00	6.77E+00
4.4	0.5	59.938	152.173	295.277	0.665	0.329	0.006	3.11E-01	1.40E+00	4.07E+00	8.95E+00	1.57E+01
4.4	0.6	63.147	218.528	382.029	0.757	0.241	0.002	1.94E+00	4.29E+00	4.16E+00	7.74E+00	1.59E+01
4.4	0.7	68.463	303.856	494.269	0.833	0.167	0.001	1.90E+00	4.66E+00	4.17E+00	9.95E+00	2.03E+01
4.4	0.8	76.052	421.154	639.485	0.891	0.109	0.000	7.19E-01	1.47E+00	3.80E+00	1.35E+01	2.57E+01
4.4	0.9	86.168	660.973	827.365	0.933	0.067	0.000	1.14E+00	3.58E+00	3.44E+00	1.37E+01	2.65E+01
4.5	0.2	70.029	99.422	141.154	0.344	0.596	0.060	8.28E-06	2.00E-05	2.32E-05	3.84E-05	4.31E-05
4.5	0.3	66.175	112.826	192.353	0.453	0.516	0.031	8.52E-05	1.98E-04	2.02E-04	2.97E-04	3.28E-04
4.5	0.4	64.977	134.298	252.228	0.561	0.424	0.015	1.93E-01	7.25E-01	1.87E+00	3.87E+00	6.79E+00
4.5	0.5	66.246	168.189	326.332	0.665	0.328	0.006	3.11E-01	1.40E+00	4.07E+00	8.95E+00	1.57E+01
4.5	0.6	69.792	241.510	422.208	0.757	0.241	0.002	1.94E+00	4.29E+00	4.15E+00	7.74E+00	1.59E+01
4.5	0.7	75.666	335.813	546.252	0.833	0.167	0.001	1.90E+00	4.65E+00	4.17E+00	9.95E+00	2.03E+01
4.5	0.8	84.051	465.447	706.740	0.891	0.109	0.000	7.19E-01	1.47E+00	3.80E+00	1.35E+01	2.57E+01
4.5	0.9	95.231	730.488	914.380	0.933	0.067	0.000	1.14E+00	3.58E+00	3.44E+00	1.37E+01	2.65E+01
4.6	0.2	77.619	110.196	156.438	0.350	0.592	0.058	1.16E-04	3.25E-04	4.40E-04	5.36E-04	5.89E-04
4.6	0.3	73.102	124.640	212.503	0.453	0.516	0.031	2.62E-04	3.13E-04	2.73E-04	3.08E-04	2.93E-04
4.6	0.4	71.804	148.404	278.755	0.561	0.424	0.015	1.93E-01	7.25E-01	1.87E+00	3.87E+00	6.78E+00
4.6	0.5	73.202	185.855	360.652	0.665	0.329	0.006	3.11E-01	1.40E+00	4.07E+00	8.95E+00	1.57E+01
4.6	0.6	77.126	266.910	466.612	0.757	0.241	0.002	1.94E+00	4.29E+00	4.16E+00	7.74E+00	1.59E+01

Table 4.6. (continued)

μ	σ	x_1'	x_2'	x_3'	ω_1'	ω_2'	ω_3'	F.E. ¹	F.E. ²	F.E. ³	F.E. ⁴	F.E. ⁵
4.6	0.7	83.621	371.131	603.702	0.833	0.167	0.001	1.90E+00	4.66E+00	4.17E+00	9.95E+00	2.03E+01
4.6	0.8	92.892	514.399	781.069	0.891	0.109	0.000	7.19E-01	1.47E+00	3.80E+00	1.36E+01	2.57E+01
4.6	0.9	105.246	807.314	1010.546	0.933	0.067	0.000	1.14E+00	3.58E+00	3.44E+00	1.37E+01	2.65E+01
4.7	0.2	85.334	121.174	172.078	0.339	0.600	0.062	1.75E-04	1.63E-04	2.32E-04	2.84E-04	3.10E-04
4.7	0.3	80.824	137.790	234.898	0.453	0.516	0.031	3.23E-06	1.83E-04	2.68E-04	3.85E-04	4.69E-04
4.7	0.4	79.361	164.025	308.071	0.561	0.424	0.015	1.93E-01	7.26E-01	1.87E+00	3.87E+00	6.79E+00
4.7	0.5	80.898	205.396	398.583	0.665	0.329	0.006	3.11E-01	1.40E+00	4.07E+00	8.95E+00	1.57E+01
4.7	0.6	85.241	294.981	515.686	0.757	0.241	0.002	1.94E+00	4.29E+00	4.16E+00	7.74E+00	1.59E+01
4.7	0.7	92.417	410.163	667.194	0.833	0.167	0.001	1.90E+00	4.66E+00	4.17E+00	9.95E+00	2.03E+01
4.7	0.8	102.660	568.499	863.215	0.891	0.109	0.000	7.19E-01	1.47E+00	3.80E+00	1.35E+01	2.57E+01
4.7	0.9	116.315	892.220	1116.826	0.933	0.067	0.000	1.14E+00	3.58E+00	3.44E+00	1.37E+01	2.65E+01
4.8	0.2	94.666	134.422	190.868	0.347	0.594	0.059	5.49E-05	1.86E-04	3.41E-04	4.50E-04	5.79E-04
4.8	0.3	89.178	152.037	259.218	0.451	0.518	0.032	1.66E-04	1.34E-04	1.68E-04	1.72E-04	1.68E-04
4.8	0.4	87.719	181.296	340.472	0.561	0.424	0.015	1.93E-01	7.26E-01	1.87E+00	3.88E+00	6.79E+00
4.8	0.5	89.409	226.997	440.502	0.665	0.329	0.006	3.11E-01	1.40E+00	4.07E+00	8.95E+00	1.57E+01
4.8	0.6	94.199	326.005	569.921	0.757	0.241	0.002	1.94E+00	4.29E+00	4.17E+00	7.74E+00	1.59E+01
4.8	0.7	102.137	453.301	737.363	0.833	0.167	0.001	1.90E+00	4.65E+00	4.17E+00	9.95E+00	2.03E+01
4.8	0.8	113.456	628.288	954.000	0.891	0.109	0.000	7.19E-01	1.47E+00	3.80E+00	1.35E+01	2.57E+01
4.8	0.9	128.548	986.056	1234.284	0.933	0.067	0.000	1.14E+00	3.58E+00	3.44E+00	1.37E+01	2.65E+01
4.9	0.2	104.883	148.892	211.351	0.352	0.590	0.058	1.05E-04	1.55E-04	1.42E-04	1.35E-04	1.19E-04
4.9	0.3	98.667	168.208	286.760	0.452	0.516	0.031	6.93E-05	7.27E-05	9.82E-05	1.25E-04	1.73E-04
4.9	0.4	96.925	200.336	376.279	0.561	0.424	0.015	1.93E-01	7.26E-01	1.87E+00	3.87E+00	6.79E+00
4.9	0.5	98.817	250.885	486.830	0.665	0.329	0.006	3.11E-01	1.40E+00	4.07E+00	8.95E+00	1.57E+01
4.9	0.6	104.111	360.291	629.860	0.757	0.241	0.002	1.94E+00	4.29E+00	4.16E+00	7.74E+00	1.59E+01
4.9	0.7	112.880	500.975	814.912	0.833	0.167	0.001	1.90E+00	4.65E+00	4.17E+00	9.95E+00	2.03E+01
4.9	0.8	125.389	694.366	1054.333	0.891	0.109	0.000	7.19E-01	1.47E+00	3.80E+00	1.35E+01	2.57E+01
4.9	0.9	142.067	1089.760	1364.095	0.933	0.067	0.000	1.14E+00	3.58E+00	3.44E+00	1.37E+01	2.65E+01
5.0	0.2	115.227	163.614	232.334	0.339	0.599	0.061	8.84E-05	8.84E-05	8.31E-05	6.97E-05	8.36E-05
5.0	0.3	108.991	185.823	316.819	0.452	0.517	0.031	1.35E-04	1.13E-04	1.04E-04	8.73E-05	9.89E-05
5.0	0.4	107.123	221.407	415.853	0.561	0.424	0.015	1.93E-01	7.25E-01	1.87E+00	3.87E+00	6.79E+00
5.0	0.5	109.214	277.283	538.030	0.665	0.328	0.006	3.11E-01	1.40E+00	4.07E+00	8.95E+00	1.57E+01
5.0	0.6	115.059	398.183	696.103	0.757	0.241	0.002	1.94E+00	4.29E+00	4.17E+00	7.74E+00	1.59E+01
5.0	0.7	124.751	553.663	900.617	0.833	0.167	0.001	1.90E+00	4.65E+00	4.17E+00	9.95E+00	2.03E+01
5.0	0.8	138.577	767.393	1165.218	0.891	0.109	0.000	7.19E-01	1.47E+00	3.80E+00	1.36E+01	2.57E+01
5.0	0.9	157.007	1204.371	1507.558	0.933	0.067	0.000	1.14E+00	3.59E+00	3.44E+00	1.37E+01	2.65E+01
5.1	0.2	127.557	181.144	257.247	0.343	0.597	0.060	2.57E-04	3.13E-04	3.87E-04	4.85E-04	5.22E-04
5.1	0.3	120.419	205.304	350.034	0.451	0.517	0.032	2.33E-04	2.28E-04	2.96E-04	3.78E-04	4.50E-04
5.1	0.4	118.402	244.711	459.589	0.561	0.424	0.015	1.93E-01	7.25E-01	1.87E+00	3.87E+00	6.79E+00
5.1	0.5	120.689	306.415	594.615	0.665	0.329	0.006	3.11E-01	1.40E+00	4.07E+00	8.95E+00	1.57E+01

Table 4.6. (continued)

μ	σ	x_1'	x_2'	x_3'	ω_1'	ω_2'	ω_3'	F.E. ¹	F.E. ²	F.E. ³	F.E. ⁴	F.E. ⁵
5.1	0.6	127.163	440.060	769.313	0.757	0.241	0.002	1.94E+00	4.29E+00	4.16E+00	7.74E+00	1.59E+01
5.1	0.7	137.871	611.892	995.336	0.833	0.167	0.001	1.90E+00	4.65E+00	4.17E+00	9.95E+00	2.03E+01
5.1	0.8	153.151	848.100	1287.765	0.891	0.109	0.000	7.19E-01	1.47E+00	3.80E+00	1.36E+01	2.57E+01
5.1	0.9	173.521	1331.036	1666.109	0.933	0.067	0.000	1.14E+00	3.58E+00	3.44E+00	1.37E+01	2.65E+01
5.2	0.2	141.087	200.325	284.438	0.345	0.595	0.060	2.66E-05	2.39E-05	1.82E-05	2.60E-05	3.90E-05
5.2	0.3	133.204	227.092	387.156	0.452	0.516	0.031	1.02E-04	8.24E-05	6.48E-05	1.05E-04	9.63E-05
5.2	0.4	130.843	270.423	507.924	0.561	0.424	0.015	1.93E-01	7.25E-01	1.87E+00	3.87E+00	6.78E+00
5.2	0.5	133.380	338.633	657.152	0.665	0.329	0.006	3.11E-01	1.40E+00	4.07E+00	8.95E+00	1.57E+01
5.2	0.6	140.531	486.342	850.222	0.757	0.241	0.002	1.94E+00	4.29E+00	4.17E+00	7.74E+00	1.59E+01
5.2	0.7	152.371	676.245	1100.017	0.833	0.167	0.001	1.90E+00	4.65E+00	4.17E+00	9.95E+00	2.03E+01
5.2	0.8	169.258	937.296	1423.200	0.891	0.109	0.000	7.19E-01	1.47E+00	3.80E+00	1.35E+01	2.57E+01
5.2	0.9	191.770	1471.023	1841.335	0.933	0.067	0.000	1.14E+00	3.59E+00	3.44E+00	1.37E+01	2.65E+01
5.3	0.2	155.977	221.472	314.475	0.345	0.595	0.060	2.39E-05	3.97E-05	4.97E-05	1.15E-04	1.49E-04
5.3	0.3	147.150	250.856	427.657	0.452	0.517	0.031	4.18E-05	4.41E-05	8.39E-05	9.66E-05	1.09E-04
5.3	0.4	144.572	298.795	561.343	0.561	0.424	0.015	1.93E-01	7.24E-01	1.87E+00	3.87E+00	6.77E+00
5.3	0.5	147.412	374.262	726.265	0.665	0.329	0.006	3.11E-01	1.40E+00	4.07E+00	8.95E+00	1.57E+01
5.3	0.6	155.319	537.491	939.641	0.757	0.241	0.002	1.94E+00	4.29E+00	4.16E+00	7.74E+00	1.59E+01
5.3	0.7	168.392	747.366	1215.706	0.833	0.167	0.001	1.90E+00	4.66E+00	4.17E+00	9.95E+00	2.03E+01
5.3	0.8	187.054	1035.872	1572.880	0.891	0.109	0.000	7.20E-01	1.47E+00	3.80E+00	1.35E+01	2.57E+01
5.3	0.9	211.938	1625.731	2034.990	0.933	0.067	0.000	1.14E+00	3.59E+00	3.44E+00	1.37E+01	2.65E+01
5.4	0.2	172.033	244.238	346.768	0.341	0.598	0.061	3.15E-05	2.58E-05	5.95E-05	5.08E-05	6.08E-05
5.4	0.3	162.574	277.162	472.523	0.451	0.517	0.031	5.46E-05	1.79E-04	2.28E-04	2.63E-04	2.50E-04
5.4	0.4	159.805	330.276	620.380	0.561	0.424	0.015	1.93E-01	7.25E-01	1.87E+00	3.87E+00	6.78E+00
5.4	0.5	162.922	413.641	802.647	0.665	0.329	0.006	3.11E-01	1.40E+00	4.07E+00	8.95E+00	1.57E+01
5.4	0.6	171.652	594.020	1038.464	0.757	0.241	0.002	1.94E+00	4.29E+00	4.16E+00	7.74E+00	1.59E+01
5.4	0.7	186.108	825.968	1343.563	0.833	0.167	0.001	1.90E+00	4.65E+00	4.17E+00	9.95E+00	2.03E+01
5.4	0.8	206.735	1144.816	1738.301	0.891	0.109	0.000	7.19E-01	1.47E+00	3.80E+00	1.36E+01	2.57E+01
5.4	0.9	234.228	1796.711	2249.012	0.933	0.067	0.000	1.14E+00	3.59E+00	3.44E+00	1.37E+01	2.65E+01
5.5	0.2	190.543	270.549	384.152	0.346	0.595	0.059	9.63E-05	1.48E-04	1.94E-04	2.49E-04	2.44E-04
5.5	0.3	179.827	306.575	522.648	0.453	0.516	0.031	9.24E-05	6.84E-05	7.39E-05	9.18E-05	1.11E-04
5.5	0.4	176.642	365.086	685.626	0.561	0.424	0.015	1.93E-01	7.26E-01	1.87E+00	3.88E+00	6.79E+00
5.5	0.5	180.056	457.145	887.062	0.665	0.329	0.006	3.11E-01	1.40E+00	4.07E+00	8.95E+00	1.57E+01
5.5	0.6	189.709	656.493	1147.680	0.757	0.241	0.002	1.94E+00	4.29E+00	4.16E+00	7.74E+00	1.59E+01
5.5	0.7	205.684	912.835	1484.867	0.833	0.167	0.001	1.90E+00	4.65E+00	4.17E+00	9.95E+00	2.03E+01
5.5	0.8	228.473	1265.217	1921.120	0.891	0.109	0.000	7.19E-01	1.47E+00	3.80E+00	1.35E+01	2.57E+01
5.5	0.9	258.863	1985.673	2485.543	0.933	0.067	0.000	1.14E+00	3.58E+00	3.44E+00	1.37E+01	2.65E+01

CHAPTER 5. CONCLUSION

5.1 Remark on Limitation of the Proposed Method

Mathematically, the variance estimates $\text{Var}[Y] = E[(Y - \mu_Y)^2]$ of a response Y must be positive (μ_Y is the mean of Y). However, a negative variance value may appear when the numerical approximations of $E[Y^2]$ and/or $E[Y]^2$ happen to lead to unexpected values. For instance, when our target response $Y = F_{min}$, the peak shear force capacity in the negative direction, the 4D MM variance estimation using 9 index points is given by

$$\text{Var}[F_{min}] = \sum_{i=1}^9 \omega_i F_{min}^2(X_i) - \left[\sum_{i=1}^9 \omega_i F_{min}(X_i) \right]^2 \quad (5.1)$$

In view of the fact that the weight ω_i is determined from the $\text{PDF}(X)$, when $F_{min}(X_i)$, the response approximation at X_i , is different from the true response, Eq. (5.1) may result in, albeit very rarely, the following inequality:

$$\sum_{i=1}^9 \omega_i F_{min}^2(X_i) < \left[\sum_{i=1}^9 \omega_i F_{min}(X_i) \right]^2 \quad (5.2)$$

which eventually leads to unrealistic negative variance. Figure 5.1 graphically illustrates this circumstance. Figure 5.2a shows the normal distribution of X_i we assumed, and the distribution of true response of $F_{min}(X)$ is shown in Figure 5.2b. In Figure 5.2b, circle marks the true response F_{min} at X_i while cross marks the simulated response, which naturally has errors for various reasons such as numerical error, material and geometrical modeling error, etc. Combined with the fixed weight ω_i , the inequality of Eq. (5.2) can arise in the numerical moment matching task.

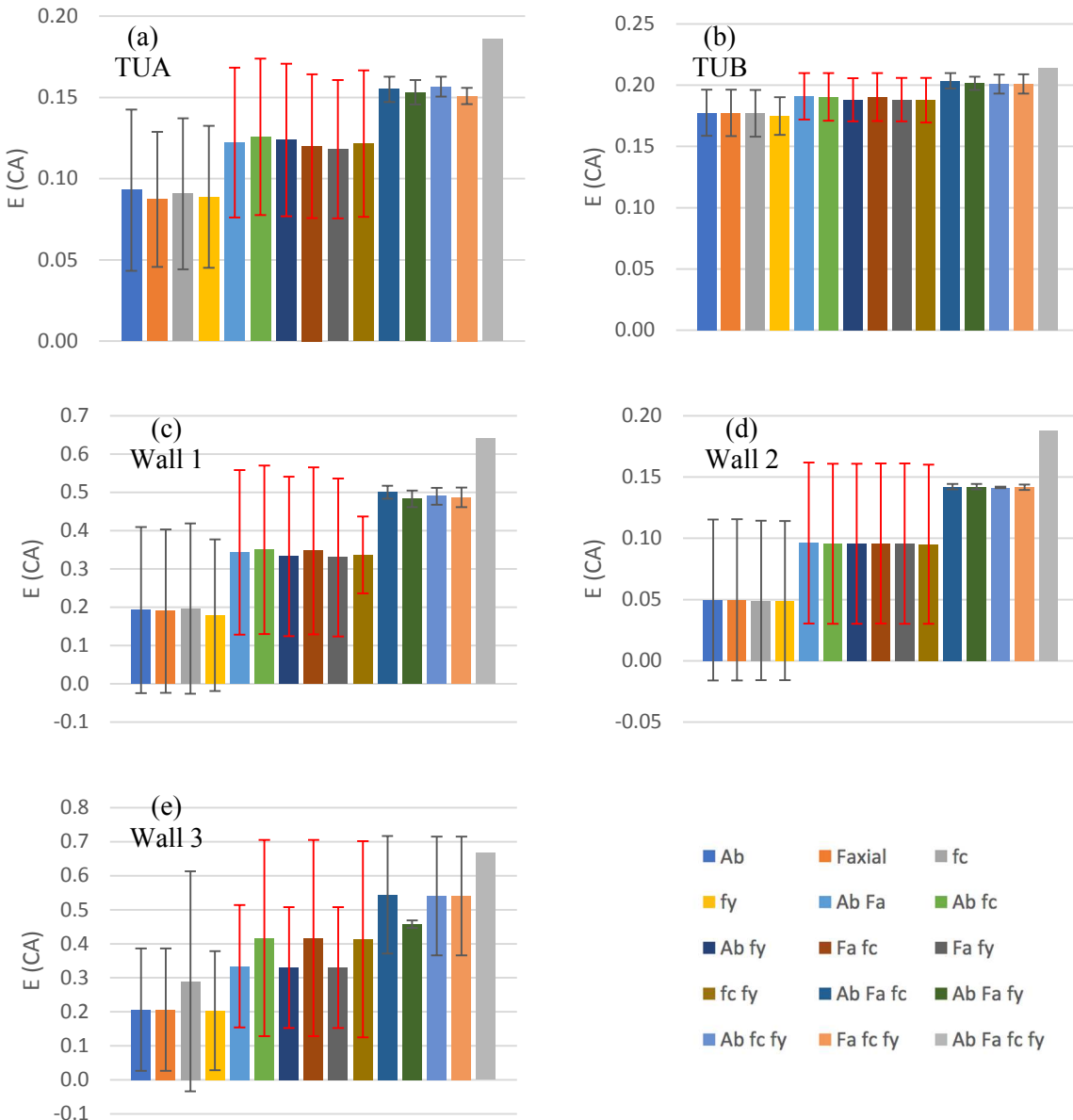


Figure 5.1. Expectations of the crushed area ratio (denoted as $E[CA]$) derived from PM-FEA coupled with multi-dimensional MM ranging from 1D through 4D: (a) TUA; (b) TUB; (c) Wall 1; (d) Wall 2; (e) Wall 3. Error bar indicates $\pm\sigma$. Large error bars are produced by MM which implies there are substantial uncertainties in the crushed areas and progressive bar buckling of five U-walls.

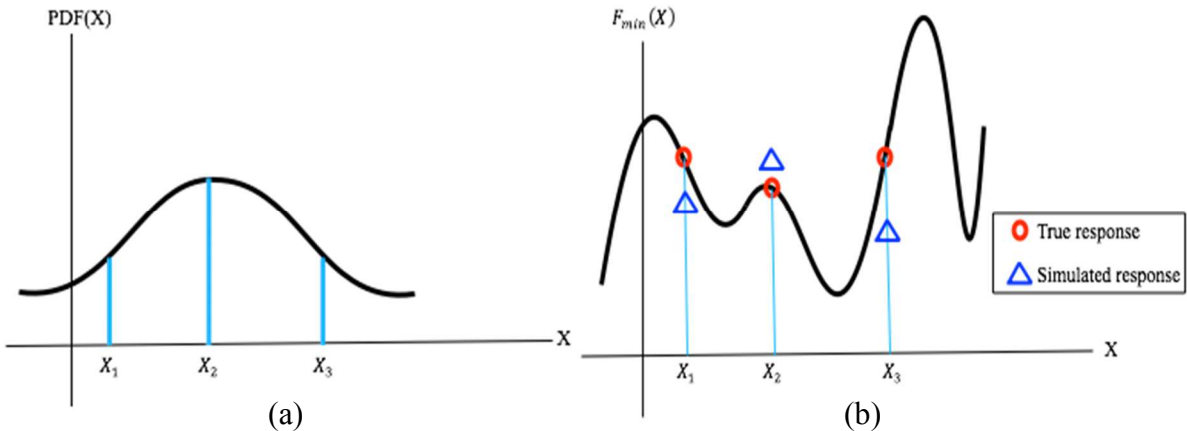


Figure 5.2. (a) PDF of variable X ; (b) True and simulated responses at various X .

This circumstance occurs for the 4D MM estimation of $\text{Var}[F_{min}]$ of TUA and TUB. However, the variance estimate returns to positive values by slightly adjusting the simulated responses within an acceptable error range: e.g., when $F_{min}(X_2)$ is greater than -528.512 kN for TUA; when $F_{min}(X_2)$ is greater than -485.860 kN for TUB. Such *ad hoc* adjustment is not a fundamental solution, and improvement of computer simulation accuracy would be a remedy that is more essential. The accuracy improvement of high-precision FEA tool can be achieved by incorporating more advanced microscopic material mechanisms, which is beyond our scope.

5.2 Conclusion

As a fast and robust method for uncertainty quantification of complex RC structures, this study presents a combination of MM and a high-precision PM-FEA. We demonstrated how MM can dramatically reduce the required sample points to only a few, thereby enabling precise uncertainty quantification behind global and microscopic performances. We demonstrate the method by using five U-shaped RC walls collected from the literature. The combination of MM and PM-FEAs appears to be promising. The combination reveals that a

superior test condition (i.e., the variability of salient experimental parameters is highly low) may lead to substantially large and irregular patterns of uncertainty in predictions depending upon unique features of the specimens. Importantly, the present methodology offers new access to identifying uncertainty behind microscopic damage phenomena of complex RC structures. As an apt application, this study demonstrated that the combination of MM and PM-FEA can be efficiently used to quantify uncertainty behind PBB behavior. Compared to uncertainty behind global performances, Uncertainties of PBB appears to be highly sensitive to subtle changes of design factors, necessitating due care in interpreting prediction results of PBB and other microscopic behaviors. The combination of MM and PM-FEA is believed an efficient, reliable method to improve our understanding of complex causal pathways between intrinsic variability of design variables and uncertainty behind global performances as well as microscopic damage phenomena of complex RC structures.

The combination of genetic algorithm and numerical moment matching successfully overcomes the severe numerical divergence and initial-value dependency. Leveraging off GA-NMM, this study offers three tables for searching required locations and weights based on common collapse capacity. The three tables include the exact solution, the solution revised using common remedy, and adjusted remedy. The future research will focus on not only extending the range of the table and reducing the errors for the adjusted remedy, but also investigating more features, i.e., yearly repair cost. Leveraging off GA-NMM, we are capable to generate the exact solution for lognormally distributed collapse capacity. For all 424 cases, the error rate are all smaller than 1E-14 percent, which means the exact errors are lower than 1E-16, that is, 0 error due to computational double precision.

The exact solution has small error that approaches 0. Nevertheless, two locations (x_2 and x_3) are on the upper tail of the lognormal distribution significantly. To fix the problem statistically, we provide two remedies, common remedy and adjusted remedy, by moving locations based on percentiles. The error of common remedy is acceptable till $\sigma = 0.5$ while the adjusted remedy reduces approximately 50% of the error from the common remedy. Engineers or researchers can quickly obtain intended collapse capacities from the adjusted remedy.

In this study, we investigate collapse capacity within common range of μ and σ . However, there exists various features, i.e., yearly repair cost, to be investigated in the future. Therefore, the future work will focus on not only lowering the error rate of the adjusted remedy and covering more cases, but also investigating more features and providing convenient tables for researchers and engineers to use.

REFERENCES

- [1] Heredia-Zavoni, E., Zeballos, A., and Esteva, L., 2000. Theoretical models and recorded response in the estimation of cumulative seismic damage on non-linear structures, *Earthquake Engng Struct. Dyn* **29**, 1779-1796.
- [2] Iervolino, I., Fabbrocino, G., and Manfredi, G., 2004. Fragility of standard industrial structures by a response surface based method, *Journal of Earthquake Engineering* **8**(6), 927-945.
- [3] Aslani, H., Miranda, E., 2004. Component-level and system-level sensitivity study for earthquake loss estimation, *13th World Conference on Earthquake Engineering*, Paper No.1070.
- [4] Akkar, S., Sucuoglu, H., and Yakut, A., 2005. Displacement-based fragility functions for low- and mid-rise ordinary concrete buildings, *Earthquake Spectra* **21**(4), 901-927.
- [5] Iervolino, I., Manfredi, G., Polese, M., Verderame, G. M., and Fabbrocino, G., 2006. Seismic risk of R.C. building classes, *Engineering Structures* **29**, 813-820.
- [6] Bal, E., Crowley, H., Pinho, R., Gulay, G., 2007. Detailed assessment of structural characteristics of Turkish RC building stock for loss assessment models, *Soil Dynamics and Earthquake Engineering* **28**, 914-932.
- [7] O'Brien, P., Eberhard, M., Haraldsson, O., Irfanoglu, A., Lattanzi, D., Lauer, S., and Pujol, S., 2011. Measures of the seismic vulnerability of reinforced concrete buildings in Haiti, *Earthquake Spectra* **27**(S1), S373-S386.
- [8] Bal, I., Bommer, J. J., Stafford, P. J., Crowley, H., and Pinho, R., 2011. The influence of geographical resolution of urban exposure data in an earthquake loss model for Istanbul, *Earthquake Spectra* **26**(3), 619-634.
- [9] Avsar, O., Yakut, A., and Caner, A., 2011. Analytical fragility curves for ordinary highway bridges in Turkey, *Earthquake Spectra* **27**(4), 971-996.
- [10] Lang, D. H., Singh, Y., and Prasad, J. S. R., 2012. Comparing empirical and analytical estimates of earthquake loss assessment studies for the city of Dehradun, India, *Earthquake Spectra* **28**(2), 595-619.
- [11] Ozhendekci, N., and Ozhendekci, D., 2012. Rapid seismic vulnerability assessment of low- to mid-rise reinforced concrete buildings using Bingöl's regional data, *Earthquake Spectra* **28**(3), 1165-1187.
- [12] Silva, V., Crowley, H., Varum, H., Pinho, R., and Sousa, R., 2014. Evaluation of analytical methodologies used to derive vulnerability functions, *Earthquake Engng Struct. Dyn.* **43**, 181-204.

- [13] Fajfar, P., 1999. Capacity spectrum method based on inelastic demand spectra. *Earthquake Engineering and Structural Dynamics* **28**(9), 979–993.
- [14] Antoniou, S., and Pinho, R., 2004. Development and verification of a displacement-based adaptive pushover procedure. *Journal of Earthquake Engineering* **8**(5), 643–661.
- [15] Rosenblueth, E., 1975. Point estimates for probability moments. *Proc. Nat. Acad. Sct. USA* **72**(10), 3812-3814.
- [16] Ching, J., Porter, K. A., and Beck, J. L., 2009. Propagating uncertainties for loss estimation in performance-based earthquake engineering using moment matching, *Structure and Infrastructure Engineering* **5**(3), 245-262.
- [17] Abramowitz, M. and Stegun, I. A. (Eds), 1972. *Handbook of Mathematical Functions with Formulas, Graphs, and Mathematical Tables*, 9th printing, (Dover: New York).
- [18] Cho, I., and Porter, K. A., 2016. Modeling building classes using moment matching, *Earthquake Spectra* **32**(1), 285-301.
- [19] Baker, J. W., and Cornell, C. A., 2003. Uncertainty specification and propagation for loss estimation using FOSM methods. In *Proceedings of Ninth International Conference on Applications of Statistics and Probability in Civil Engineering*.
- [20] Borzi, B., Pinho, R., and Crowley, H., 2008. Simplified pushover-based vulnerability analysis for large- scale assessment of RC buildings, *Engineering Structures* **30**, 804-820.
- [21] Beyer, K., Dazio, A., and Priestley, M. J. N., 2008. Quasi-static cyclic tests of two u-shaped reinforced concrete walls. *Journal of Earthquake Engineering*, **12**(7):1023-1053.
- [22] Cho I., 2013. Virtual earthquake engineering laboratory capturing nonlinear shear, localized damage and progressive buckling of bar. *Earthquake Spectra* **29**(1), 103-26.
- [23] Rossetto, T., Elnashai, A., 2005. A new analytical procedure for the derivation of displacement-based vulnerability curves for populations of RC structures, *Engineering Structures* **27**(3), 397-409.
- [24] Cho, I. and Hall, J. F., 2014. General Confinement Model based on Nonlocal Information, *Journal of Engineering Mechanics* **140**(6). [10.1061/(ASCE)EM.1943-7889.0000724].

- [25] N. Ile., and Reynouard, J. M., 2015. Behavior of u-shaped walls subjected to uniaxial and biaxial cyclic lateral loading, *Journal of Earthquake Engineering* **9**(1), 67-94, DOI:10.1080/13632460509350534.
- [26] Cho, I., 2017, Deformation gradient-based remedy for mesh objective three-dimensional interlocking mechanism, *Journal of Engineering Mechanics* (in press).
- [27] Cho. I., and K. Porter, 2014. Structure-independent parallel platform for nonlinear analyses of general real-scale RC structures under cyclic loading, *Journal of Structural Engineering* **140**(8).
- [28] Beck. J.L., Porter, K. A., Shaikhutdinov, R., Mizukoshi., K., and et al., 2002. Impact of seismic risk on lifetime property values. *Rep. No. EERL 2002-04.*
- [29] Haselton, C. B., Goulet, C. A., Judith, M., and et al, 2008. An assessment to benchmark the seismic performance of a code-conforming reinforced concrete moment-frame building.
- [30] Lazar. N., and Dolsek, M., 2013. Incorporating intensity bounds for assessing the seismic safety of structures: Does it matter?, *Earthquake engineering and Structural Dynamic* **43**(5), 717-738. DOI: 10.1002/eqe.2368.
- [31] Blume Earthquake Engineering Research Center, 2001. *Assembly-based vulnerability of buildings and its uses in seismic performance evaluation and risk-management decision-making*, PEER Rep. 139, Stanford, CA.
- [32] Cho. I., Song. I., and Teng Y. L., 2018. Numerical moment matching stabilized by a genetic algorithm for engineering data squashing and fast uncertainty quantification. *Computers and Structures*, **204**, 31-47.
- [33] Cho. I. Program for GANMM.
<https://sites.google.com/site/ichoddese2017/home/type-of-trainings/numerical-moment-matching-coupled-with-generalized-genetic-algorithm-ga-nmm-v10>; 2018.
- [34] Johnson, N. L., Kotz, S., Balakrishnan, N., 1994. Lognormal distributions, in *Probability and Mathematical Statistics: Applied Probability and Statistics (2nd ed.)*, New York, NY, 115.